A STUDY OF THE INFLUENCE OF DIFFERENT STRUCTURES ON RESISTIVITY OF CONDUCTIVE KNITTED FABRICS

LIU SU

Ph.D

The Hong Kong Polytechnic University

2017

THE HONG KONG POLYTECHNIC UNIVERSITY

INSTITUTE OF TEXTILES AND CLOTHING

A STUDY OF THE INFLUENCE OF DIFFERENT STRUCTURES ON RESISTIVITY OF CONDUCTIVE KNITTED FABRICS

Liu Su

A thesis submitted in partial fulfillment of the requirements for the degree of Doctor of Philosophy

June 2016

CERTIFICATE OF ORIGINALITY

I hereby declare that this thesis is my own work and that, to the best of my knowledge and belief, it reproduces no material previously published or written, nor material that has been accepted for the award of any other degree or diploma, except where due acknowledgement has been made in the text.

______________________ (Signed)

________Liu Su________ (Name of student)

To My Family

For the Love, Patience and Support

ABSTRACT

The research progress made in the field of materials science and the efforts put forth by many researchers have resulted in many research works that focus on wearable electronic textiles. Nowadays, wearable electronic textiles have progressed from the research lab into the industry and subsequently commercialized. The different ways of incorporating conductive fibers and electronic components into traditional textiles have been receiving much attention due to the potentially significant commercial value. However, the industry does not appear to have the means to new knowledge and knowledge transfer. For example, the industry does not have the resources to calculate and control yarn resistance on fabrics simply based on current textile knowledge, and wearable electronic products thus cannot be further developed. Nevertheless, the results of research on such products are not significant or adequate due to the complexity of the interdisciplinary efforts required for their success. Therefore, there is a need to establish a systematic method to provide the industry with a reference source to produce wearable electronics. The relationship between different stitches and the properties of conductive materials needs to be elaborated.

This study conducts a series of experiments on the resistivity of conductive knitted fabric with different knitwear structures. Based on a previous study that modeled the resistance of plain jersey fabric with different numbers of wales and courses, planar geometric models are established for 1 x n float and Single Pique structures. Resistive network models are developed for different external voltages to

determine the resistance values of conductive knitted fabrics with different numbers of wales and courses. Corresponding experiments are carried out to verify the proposed models. The simulated results obtained through modeling agree well with the experimental data with an acceptable range of error. Finally, a comparison of jersey (knit), float and tuck stitches is carried out with the relative wales and courses. It is concluded that both float and tuck stitches could reduce the total resistance of conductive knitted fabrics, and between them, tuck structures can provide lower resistance as well as a more aesthetically pleasing appearance. On the other hand, float structures are more economical, as conductive yarn is expensive so its cost is reduced with use of float stitch as the loop length is much shorter than that of the tuck stitches.

Three thermal knitwear garments are developed in the experiments to test the thermal performance to determine the optimal design from the different knitted structures. It is concluded that the thermal properties are influenced by the different knitted structures and Single Pique has the most optimal performance in terms of the heating effect among the three types of selected structures.

The newly developed resistance models in this study will provide significant benefits to the commercialization of wearable electronic textiles, as well as to the apparel industry as they can now offer apparel products that are not only aesthetically pleasing and multi-functional, but also have high added value.

PUBLICATIONS ARISING FROM THE THESIS

Journal paper

1. Liu S, Tong J, Li L. The impact of different proportion of knitting elements on resistive properties of conductive fabrics. Textile Research Journal, in submission.

2. Liu S, Tong J, Yang C, Li L. 2016. Smart E-textile: Resistance Properties of Conductive Knitted Fabric – Lacoste. Textile Research Journal 2016, 0040517516658509.

3. Liu S, Yang C, Zhao Y, Tao X, Tong J, Li, L. The impact of float stitches on the resistance of conductive knitted structures. Textile Research Journal 2016, 86(14): 1455-1473

4. Tong J, Liu S, Yang C, Li L. Modeling of package-free flexible conductive fabric with thermal regulation where temperature can be customized. Textile Research Journal 2015, 85(6): 590-600.

Patent

1. Li L, Liu S, Zhao Y F, Yang C X. The selection method and application for a thermal silver coated yarn. (一種可發熱鍍銀導電線的選擇方法及其應用). (2014)

Awards

1. Li L, Wan K M, Tong J H, Zhao Y F, Chan Y F, Chui Y T, Liu S. Thermal fabric with the temperature control. International Inventions of Geneva 2014. Silver Award.

2. Liu S. Circular Water. Shenghong Cup China Fiber Creative Works Exhibition 2013, The Best Technology Awards.

Conference Paper

1. Liu S, Li L. The resistance properties of conductive Lacoste Fabrics. TBIS 2015, the 8th Textile Bioengineering and Informatics Symposium. June 14-17, 2015 in Zadar, Croatia.

ACKNOWLEDGEMENTS

I registered to be a Ph.D research student four years ago. During this period, I cannot persist until today without supports and assistances from many others. I would like to take this opportunity to express my sincere appreciation.

First of all, I would like to express my great and sincere appreciation to my Chief supervisor, Dr. Li Li, Associate Professor of Institute of Textiles and Clothing, The Hong Kong Polytechnic University. She is not only an excellent supervisor in academic, but also a wonderful supervisor in spirit. I am very thankful for her great patience and tolerance to guide, instruct and support me during my study. The sincere gratitude would also be expressed to my Co-supervisor Prof. Hu Hong and Prof. Au Raymond Wai Man, Professor of Institute of Textiles and Clothing, The Hong Kong Polytechnic University. Without their advice, guidance and instruction, I will not be brave enough to work on a Ph.D study.

Secondly, I would like to sincerely thank Dr. Zhou Jinyun, Instructor of Institute of Textiles and Clothing, The Hong Kong Polytechnic University. His unlimited tolerance and understanding afford me a very friendly background to balance my work and study.

I also would like to appreciate my friends and my team members Dr. Liu Yanping, Mr Tong Jiahui, Mr Liu shirui, Ms Liu Su, Ms Han Xiao, Miss Yan Ou, Miss Yang Chenxiao, Dr. Chui Yin-Ting, Dr. Kitty Lam, Ms Zhao Yuanfang, who afford me a lot of assistances and friendship.

Last but not least, I would like to express my special appreciation to my family. Without their encouragement and great support, I could not stick to my study all along the way.

Thanks so much to all of you!

TABLE OF CONTENTS

LIST OF FIGURES

LIST OF TABLES

CHAPTER1 INTRODUCTION

1.1 Background

A new emerging domain in the textiles field is wearable electronic textile, namely, textile that has incorporated electrical functions. For instance, these functions include provision of heat, emitting of light, sensing ability, electromagnetic shielding, electrode functions, etc. The field of wearable electronic textiles is developing rapidly due to the creation of new types of fibers and fiber-composites. Conductive yarn is an innovative textile material in the family of smart materials, which also include for example, piezoelectric, chromogenic, optical, and shape memory materials (Mattila, 2006). Conductive yarn has widespread applications due to its advantages including exceptional electrical conductivity, high-intelligence, stability, washability, etc.

In the last few decades, numerous researchers and their project teams have put forth a significant amount of effort into the development of electrical textiles, starting with electronically conductive textile fibers by Sanders (1974). Nowadays, wearable electronic textiles have progressed from the research lab into the industry and subsequently commercialized. The different ways of incorporating conductive fibers and electronic components into traditional textiles have been receiving much attention due to the potentially significant commercial value. To meet the requirements of both aesthetics and function rather than appearing to be overly ‘technical’, the textiles technology and garment design methods are important for marketing success. In the earlier days, the methods of incorporating electronic components were to mainly attach an additional device onto a non-functional garment to satisfy the required function; however, this not only compromises the aesthetics but also inconveniences wearers. In recent studies on electrical textiles, prototypes now tend to be more and more esthetically pleasing and commercially practical. Traditional methods are now gradually being replaced by embedding conductive yarn into fabrics during the production process. In previous research, the general methods of embedment were mainly carried out in four ways (weaving, knitting, embroidery and coating), and knitting has proven to be the most efficient way due to the resultant good elasticity and shape formation flexibility (Bonfiglio et al., 2011).

Nowadays, the combination of conductive materials and knits results in wearable electrical textiles, and their applications are found in the areas of sports, healthcare, fashion and entertainment, military, public sector and safety, etc. (Lymberis & Paradiso, 2008; Van Langenhove & Hertleer, 2004). Conductive knitting is one of the most significant and promising areas of research and the focus of many researchers. Conductive knitting is traditional knitting that uses electronic yarns or fibers to create innovative functional garments, for example, thermal and sensor knitwear (Park & Jayaraman, 2003) which have the advantages of knits in terms of their flexibility, lightness in weight, soft handle, etc.

Wearable electronic textiles is a very promising field since statistical data show that the development of wearable electronics dates back to the portable music cassette player (Japanese Sony®) (McCann & Bryson, 2009), and predicted revenue is anticipated to increase from over $14 billion in 2014 to over $70 billion in 2024 worldwide (Swapnil, 2015). In the recent decade, the development of wearable electronics for commercialization has gradually increased, which means that scientific research on conductive knitting is increasing in academic importance. However, most of the research work has focused on the development of conductive yarns with high performance and value added properties, which are mainly in the improvement of production and formulation. Little attention has been given to the applications of conductive yarns, for example, their properties when embedded into knitted fabrics which are very important areas of study as knitted fabric is very flexible and elastic so that traditional electronic textile knowledge is not directly applicable. There is therefore the need to further systematically analyze the properties of conductive knitted fabrics with different structures since they have variations in mechanical and geometrical performances, which will directly affect the electrical performance of the knitted structures. However, if more research work is carried out to determine the properties of conductive yarn when embedded into fabrics, the issues will be addressed and new techniques developed.

In previous work, the knitting techniques to produce conductive-textile products have been very complicated. For example, Liu et al. (2012) changed the fabric structure on plain knits by using 2x1 rib, miss-knit stitches and a mesh structure. In Li et al. (2009b) intelligent clothing was examined by studying different knitting structures. Another instance is Çeken et al. (2012b), who researched the electromagnetic shielding properties of conductive knitted fabrics by investigating several different types of knitted structures, such as cross-miss 1x1 plain knit, Single Pique, interlock and double pique. These researchers found that conductive fabric with different knitted structures provide different properties although the same materials and the same stitch length are used. Their results demonstrate that the knitted structure is an important factor during the fabrication of electro-conductive fabrics. However, there is the need to further systematically study the relationship between different knitted structures and electrical properties of conductive knitted fabrics.

However, to apply electrical properties to fabrics by using conductive fibers, the complex and elastic fabric structure would need to be modeled. Thanks to the technological progress and the efforts of numerous researchers, there are now many research examples on the modeling of conductive knitted fabrics. Li et al. (2009a) developed an equivalent resistive network to predict the resistance of plain jersey fabric with different numbers of wales and courses. R_L and R_C are used to represent the linear and contact resistances, respectively. The length of the conductive yarn generates linear resistance and contact resistance is generated by the contact of two or more overlapping conductive yarns. The theory in which R_L and R_C both contribute to the total resistance of knitted fabrics has been accepted by most researchers. Li et al. (2012) also conducted a series of experiments and developed corresponding empirical equations to establish the relationships among resistance, tensile force, and fabric length and width. A series of applications have been published based on the models (Tong & Li, 2015). Besides these research works, some related research has also focused on the study of the resistance of plain jersey under external extension. For example, In Zhang et al. (2006), a matrix expression was introduced to obtain the resistance value of single jersey on the basis of a loop model to simulate conductive knitted fabric as a large-strain gauge under high temperatures. Recently, Wang et al. (2014a; 2014b) developed a hexagonal model to predict the electromechanical properties of conductive knitted elastic fabrics under biaxial extension. By using Holm's electrical contact theory, two classical models on the mechanics of knitted fabric were used to calculate the contact resistance of the knitted fabric together with contact load and deformation. However, the modeling was mainly carried out on single jersey structures with a onefold template. There is little related modeling work done on different structures, which would affect the properties of conductive knitted fabrics.

Therefore, the present study will establish a relationship between knitted structures and the conductive properties of fabric based on knit, float and tuck stitch models. The aim is to provide a systematical means for the production of conductive knitted fabric, which will contribute to the commercialization of wearable electronic textiles and intelligent textile products. The newly developed system will provide a powerful theoretical foundation for the innovation of intelligent knitwear fashion.

1.2 Aim and Objectives

The aim of this study is to contribute to the fundamental knowledge on conductive knitting with the use of three basic stitches. Equivalent resistive network models for differential kinds of conductive knitted fabrics are established based on geometrical modeling of knitted structures.

The primary objectives are as follows:

To study the influence of knitted structure on the conductivity of fabric with a comprehensive investigation and theoretical analysis.

To investigate the practical properties of conductive knitted fabrics by conducting experiments based on the deduced influential factors.

To model the relationship between knitted structure and electrical properties and establish a means for the design of fabric structure when fabricating conductive knitted garments.

To design a series of conductive knitwear which have good conductive properties and aesthetics.

1.3 Significance and Value

The developed system is expected to address the multidisciplinary research gaps and contribute to knowledge on wearable electronic functional textiles in terms of application and commercialization. The proposed system is not only limited to modeling functional protective garments but can be also used for healthcare/medical textiles and where soft thermals are required. The study will also generate knowledge in the fields of electronics, textile technology and knitwear design. Thus, the work here will add to the innovative development of smart textiles. This study will also serve as the basis for future studies and may be extended to other potential applications in the future. In addition, the proposed methods can be used as a reference for laboratory research, industrial production and commercial marketing.

1.4 Methodologies

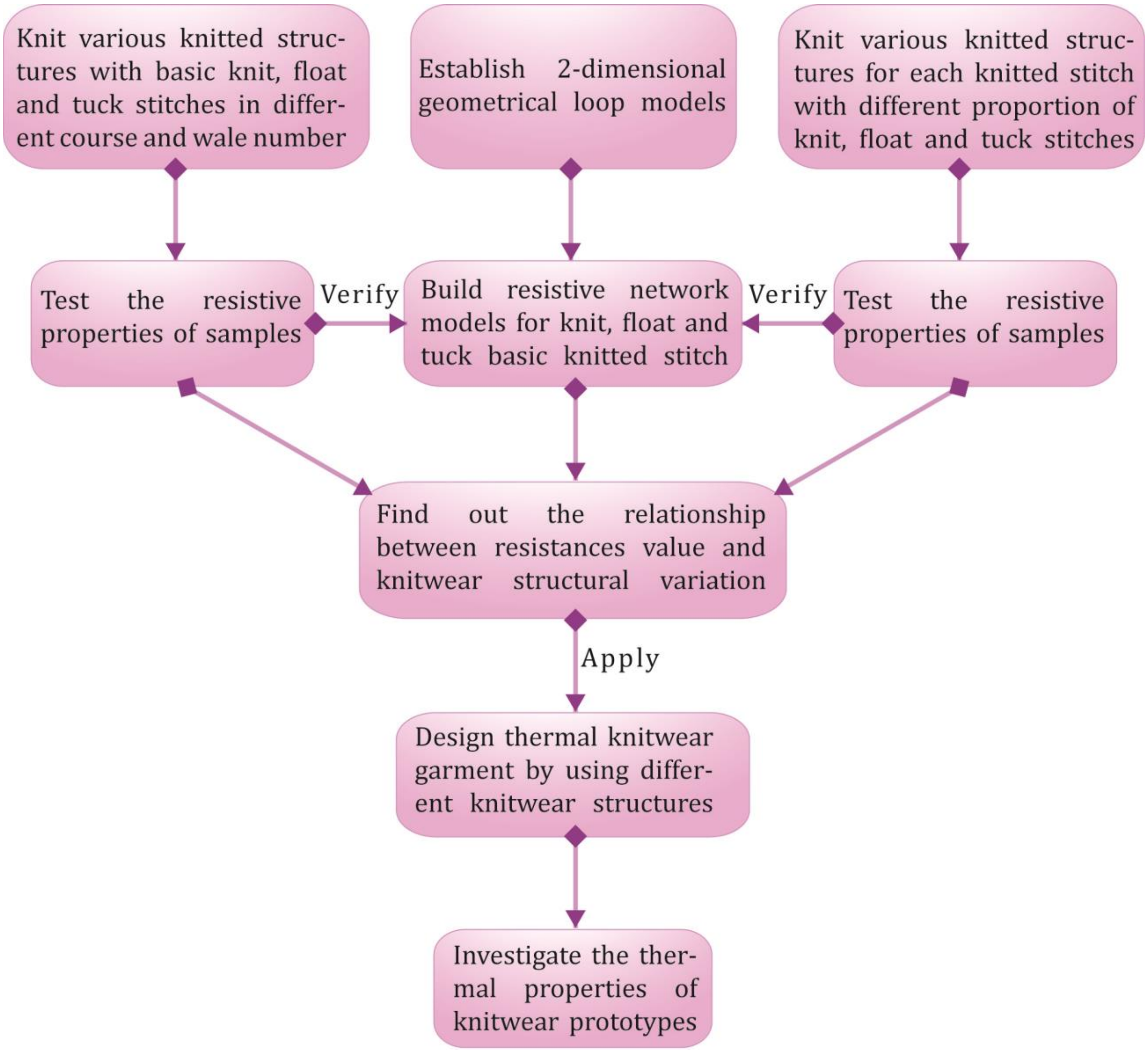

Figure 1.1 The methodology used in this study.

Based on the past research work as mentioned previously, the research methods adopted in this study to investigate the impact of different knit structures on the properties of conductive knitwear will be carried out per Figure 1.1.

1.5 Outline of the thesis

The organization of this thesis is provided as follows, which comprises a total of 8 chapters.

Chapter 1: A brief introduction on this research work, which includes background information, aim and objectives, methodologies, significance and value, and thesis organization, is provided. In this chapter, the research gap is discussed by demonstrating the limitations of previous research work. The objectives are established followed by a brief description of the research methods and potential contribution of the study.

Chapter 2: A systematical review of the related literature will be provided, which includes current work on electronic textiles, conductive paths of conductive knitted fabrics and thermal fabric functions. Literature in related fields is reviewed and previous works and outputs are elaborated with discussion of their limitations.

Chapter 3: A description of the research methods will be provided in detail. In this chapter, the methods used in the present study are outlined and will be further elaborated in the following chapters.

Chapter 4: A discussion will be carried out on a fundamental study of the resistivity of conductive knitted structures with float stitches. In this chapter, the resistive network modeling of basic conductive structures with float stitches is carried out based on an established planar geometrical model for the float stitch. Corresponding experiments are carried out to verify the modeling.

Chapter 5: This is a fundamental study on the resistivity of conductive knitted structures with tuck stitches. In this chapter, resistive network modeling of typical conductive structures with tuck stitches is carried out based on an established planar geometrical model for the tuck stitch. The modeling is verified by a series of related experiments.

Chapter 6: The predicted resistivity will be examined by applying the resistive network models. In this chapter, the resistance values of conductive knitted fabrics with different proportions of knit, float and tuck stitches are tested to further verify the established models and identify the effects of different knit structures.

Chapter 7: Prototypes of thermal garments with different knitted structures in the heating areas are presented in this chapter. Three thermal garments are designed and fabricated with different knitted structures in the heating areas. It is found that there are different thermal effects, which can further verify the impacts on the resistivity due to the design of the knit structure.

Chapter 8: In this chapter, the present study will be summarized and conclusions made, and limitations are discussed. As well, recommendations for future works are provided.

CHAPTER 2 LITERATURE REVIEW

2.1 Introduction

This chapter is a review of the literature that is related to this study. First, electronic textiles will be discussed in terms of conductive yarn and fabric, their corresponding applications and then their advantages. Secondly, the conductive paths of conductive knitted fabric will be reviewed in terms of the construction of the knitted elements, electrical properties of the conductive knitted structures and the relationship between resistance and the conductive knitted structures. Thirdly, previous work on thermal textiles, the resistance of conductive knitted fabric and thermal knitted textile will be outlined. Finally, the current related literature is summarized and the research gap will be identified.

2.2 Review on current electronic textiles

2.2.1 Conductive yarn

2.2.1.1 Introduction

Conductivity can be transferred onto textile materials in three different phases: onto the fibers or yarn, during the production stage, or as an after-treatment (Schwarz & Van Langenhove, 2013). To date, textiles are increasingly incorporating conductive yarns to provide a final product with various special functions. The embedment of conductive yarns into textiles will provide a normal garment with electronic properties. Although conductive yarns and fibers have recently caught the attention of researchers, the use of metallic yarns can be actually dated back to the golden yarns produced in ancient

China (Latifi et al., 2010). With the rapid development of modern electronics, previous research has investigated various types of conductive materials and yarns so as to produce wearable electronic textiles. The most common types are listed in the following section.

2.3.1.2 Conductive yarn material

1. Carbon based fibers

(a) (b)

Figure 2.1 Carbon fibers: (a) filaments, (b) staples.

One of the most widely discussed types of conductive materials is carbon-based material, which includes carbon black (CB), graphite and carbon nanotube (CNT). CB is widely applied for shielding, heating and antistatic properties, due to its high resistance and low electro-conductivity compared with other conductive materials (Schwarz & Van Langenhove, 2013). Carbon based fibers are made by using continuous fibers or different morphologies with monofilament strands of 1000-12,000 filaments (Biró et al., 2012). Carbon monofilaments and filaments are mainly produced by using polyacrylonitrile (PAN), or isotropic, anisotropic or mesophase pitch (Figure

2.1(a)). However, only vapor-grown carbon is spun into staples (Figure 2.1(b)). Carbon fibers are classified according to their mechanical performance (Figure 2.2) based on their strength and modulus (Inagaki, 2000). It can be seen from the image that carbon fibers, which have relatively low tensile strength and modulus, around 1000MPa and 100 GPa, respectively, are classified into general- purpose grade (GP-grade). Isotropic-pitch-based and some PAN-based carbon fibers belong to this grade and are used in applications that benefit from their low weight and bulkiness.

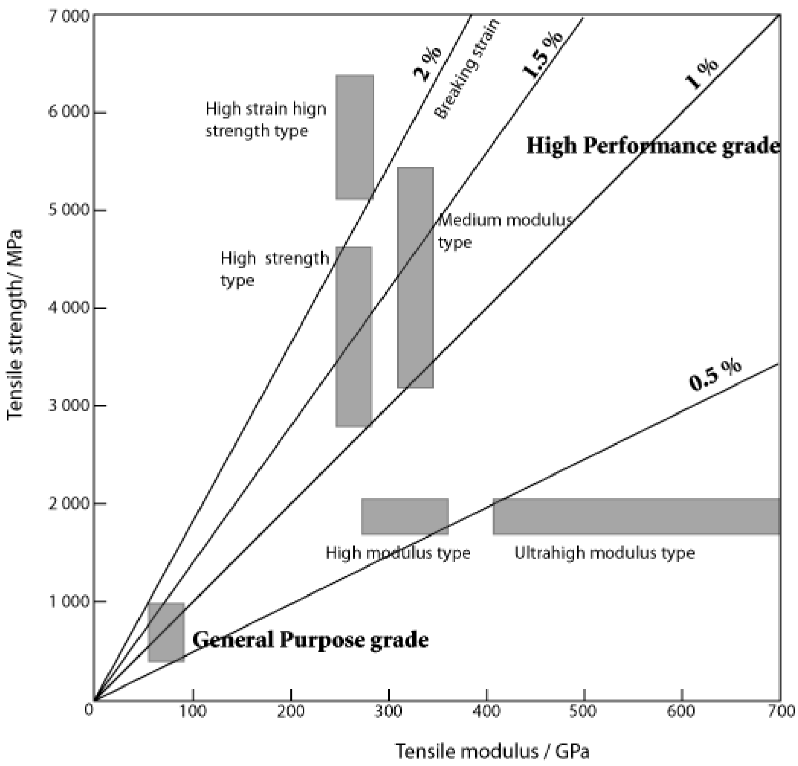

Figure 2.2 Classification of carbon fibers based on strength and modulus performance [Reproduced From (Inagaki, 2000) with permission of Elsevier Science].

Jost et al. (2013) produced supercapacitors from knitted carbon-fibers and activated carbon ink as an “energy textile”, which is the first fabrication technique that integrates energy storage devices with knits (Figure 2.3). It was concluded that knitted carbon fiber electrodes have the optimal properties in comparable mass and capacitance.

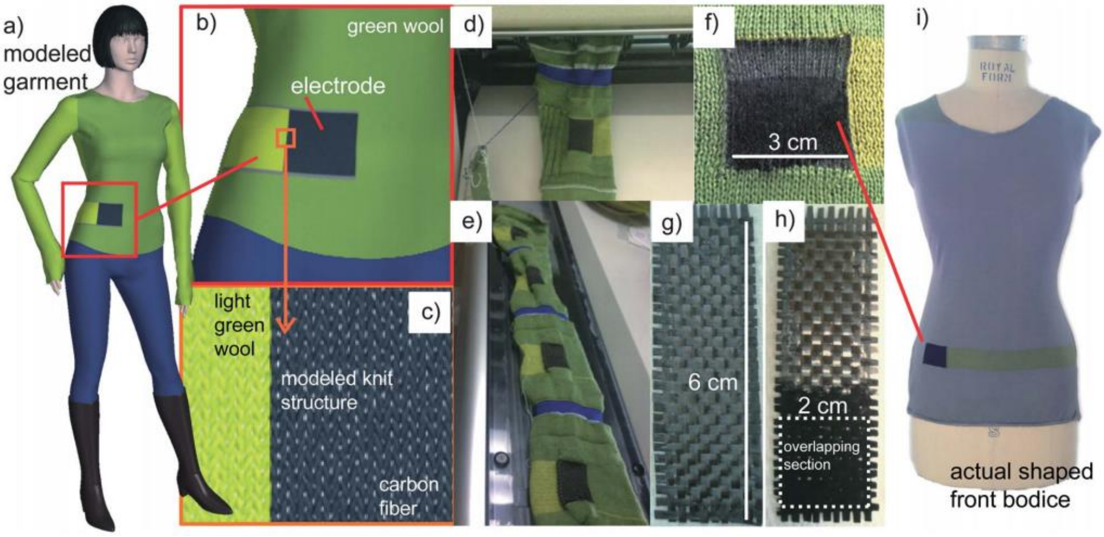

Figure 2.3 Supercapacitors produced from knitted carbon-fibers and activated carbon ink as an “energy textile” [Reproduced From (Jost et al., 2013) with permission of The Royal Society of Chemistry].

2. Intrinsically conductive polymers

Intrinsically conductive polymers (ICPs) are organic materials with electrical conductivity. Conductive fibers constituted by pure ICPs are produced through a one-step wet spinning process. Materials made of these fibers have good conductivity and stability in outside environments, but limited applications in electrical textiles due to their poor mechanical strength, fragility and difficulties in production. Some common types are poly(fluorene)s, polyphenylenes, polyanilines, polypyrrole, etc. (Figure 2.4) (BASHIR, 2013).

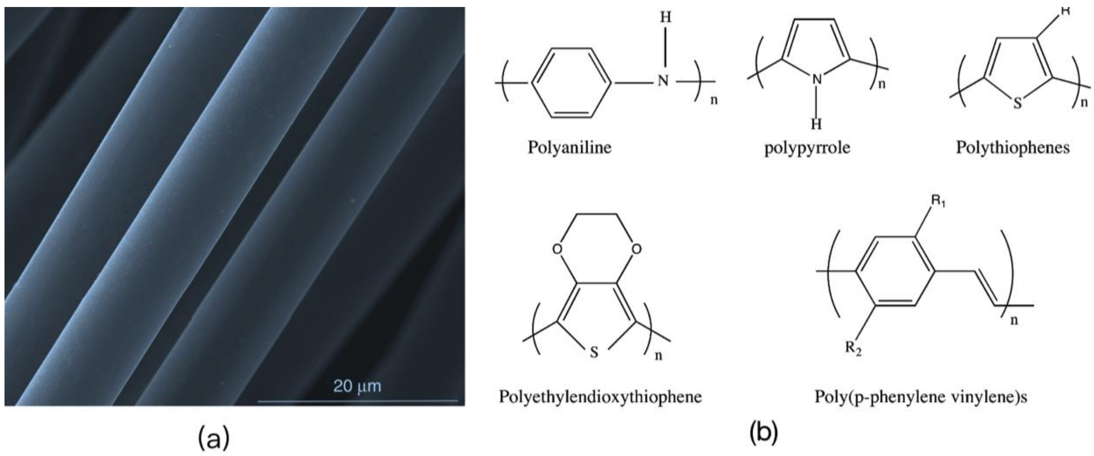

Figure 2.4 (a) Polypyrrole-coated para-aramid fibres [Reproduced From (Schwarz & Van Langenhove, 2013)with permission of Elsevier Science], (b) Chemical structure of common ICPs. (Saini & Arora, 2012).

3. Ferrous materials

Ferrous materials are magnetic and malleable. Stainless steel conductive fibers (SSCFs) are an example of a conductive fiber made of a ferrous material, or stainless steel. For instance, in the prototype of the Levi's Musical Jacket (Meoli & May-Plumlee, 2002), a stainless steel and polyester blended yarn was embroidered onto fabric to form a touch sensitive keyboard that allows control of smartphone functions. As conductive materials, SSCFs have good electrical ability. The materials were 100% metal made by using a mechanical drawing process. However, it is very difficult to use SSCFs on flexible materials such as knitted fabrics because they are extremely stiff. Generally, SSCFs only embroidered onto knitted fabrics as an inlaid yarn (Çeken et al., 2012b).

A study by Šahta et al. (2014) on the use of conductive yarns for knitting heating elements reported that stainless steel multifilament yarn is not suitable for knitting as it is inflexible and undeformed by extension. However, silver coated polyamide yarns were considered to be the most suitable for producing heating knitted elements.

(a) (b)

Figure 2.5 Stainless steel yarn: (a) stainless steel staple yarn twisted around core yarn, (b) stainless multifilament yarn [Reproduced From (Schwarz & Van Langenhove, 2013) with permission of Elsevier Science].

4. Non-ferrous materials

As conductive materials, the use of metallic yarns has had a relatively long history. In 1965, John A. Roberts created a metallic yarn structure with helically twisted outer filaments (JohnA.Roberts et al., 1968). Metallic components are generally coated (laneF.Forsgren et al., 1977), blended (Guo et al., 2012) or twisted (JohnA.Roberts et al., 1968) with other synthetic fibers, such as polyester, to enhance the elasticity of the resultant fabric (Guo et al., 2012). The metal materials used are usually copper (Qureshi et al., 2011), aluminum, nickel (Rheaume, 1982), tin (Parkova et al., 2011), tungsten and platinum (Hsu & Kuo, 2010). Table 2.1 is a list of the resistivity of different types of non-ferrous metals.

Table 2.1 Different materials and their resistivity [Reproduced From (Schwarz & Van Langenhove, 2013) with permission of Elsevier Science].

Material	Resistivity ρ (Ω/m)
Silver	1.62×10^{8}
Copper	1.69×10^{8}
Gold	2.44×10^{8}
Aluminum	2.75×10^{8}
Nickel	6.93×10^{8}
Iron	9.68×10^{8}
Platinum	10.6×10^{8}

Compared to non-metallic conductive materials, metallic yarns have the advantages of ease of processing, good conductivity and being environmentally friendly. Furthermore, among the various metallic materials, silver has more superior properties, compared to copper, which is poor in color; nickel and tungsten, which have impurities; and platinum, which is costly. Therefore, in this study, the focus will be on knitted fabrics produced with silver-coated yarns. Silver-coated yarns are one of the most popular types of conductive yarns in previous studies and for the fabrication of conductive textiles because silver has exceptional properties. To date, silver yarns have been applied on a widespread basis on medical wound dressings (Zou, 2013), and for heating purposes (McCann & Bryson, 2009), its conductivity (Zysset et al., 2010), EMI shielding (Ingle et al., 2008), antibacterial ability (Pollini et al., 2009), etc. At present, there are numerous commercial products in the textile and garment industry that use silver, such as SHIELDEX® yarns (X-STATIC, 2016), X-static® technology for wound care (X-STATIC, 2016) and Statex ® coated fabrics (Schwarz et al., 2010) (Figure 2.6). Some of the common producers of various conductive yarns are listed in Table 2.2 (Schwarz & Van Langenhove, 2013).

Table 2.2 Producers of conductive yarns [Reproduced From (Qureshi et al., 2011) with permission of Elsevier Science].

Material	Company Wires/filaments	Company Yarns
Copper	Elektrisola Feindraht Drahtwerk Waidhaus GmbH	Syscom Advanced Materials R.Stat
Silver	Elektrisola Feindraht	Statex Sauquoit Industries TIVV Greiz(Elitex) Syscom Advanced Materials Textronics Swiss Shield
Gold		Microcorax Syscom Advanced Materials
Aluminum	Imattec Gutmann	
Nickel	Western Metal Materials	Electro Fiber Technologies Syscom Advanced Materials
Stainless steel	Leoni Nippon Seisen	Bekaert Textiles Schoeller Epitropic Fibres R.Stat Créafibers IMATTEC International TibTech Innovation
Carbon black	SmartFiber	Kuraray Teijin Monofilament Ascend Performance Materials Shakespeare Conductive Fibers Unitika Fibers Barnet
Carbon nanotubes		Kuraray and Mitsui
Polypyrrole		Sterling Fibers Eeonyx Corporation

(a) (b)

Figure 2.6 (a) SHIELDEX, and (b) Statex silver-coated yarns.

2.2.1.3 Classification of conductive yarn

Electro-conductive yarns can be distinguished by their manufacturing method, which consist of pure and blend of conductive materials.

1. Yarns from pure conductive materials

The types of electro-conductive yarns that are made from pure conductive materials are normally metal, wire meshed or metallized yarns in the form of filaments (Nusko et al., 2005). Typical materials include silver, gold, metal, stainless steel, nanotube, etc. Their limitations are that they are difficult to produce and easily oxidate, and have a poor handfeel.

2. **Yarns from blend of conductive materials**

Electro-conductive yarns that are produced from a blend of conductive materials are more commonly adopted compared to those from pure materials due to their good conductivity, surface feel and appearance. These electro-conductive yarns are the so-called staple, filament and coated yarns, which are spun together with ordinary short textile fibers or filament yarns (Nusko et al., 2005). Figure 2.7 is an illustration of the different categories of typical pure and blends of electro-conductive yarns.

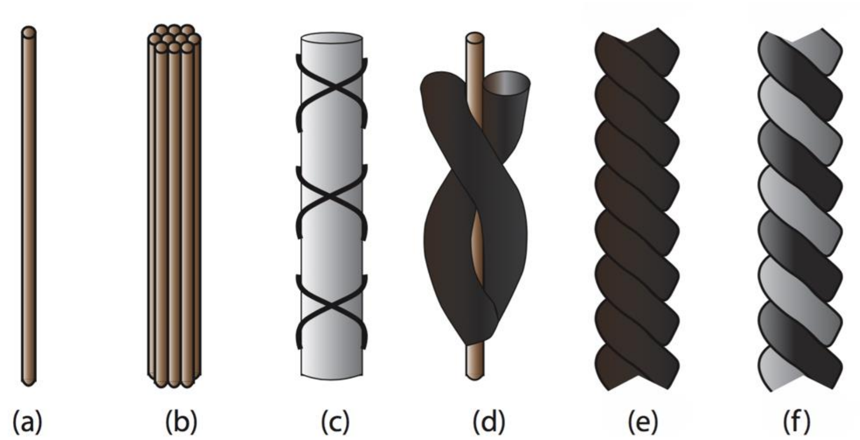

Figure 2.7 Categories of conductive yarn: (a) monofilament, (b) multifilament, (c) synthetic fiber plated with metallic yarn, (d) metal wire plated with insulating materials, (e) pure staple twisted yarn, (f) staple twisted with ordinary yarn.

Coated electro-conductive yarns are normally synthetic fibers plated with metallic materials, or a metal wire plated with insulating materials. The coating methods vary chemically and physically, which results in different functions and quality.

In reviewing the different types of conductive yarns found in the market, silver/nylon conductive yarns are the most popular for use in wearable electronic products due to their advantages, which include light in weight, flexibility, spinnability, and high mechanical stability over metal and carbon yarns (Chui et al., 2015). A large number of different conductive yarns have been developed along with the fast emergence of electronic textiles. For an optimal knitted conductive fabric, silver coated yarns are the best choice due to their flexibility, stability of conductivity, low resistivity, etc.

2.2.2 Conductive fabric (woven and knitted)

2.2.2.1 Introduction

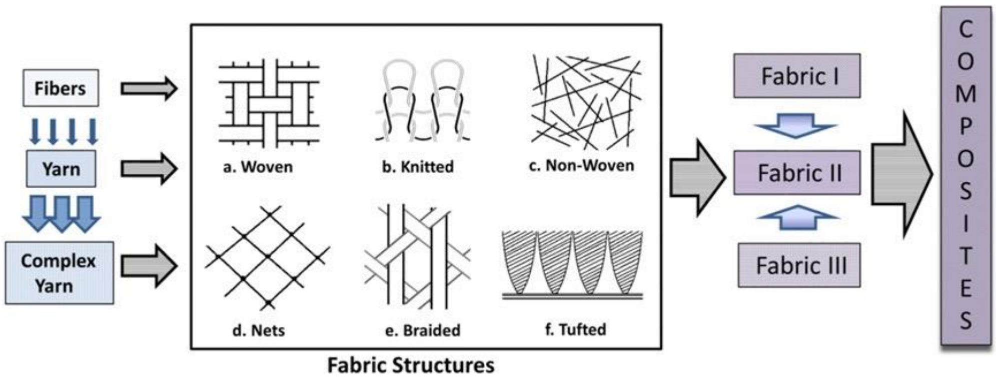

Figure 2.8 Fabric construction platform and hierarchy. Fabric structures: (a) woven, (b)knitted, (c)non-woven, (d)nets, (e)braided and (f) tufted (Castano & Flatau, 2014).

Conductive yarns or fibers can be hierarchically structured into fabrics by using a variety of techniques. Ordinary fabric is made by using different methods, which include weaving, knitting, non-weaving processes, netting, braiding and tufting, as shown in Figure 2.8 (Castano & Flatau, 2014). Among these techniques, weaving and knitting have been extensively studied as the methods of fabricating conductive fabrics, which will be highlighted and reviewed in the coming section.

2.2.2.2 Conductive weaving

Table 2.3 Typical conductive woven fabrics.

Prototype	Inventor/Institution	Description
	International Fashion Machines, Seattle, Washington, USA	**Running pad [Reprinted from (Seymour, 2008) with permission of Springer].** Double weave with black and white colors display multiple colors by combining printed conductive ink and electronic yarns. The program explores both regular and randomly generated patterns.
	Dept. of Electrical and Computer Engineering Virginia Tech	**Shape-sensing glove [Reprinted from (Martin et al., 2003) with permission of IEEE].** Sensors with novel fibers for communication networks are woven into glove materials, which can detect gestures.
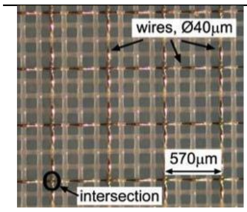	Electronics Department and the Wearable Computing Laboratory, ETH, Zürich	**PETEX hybrid fabric (Sefar Inc.)** Polyester yarns twisted with metal yarns coated with insulated materials to produce plain weave structure. Realizes customizable textile circuit by embedding copper wires.
	Dokuz Eylül University, Textile Engineering Department, İzmir, Turkey	**Read-temperature fabric [Reprinted from (Özdemir & Kılınç, 2015) with permission of De Gruyter]** Wearable and portable woven fabric reads human body temperature. 2/2 twill woven fabric with stainless steel core yarn adopted.

Conductive weaving has been primarily applied towards wearable and portable devices recently, which are woven fabrics produced by using electro-conductive yarns. Conductive woven fabric has planar and 3-dimensional configurations (Özdemir & Kılınç, 2015). Figure 2.9 shows a standard woven structure with copper yarns twisted with polyester yarns, which is developed by Electronics Department and the Wearable Computing Laboratory at ETH Zürich (Cottet et al., 2003). Table 2.3 lists several different types of conductive woven fabrics, which are found in the more recent research work.

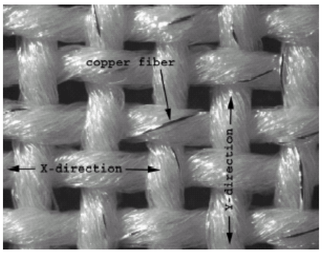

Figure 2.9 Woven fabric with copper yarns [Reprinted from (Cottet et al., 2003) with permission© 2003 IEEE].

Conductive weaving is an effective way to integrate conductive yarns into textile structures, and thus, endow ordinary textile apparel with electrical properties. The advantages and disadvantages are as follows.

a. Advantages include: (1) affording complex networks to be employed as elaborate electrical circuits that constitute of conducting and non-conducting parts; (2) flexible textiles properties which make intelligent products wearable and practical; and (3) providing the possibility of multi-layered structures for closer locating of electronic devices.

b. Disadvantages include: (1) lack of a complex and not uniform integration process to ensure comfort and a smooth handfeel of the resultant conductive fabrics, and (2) high dimensional stability reduces the stretchable sensitivity, which is beneficial for detection or monitoring purposes.

2.2.2.3 Conductive knitting

Table 2.4 Prototypes of conductive knitted fabrics.

Prototype	Inventor/Institution	Description
	Swedish School of Textiles, University College of Borås, Sweden	**Knitted Circuits and Irreversible Textile Patterns [Reprinted from (Seymour, 2008) with permission of Springer].** The interposed metal yarn affects the natural and synthetic materials in different ways; thus, dynamic patterns are created.
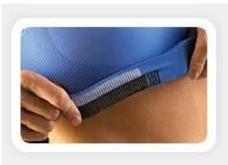	Textronics Inc, United States	**NuMetrex (Textronics Inc. , 2006)** Heart rate sensing bra with a knitted sensor can collect user's heart beat and transmit information to a monitoring watch.
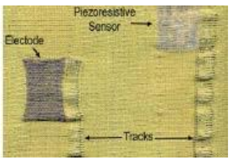	University of Pisa, Smartex srl, et al.	**WEALTHY [Reprinted from (Paradiso et al., 2005) with permission of IOS press]** Metal fibers, which comprise stainless steel fibers and viscose yarn, are knitted as fabric electrodes. The system can monitor respiration, heart rate, etc.
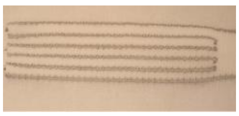	IEEE, Atalay et al.	**Weft-Knitted Strain Sensor [Reprinted from (Atalay et al., 2015) with permission of IEEE]** Interlock knitted belt made with silver plated polymeric yarn monitors respiratory rate from resistance variation in dynamic conditions.

Conductive knitting is one of the most significant and promising areas of research, which has been recently a popular topic of study by researchers. Conductive knitting is mainly the traditional knitting method that uses electronic yarn or fibers to meet the demand for innovative functional garments, for example, thermal and sensing knitwear garments (Atalay et al., 2015). It has the advantages of knitting, in terms of flexibility, lightness, softness, etc.

Knitted fabrics easily deform compared to woven or nonwoven fabrics but have much more stable dimensions. The elongation rate of knitted fabrics is much greater than that of woven or nonwoven fabrics, since their stretchability is usually more than 100% whereas the latter are normally 20-30%. Thus, knitted conductive fabric is more suitable for wearable electronic systems that are skin friendly or skin-connected (Zeng et al., 2014). Table 2.4 shows several types of knitted prototypes with conductive properties invented by the industry and academics.

Aside from weaving and knitting, embroidery, nonweaving processes and conductive printing are also good means of endowing traditional fabrics with electrical properties. Embroidery can be used on various textile fabrics and apparel products with a single layer or multiple layers due to the flexibility and freedom of the thread path (Clevertex, 2015). However, embroidered yarns need to have stronger tenacity, smoother finish and less elongation percentage than knitting yarns (Stoppa & Chiolerio, 2014). Nonwovens are usually created through fiber webs or filaments and are intensified by using different bonding techniques including mechanical, chemical or adhesive bonding, as well as thermal bonding and bonding of spunlaid webs (Russell, 2006). Modern digital printing technology can also apply conductive ink onto textiles, which is becoming increasingly popular.

Table 2.5 Knitted prototypes with conductive properties.

Prototype	Inventor/Institution	Description
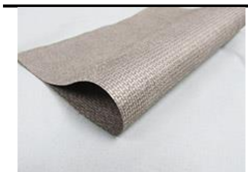	Swift Textile Metalizing	**Conductive Non-Woven Point Bonded Fabric (Swift Textile Metalizing, 2015)** Commercial products made from point-bonded non-woven nylon for breathable shielding applications.
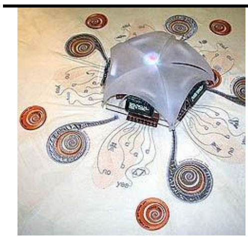	International Business Machines Corporation	**Embroidered tablecloth [Reprinted from (Post et al., 2000) with permission of ProQuest].** Tablecloth created with keypads and capacitive tag readers, which are made by using e-broidery to interact with each other and a computer.
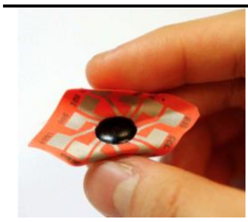	Electrical Engineering, KAIST	**Fabric resistor [Reprinted from (Kim et al., 2009) with permission of IEEE].** Resistor made by printing conductive ink onto fabric to form fashionable circuit board.

The methods for producing conductive textiles include weaving, knitting, nonwoven processes, embroidery, printing, etc. Different technologies provide unique characteristics, for example, woven and nonwoven conductive textiles are used when stable fabrics are required, and flexible and free circuits on textiles can be achieved by using embroidery and printing technology. Although the weaving technique is the most often used method in current wearable electronics, knitting has the advantages of stretchability, softness, fewer processing steps, good air permeability, low in cost, etc. Therefore, in the world of wearable electronics, the knitting technique is becoming increasingly popular and corresponding research work is being carried out on the properties of conductive knitted fabrics when embedded with wearable electronics.

2.2.3 Functions of conductive fabric

2.2.3.1 Introduction

Conductive textiles are used in many fields. In the last decade, research on the functions of conductive fabric has greatly increased. Usually, they focus on highly desirable e-textile components (substitution of traditional transistors, antennas, electric connecters and circuits), sensors and sensing networks or wearable energy harvesting and batteries (Zeng et al., 2014). Besides, with the application of electronic properties, the functions of conductive yarns such as electromagnetic shielding (Duran & Kadoğlu, 2015), antibacterial function (Yu et al., 2014), thermal properties (Tong & Li, 2015), have also been increasingly developed in recent years.

2.2.3.2 E-textile components

1. E- textile translator

Organic fibers allow for the realization of flexible e-textile translators (Lee & Subramanian, 2003). In previous research, organic fiber translators are categorized into wire electrochemical or field-effect transistors (Zeng et al., 2014). For example, Muller et al. (2011) explored electrochemical transistors with basket-weaving technology by incorporating conductive silk fibers as structural and active components (Figure

2.10(a)). Poly (3,4-ethylenedioxythiophene) (PEDOT) materials were adopted due to their high conductivity and water dispersibility. Figure 2.10(b) illustrates the work principles and images of electrochemical transistors (ECTs) with the incorporation of conjugated polyelectrolytes.

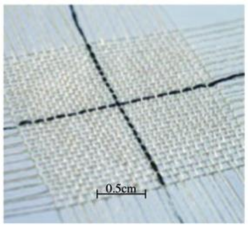

(a)

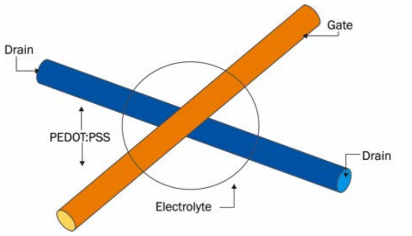

(b)

Figure 2.10(a) Electrochemical transistors with basket-weaving technology [Reprinted from (Muller et al., 2011) with permission from John Wiley and Sons], (b) Work principles for yarn-based transistor [Reproduced from (Stoppa & Chiolerio, 2014) with permission from Multidisciplinary Digital Publishing Institute].

2. Fabric-based antennas

Wearable antennas are necessary for developing flexible and autonomous systems, and make it possible for sensors integrated in apparel to communicate with a control unit or a monitoring system. Wearable antennas are required to be lightweight, thin, low in maintenance and cost, sturdy and easily inserted into radio frequency circuits. The principle for an excellent wearable antenna is that it should be positioned in a suitable area, made with correct and stable dimensions and thickness for a variety of different fabrics, and designed to be stable and robust to avoid destroying the electrical connectivity (Stoppa & Chiolerio, 2014). During the past few years, textile antennas have been widely researched in the realization of wearable products. For example, Osman et al. (2011) designed an ultra-wideband textile antenna with medical monitoring applications. The advantages are its size (compact), flexibility and washability compared to traditional extra antennas (Osman et al., 2011).

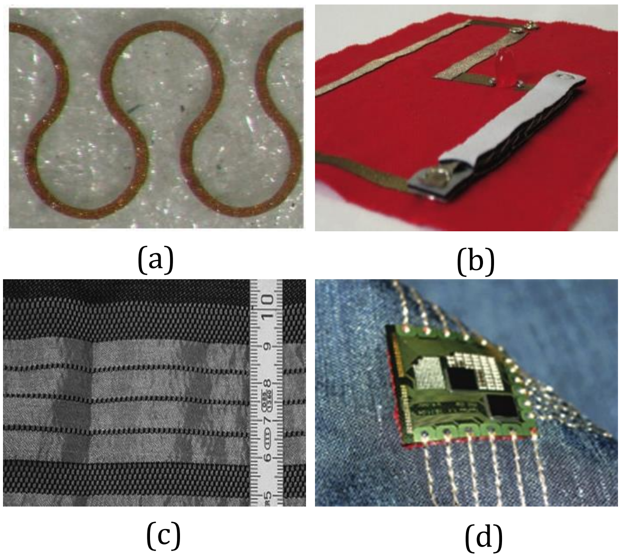

Figure 2.11 Prototypes of communication interconnections in smart textiles with the use of different technology (a) Horseshoe metal interconnectors [Reprinted from (Gonzalez et al., 2008) with permission of Elsevier], (b) Textile fabric as interconnection for a red LED sensory switch in Smart Textiles Salon 2009 in Ghent, Belgium,, (c) Weaving conductive yarns into textiles for communication interconnection by TITV Greiz e.V., (d) Embroidery interconnections by Fraunhofer IZM. [Reprinted from (Schwarz et al., 2010) with permission from Taylor & Francis Group].

3. Stretchable electric connections

Interconnections are necessary in the world of smart textiles to connect electronic components with each other. Interconnections are realized by using weaving, embroidering or knitting coupled with conductive yarns to create a variety of structures as shown in Figure 2.11 (Schwarz et al., 2010). Interconnections made with knitting are preferred due to their excellent stretchability, robustness and high recoverability.

4. Fabric circuitry

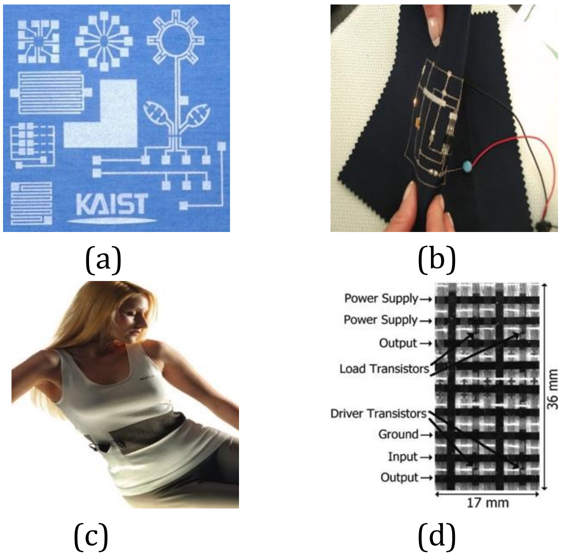

Figure 2.12 Common techniques to fabricate fabric circuits (a) silk printing on Fabric Circuit Board [Reprinted from (Kim et al., 2009) with permission of IEEE], (b) embroidery - TITV Greiz e.V., (c) knitting – WarmX [Reprinted from (Schwarz et al., 2010) with permission from Taylor & Francis Group], and (d) weaving with active component fibers [Reprinted from (Bonderover & Wagner, 2004) with permission of IEEE].

Fabric circuitry is a technique to fabricate circuits on fabric materials. The primary effect of integrating fabric circuitry is to obtain a large range of different applications in wearable electronics. Appropriate textile materials and techniques for the fabric structure are therefore important for implementation of fabric circuitry (Castano & Flatau, 2014). Common methods to carry out fabric circuitry are weaving, knitting, embroidery and conductive printing as shown in Figure 2.12.

2.2.3.3 Sensors and sensing networks

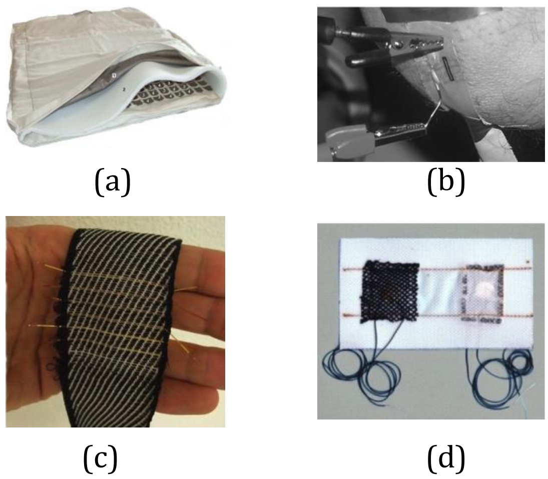

Figure 2.13 Different textile sensors and sensor networks (a) pressure sensor to determine sitting posture [Reprinted from (Meyer et al., 2010) with the permission of IEEE], (b) strain sensor for monitoring bending of knees [Reprinted from with permission of Taylor & Francis Group], (c) temperature sensitive sensor made with woven fabrics [Reprinted from (Calvert et al., 2008) with permission of IEEE], and (d) temperature sensitive sensors in textile arrangement [Reprinted from (Coyle et al., 2010) with permission of IEEE].

Fabric sensors are fabric-based materials, which can sense a diversity of physical signals (Castano & Flatau, 2014). Fabric sensors are the most successful and developed applications in terms of conductive textiles. They have been widely applied in commercial products of wearable sensors and devices. Fabric sensors can be divided into different categories in accordance with their functions, for example, strain, pressure, chemical, temperature and humidity sensors, etc. (Zeng et al., 2014).

Meyer et al. (2010) designed a pressure sensor (Figure 2.13(a)) to determine sitting postures. This textile sensor achieved the standards of commercial non-textile pressure sensing products (Meyer et al., 2010). Calvert et al. (2008) developed a strain sensor (Figure 2.13(b)) for monitoring the bending of knees. The inkjet printed conductive polymers and composites onto woven textiles produce the strain sensor (Calvert et al., 2008). Plastic foil cut into stripes was woven and fully integrated into fabric to fabricate the temperature sensitive sensors shown in Figure 2.13(c) (Kinkeldei et al., 2009). A BIOTEX EU-funded project developed sensor networks that detect physiological parameters, including sweat rate, electrocardiograms (ECGs), respiration, and blood oxygenation with chemical, humidity, conductivity, and pH sensors. Figure 2.13(d) shows humidity sensors arranged in a wearable textile to monitor the sweat rate (Coyle et al., 2010).

2.2.3.4 Wearable energy harvesting and batteries

Conductive textiles can generate electrical power through dynamic and thermal energy of users or the ambient environment (Castano & Flatau, 2014). A large number of works has been reported on wearable energy harvesting and batteries due to its feasibility and attractiveness in wearable electronics (Zeng et al., 2014).

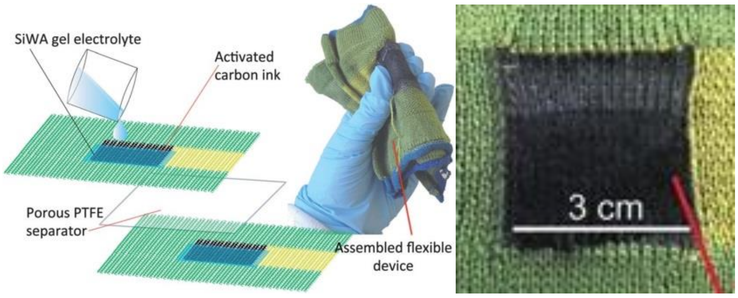

Figure 2.14 Knitted carbon fabric assembled in wearable supercapacitor [Reprinted from (Jost et al., 2013) with permission of Royal Society of Chemistry].

Relative mature work on conversion and storage of energy by fabric has been reported. For example, to make flexible and strong textile supercapacitor electrodes that would substitute traditional batteries and supercapacitors, knitted carbon fibers combined with screen-printing techniques as shown in Figure 2.14 have been used (Jost et al., 2013). Figure 2.14 illustrates how a knitted carbon fabric can be assembled with other electrochemical electrolytes to form an almost free-bent wearable device. As well, Hu et al. (2010) created flexible and stretchable conductive textiles by using a “dipping and drying” process to make supercapacitors with advanced areal capacitance, advanced specific energy and strong adhesion between carbon nanotubes and textile (Figure 2.15).

However, the challenge is the brittleness of the conductive polymer and developing economical and durable devices. Consequently, Liu et al. (2015) developed a fiber-based composite electrode with graphene–metallic materials which are flexible, tough and suitable for integration into wearable devices by using embroidery and weaving.

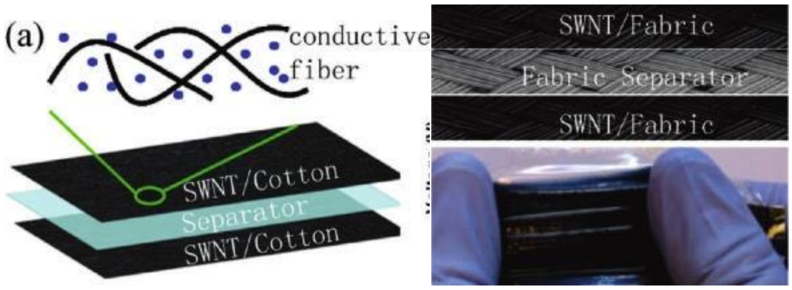

Figure 2.15 Supercapacitors made by using conductive carbon textiles [Reprinted from (Hu et al., 2010) with permission of American Chemical Society].

2.2.3.5 Other functions of conductive yarns with special properties

Aside from the applications developed by using the conductive properties of conductive textiles, conductive fabrics can also exhibit many other properties , such as, electromagnetic shielding effectiveness (EMSE) , heating of materials, static - discharge, antibacterial properties, etc.

EMSE is used to determine the degree of shielding against electromagnetic interference by using a fixed frequency. Textile products that contain conductive yarns have proven to reduce electromagnetic waves by researchers (Latifi & Payvandy, 2010). For example, a series of conductive knitted fabrics were developed on a flat knitting machine for the application of EMSE materials (Çeken et al., 2012a) Another example is where eight different types of knitted fabrics were designed and produced to meet the demand for flexibility, comfort and electrostatic shielding effectiveness (ŽUravliova et al., 2013).

Conductive yarns are more optimal for protective clothing for various work purposes to eliminate static electricity; thus, electrostatic discharge can be easily dissipated. Anti-electrostatic materials are mostly applied in automotive and home textiles, for example, blankets, insulated shelters, carpets, etc. (Xie & Tamaki, 2008).

Antibacterial textiles are also a long established application of conductive yarns. Since the 1990s, silver coated fibers have been used in medical applications, such as bandages and dressings to give them antimicrobial and anti-fungal functions. In recent studies, the effect of microbial inactivation in conductive yarns is considered (Latifi & Payvandy, 2010). For example, silver nanoparticles were placed onto cotton fibers by Xue et al. (2012) to fabricate textiles with high antibacterial properties against gram-negative bacteria.

2.2.4 Advantages of application of conductive yarns in wearable electronics

In this section, a review of electronic textiles will be provided in terms of the materials, fabrications and applications. The conductive yarns are discussed in terms of the materials and processes used. From the review, the advantages of applying conductive yarns into wearable electronics are concluded as follows.

1. The use of conductive yarns simplifies the fabrication process of wearable electronics. They allow the integration of electronic elements into garments with fabric manufacturing.
2. Conductive fabrics give the following properties to electronics: light in weight, softness, flexibility and comfort.

3. The invention of conductive textiles means that wearable electronics no longer have a heavy and cumbersome appearance and can be commercialized with good qualities.
4. Conductive yarns have many special functions aside from electroconductive performance, such as EMSE, heating, anti-static and anti-bacteria properties, etc. These greatly enlarge the different applications of wearable electronics.

2.3 Conductive paths in conductive knitted fabrics

2.3.1 Introduction

Conductive yarns or conductive fabrics can usually provide multiple fabric-based conductive paths (FCP) to interconnect different electric parts in wearable textiles. FCPs are mainly fabricated by embroidering conductive yarns onto fabric substrates, weaving and knitting conductive yarns along with non-conductive yarns, depositing or printing and chemical treating conductive textile substrates (Mattila, 2006). The conductive path is the conductive network of conductive fabrics (Li et al., 2014). Research works on conductive paths have become important in the development of integration technology in wearable electronics.

(a) (b) (c)

Figure 2.16 Three basic knitted elements: (a) knit, (b) float, and (c) tuck.

In weft knitting, knit, float and tuck are the three basic knitted elements, which constitute thousands of different knitted structures. As shown in Figure 2.16, the three basic knitted elements can provide different geometrical constructions in knitted fabrics (Spencer, 2001). It is evident that conductive yarns can therefore access different paths with the use of a different basic knitted element. Therefore, it is necessary to study the electrical properties from the view of geometrical models for these different knitted elements.

Various geometrical models have been proposed by, for example, (Perice, 1947), (Leaf & Glaskin, 1955), (Munden, 1959), (Postle, 1974) and (Semnani et al., 2003). In most of these geometrical models, the common assumption is that every loop has the same planar geometry with no out of plane behavior during deformation. The geometrical loop model has proven to be a very important tool for studying the properties of knitted fabrics in simulation and visualization; therefore, many analyses on knitted fabrics have been established on the basis of a diversity of geometrical models. For example, a 2-dimensional model is proposed to predict the kinetic actuation performance of knitted shape memory alloy actuators. Figure 2.17(a) illustrates the basic parameters in a knit unit cell of the model (Abel et al., 2012). This model can be employed to calculate the deformation of knitted loop under an external load.

Another example is one of the simplest topological representations as shown in Figure 2.17(b) (Chen, 2010), where B denotes the loop height, L denotes the loop width, A denotes the course distance, K denotes the distance between the feet and yB denotes the height at this distance. With these parameters, the coordinates of these points for the loops of the wale and course can be defined. It is found that the geometrical models are very helpful when modeling and predicting textile behavior. Therefore, appropriate models will be established in this study.

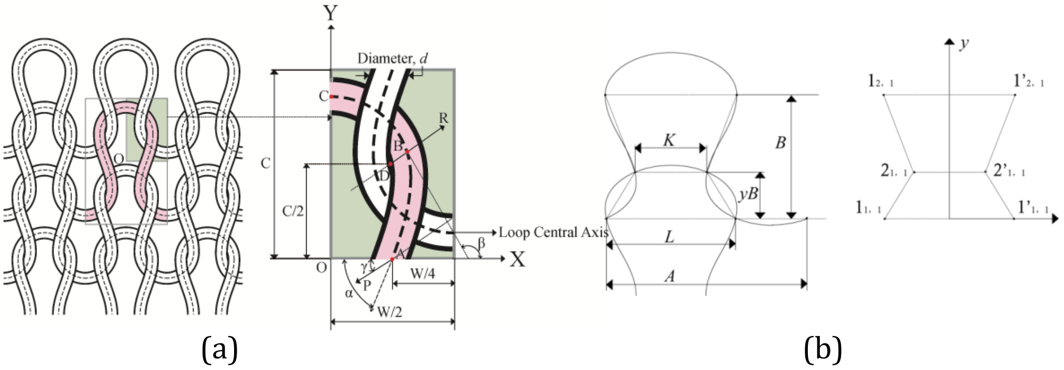

Figure 2.17 (a) Knit unit cell - one quarter of a knit loop (shown in red) and defined by geometric parameters (course height-C, wale width-W, loop length-L, wire diameter-d) and unknown characteristic angles (the angle of the connecting leg at A-α, the angle of the reaction force (R) between adjacent loops β and the angle of force P at A-γ). [Reprinted from (Abel et al., 2012) with permission of IOP Science], (b) Loop and anchor points for building 2D loop topology [Reprinted from (Chen, 2010) with permission of Elsevier].

2.3.2 Studies on electrical properties of conductive knitted structures

As known, knitted structures vary based on the different combinations used of the three basic knitted elements; thus, the electrical properties are influenced by the changes in the conductive paths in various knitted structures. Recently, more and more attention is given to the structural variations of knitted fabric for their significant influence on the electrical properties.

As early as 1989, Bryant improved the electrical charge dissipation properties by improving the knitted structure, which demonstrated that the electrical properties could be improved (Bryant, 1989). Rock and Sharma (2005) invented an EMI shielding fabric with the use of terry knitting. At least one of the two sides of the fabric had a fleece effect. The electrically conductive fibers were embedded between the technical face and back to form the stitch loop. The authors pointed out the shielding effect changes by varying the knitting parameters (Rock & Sharma, 2005). Plain jersey, weft-in-laid plain jersey, 1x1 rib, weft-in-laid 1x1 rib manufactured by using copper wire incorporated into cotton yarn were examined to compare their EMSE. It was concluded that the fabric construction could affect EMSE with a certain frequency range (Soyaslan et al., 2010). Qureshi et al. (2011) conducted an experiment to develop a knitted stretch sensor as a breathing rate indicator. In their investigation, four different kinds of conductive yarns were utilized to test four ordinary knitted structures: plain jersey, 1x1 rib, interlock and floating. The results showed that floating and interlock are the more practicable structures compared to the 1x1 rib as they provide a better elastic recovery (Qureshi et al., 2011). Liu et al. (2012) developed an incontinence monitoring system by using the moisture-sensitive property of conductive knitted fabric. In their research, they used seamless knitting, several common knitted structures–miss-knit stitch (2x1 rib effect), plated single jersey, miss-knit stitch (1x1 rib effect), and one-needle transfer stitch, which were distributed in the center or the sides of both the outer and inner layers in accordance with the comfort and aesthetic functional requirements (Liu et al., 2012). An experiment by Çeken et al. (2012) at the Dokuz Eylul University also investigated the EMSE of conductive knitted fabric. Stainless steel conductive yarn was embedded into the backside of plain knitted fabrics by using different knitting techniques of miss, tuck and plating. The study also verified that different loop forms influence the EMSE.

At the same time, the measurement of EMSE was realized in both the vertical and horizontal directions of the knitted fabric, which showed the different behaviors and EMSE values in two cases (Çeken et al., 2012b).

All of the prior research work revealed that conductive paths affect the conductive properties of knitted fabric. Therefore, it is necessary to systematically study the relationship between conductive paths and the properties of conductive knitted fabrics. The related literature is reviewed in the following.

2.3.3 Relationship between resistance and conductive knitted structures

In the numerous properties of conductive knitted fabric, the resistance value is one of the most important indexes that affect the performance of fabrics. Therefore, many researchers have put forth effort to study the resistance of conductive knitted fabrics. From previous related work, it is found that knitted constructions can drastically affect the properties of fabrics. In this section, related studies that provide calculations of the resistance value for conductive knitted fabrics will be discussed.

In an investigation carried at the University of Manchester conducted by Hamdani et al. (2013) to observe the thermo-mechanical behavior of knitted heating fabric, three different structures (plain jersey, rib and interlock) were analyzed based on the knitted loop geometry. However, the conductive knitted loops did not overlap each other, i.e. the knitted courses of the silver yarn were separated by courses of normal yarn, thus, there was only linear resistance but not contact resistance that contributed to the resistance of the whole conductive fabric (Hamdani et al., 2013). Li et al. (2009)

discussed the flexibility of knitted structures, in which eight different knitted structures – jersey, plating, 2x2 rib, full needle, tubular, full Milano double, intarsia, tubular and color striping stitches were studied to determine the influence of variations in the knitted structure in terms of the confining pressure of garments. At the same time, the resistance per unit length of eight different kinds of knitted fabrics was calculated, in which they concluded that the resistance per unit length of the knitted fabric is closely related to the structure (Li et al., 2009b). They also indicated that the differences could be even twice as much; however, the theoretical analysis is weak and the results are only taken from experimental data.

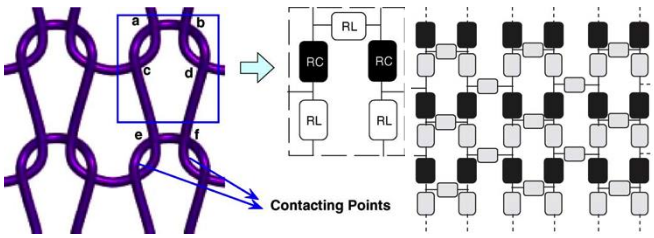

(a) (b)

Figure 2.18 (a) Circuit simulation of a unit loop, (b) Circuit network simulation of fabric [Reprinted from (Kun et al., 2009) with permission of IEEE].

Theoretical studies on the resistance of conductive knitted fabrics based on circuit networks were conducted as well. They concluded that length-related and contact resistances contribute to the whole resistance (Li et al., 2012; Shyr et al., 2011). Some of the research introduces a matrix expression to obtain the resistance value of single jersey and 1x1 rib on the basis of a loop model as shown in Figure 2.18 (Kun et al., 2009; Zhang et al., 2006). However, matrix expressions are overly complicated because they can only calculate for very small units, for example, a square area with 4 loops in the horizontal direction and 5 loops in the vertical direction (Soyaslan et al., 2010). A simple way was proposed in Holland (2013), but his theory on the resistance network lacks modeling at the micro level from the view of the knitted construction.

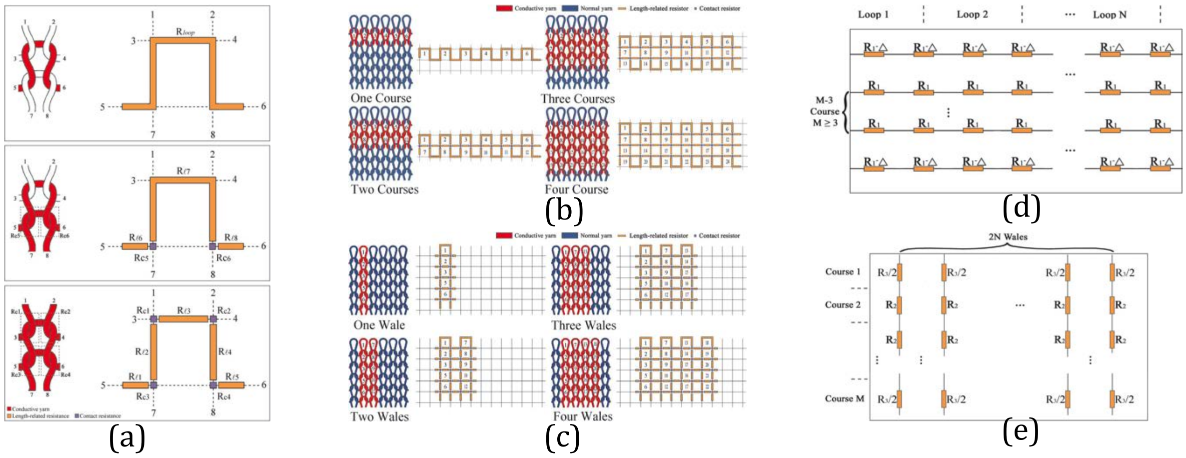

Figure 2.19 Resistive network for conductive knitted stitches: (a) resistance segments in a knitted loop, Original resistive network for (b) course direction, and (c) wale direction, Simplified equivalent resistive network for (d) course direction, and (e) wale direction [Reprinted from (Li et al., 2009a) with permission of SAGE publications].

To obtain a universal method to predict the resistance of conductive plain knitted fabrics, Li et al. (2009) developed an equivalent resistive network to predict the resistance of plain jersey fabric with different wale and course numbers based on loop units. In this resistive network for plain jersey structure, the contact resistance R_c is located on the crossover neighborhood with four length-related resistances. To simplify the network, an equivalent resistive network was proposed by dividing R_c into four quarters absorbed by the four neighboring length-related resistances. The conductive knitted stitches for different numbers of courses and wales could be modeled as a resistive network (Figure 2.19), which consists of a distributive length-related resistor and a contact resistor. The resistive network models for float stitches and woven fabrics have also been established in a similar way (Li et al., 2009a).

An analytic equation of the equivalent resistance for a conductive knitted fabric along the course and wale directions with M courses and N wales is given by Equations (2.1) and (2.2), respectively.

$$R_{eq} = \begin{cases} \mathrm{NR_{loop}} & \mathrm{M} = 1 \\ 2NR_{1\|3} & M = 2 \\ \dfrac{\mathrm{2NR_1\ (R_1 + R_{1\|3})}}{\mathrm{(M+1)\ R_1 + \ (M-3)\ R_{1\|3}}} & M \geq 3 \end{cases} \tag{2.1}$$

$$\mathrm{R_{eq}} = \frac{\mathrm{(M-2)R_2 + R_3}}{\mathrm{2N}} \tag{2.2}$$

where N denotes the loop number in the horizontal direction, M denotes the loop number in the vertical direction, and $\mathrm{R_{loop}}$, $\mathrm{R_{1\|3}}$ and $\mathrm{R_1}$ are the length-related resistances in a loop model (Pollini et al., 2009).

Besides the cases without outside forces, there are also some studies that focused on the resistance of conductive knitted fabrics under external tensions. For example, Li et al. (2012) derived an equation to calculate the resistance of conductive knitting fabric under unidirectional extension. The relationship among resistance, tensile force, fabric length and width was discussed (Li et al., 2012). They were able to calculate the length-related and contact resistances in a knitted fabric.

For length-related resistance, the electrical resistance R_l of a conductor can be calculated by using Equation (2.3) in accordance with Ohm's law as follows:

$$R_l = \rho \frac{L}{A} \tag{2.3}$$

where L (m) is the length of the conductor, A (m^2) is the cross sectional area of the conductor, and ρ (Ω/m) is the resistivity of the conductor.

For coated conductive yarns, the equation is modified and shown below:

$$R_l = \rho \frac{L}{A^k} \tag{2.4}$$

where k is a multiplicative exponent constant, dependent on the ratio between the sectional area of the conductive and non-conductive materials in the coated conductive yarn.

The value of the contact resistance R_c can be determined by using Equation (2.5).

$$R_c = \frac{\rho}{2}\sqrt{\frac{\pi H}{nP}} \tag{2.5}$$

where ρ is the electrical resistivity, H is the material hardness, n is the number of contact points, and P is the contact pressure between the conductive yarns .

Equation (2.6) is the proposed model that could be used to calculate the resistance of conductive knitting fabrics under unidirectional extension.

$$R(F, L, W) = \frac{1}{w}\left(\sum_{n=0}^{N}\sum_{m=0}^{N} C_{mn}\, F^n L^n + \frac{a_1}{P_0 + a_0 F}\right) + W \cdot b_0 \tag{2.6}$$

where, F is the tensile force, L is the fabric length, W is the total number of conductive yarn wales of a knitted fabric, b_0 is an offset coefficient to account for the terminal resistance between the connector and the fabric tested, P_0 is the initial contact pressure in natural relaxed state, a_0 is a constant coefficient, and C_{mn} is the coefficient that is to be determined in the experiment (Li, 2010).

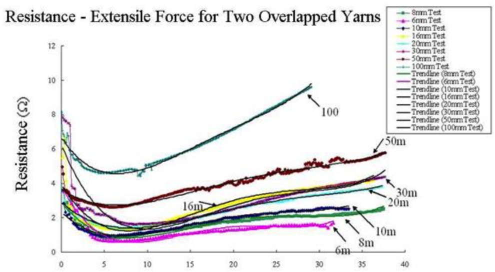

(a)

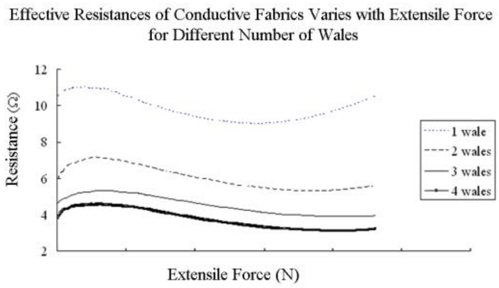

(b)

Figure 2.20 (a) Resistance vs extensile force of two overlapping yarns, (b) Variation of effective resistance in conductive fabric with extensile force. (Li, 2010)

The model indicates that the contact resistance R_c controls the overall resistance of the conductive knitted fabric at the beginning of the extension, whereas the length-related resistance controls the overall resistance when there is a large extensile force. Tests on the resistance of two overlapping yarns and fabrics with extensile force are shown in Figure 2.20.

However, the model was just based on experiments without theoretical basis. Therefore, Wang et al. (2014) reported that a hexagonal model (Figure 2.21(a)) could be used to predict the electromechanical properties of conductive knitted fabrics (Wang et al., 2014a; Wang et al., 2014b). Based on the relationship between the resistance and the load on the fabric under biaxial extension, the equivalent resistance of the fabric was obtained by solving circuit network equations. The contact resistance was ignored. The circuit diagram for a 2x1 unit loop is shown in Figure 2.21(b).

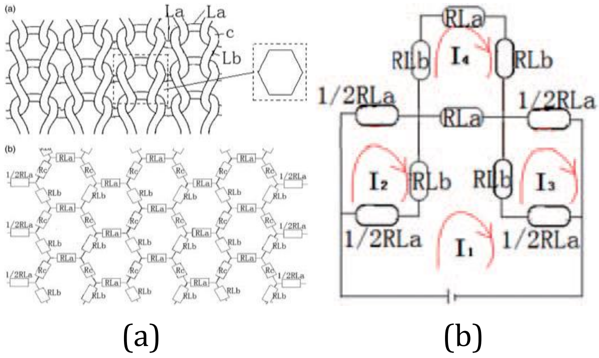

Figure 2.21 Hexagonal resistance model, (b) Resistance of 2x1 unit loop knitted fabric [Reprinted from (Wang et al., 2014a; Wang et al., 2014b) with permission of SAGE publications].

A similar method was adopted to predict the electro-mechanical properties of a knitting sensor, which focused on the relationship between the equivalent and length resistance variations of loop segments under strip biaxial elongation (Xie & Long, 2014). Figure 2.22 shows the loop shape in the initial state (a) and under strip biaxial elongation (b) and (c) in the course and wale directions, respectively.

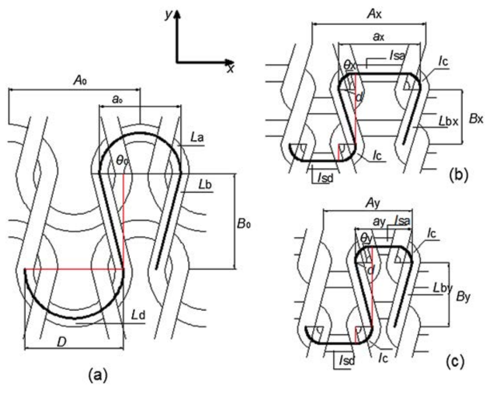

Figure 2.22(a) Loop structure models under relaxed state, (b) strip biaxial elongation in course direction, and (c) strip biaxial elongation in wale direction [Reprinted from (Xie & Long, 2014) with permission of Elsevier].

It can be found that the resistance can affect the properties of conductive knitted fabrics; therefore, to modify the properties of conductive knitted fabrics, changing their resistance can be taken into consideration. At the same time, previous work has revealed that the resistance value is greatly influenced by the knitted structure. At present, only the resistive model for the plain jersey structure is established and there is still no sufficient and systematic method to present the relationship between resistance value and different knitted structures. As a consequence, it is important to determine the means to academically describe this relationship.

2.3.4 Problem Statements

Several methods that are used to predict the resistance of plain knitted conductive fabrics have been discussed along with the proposed empirical or theoretical models. With the application of the electrical theory, the corresponding equations are formulated. It can be concluded that these models could theoretically simulate the properties of knitted stretch sensors and are verified through a series of experiments. However, to better apply them into smart textiles, there are some critical challenges that need to be addressed. First, structural variation is an important factor that affects the performance of conductive knitted fabrics. However, there is a lack of mathematical analysis of the different knitted structures including tuck and float stitches. Secondly, in the models discussed above, the processes are very complicated which is not convenient for predicting the resistance of conductive knitted fabrics. More simplified calculations will mean ease of the commercialization of conductive knitted fabrics.

2.4 Fabric for thermal knitwear

2.4.1 Introduction

Thermal comfort is an important criterion of wearable garments. Traditional thermal comfort is obtained through the thickness of materials or the micro mechanism of fibers (e.g. wool fibers) (Fayala et al., 2008; Özdil et al., 2007). The first heatable textile material was invented in 1930 (Kearsley, 1946). After that, scientific researchers developed various types of heated textile fabrics.

Modern conductive textile technology enables thermal comfort. One of the most popular applications of conductive knitted fabrics is in thermal garments, which are diffusely used to heat the human body, applied in physicotherapeutics, and assist with drug delivery. The thermal property of conductive textiles has extremely elicited the interest of researchers due to the good heat performance when establishing an electric circuit. It is very useful for producing lightweight, thermal and low-cost garments with a good appearance. The type of conductive yarn and knitted structure control the temperature of thermal garments through different resistance values.

A better understanding of the relationship between thermal properties and parameters of conductive knits (including material and knitted structures) can provide better performing and cost-effective products. A better comprehension of thermal properties of knits not only means improvement in thermal garment technology but also affects humans (Tong & Li, 2015). The following section gives a brief review of previous works on garments of thermal knitwear from work principles to products.

2.4.2 Products of conductive knitted fabrics

Table 2.6 Prototypes of thermal conductive knitted products.

Prototype	Institution/ Inventor	Description
	Nottingham Trent University	**Seamless heated glove** (School of Art & Design, 2014) Thermal glove can be washed and tumble-dried and available at a low cost for commercialization. Worn for outdoor sports. Also for treating Raynaud's disease.
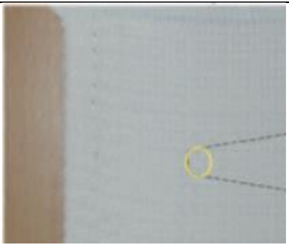	NED University of Engineering & Technology, University of Manchester and Nottingham Trent University	**Temperature Sensor Fabric (TSF) [Reprinted from (Husain et al., 2014) with permission of SAGE Publications]** An industrial scale TSF created on computerized flat knitting machine. Principle is that resistance of knitted fabric changes with temperature variations.
	Ghent University, Istanbul Technical University, RWTH Aachen University and Polytechnic University of Tiran.	**Thermal comfortable shirt Reprinted from** (De Mey et al., 2014) **with permission of Tekstil ve Konfeksiyon"].** Heatable shirt by inserting electroconductive yarns and using portable voltage supply. Used in medical therapy and for generating energy.
	Dokuz Eylul University	**A narrow warp knitted band Reprinted from** (Kayacan et al., 2009) **with permission of SAGE Publications].** Heated garment uses a narrow warp for knitted band with steel-based yarn for heating panel.

As far back as 1996, knitted fabric was used as an element for electric heating (Roell, 1996). Conductive knitted fabrics are becoming increasingly popular as electrically heated materials. Knitted fabrics can be produced by using different knitting machines including those that allow for weft and warp knitting as shown in Figure 2.23. Among the equipment, the heating element is best manufactured on computerized flat knitting machines. They have the ability to make almost any fabric shape and the elasticity property of knitted fabrics allow heating elements from knit fabric to overcome the issues of traditional planar elements.

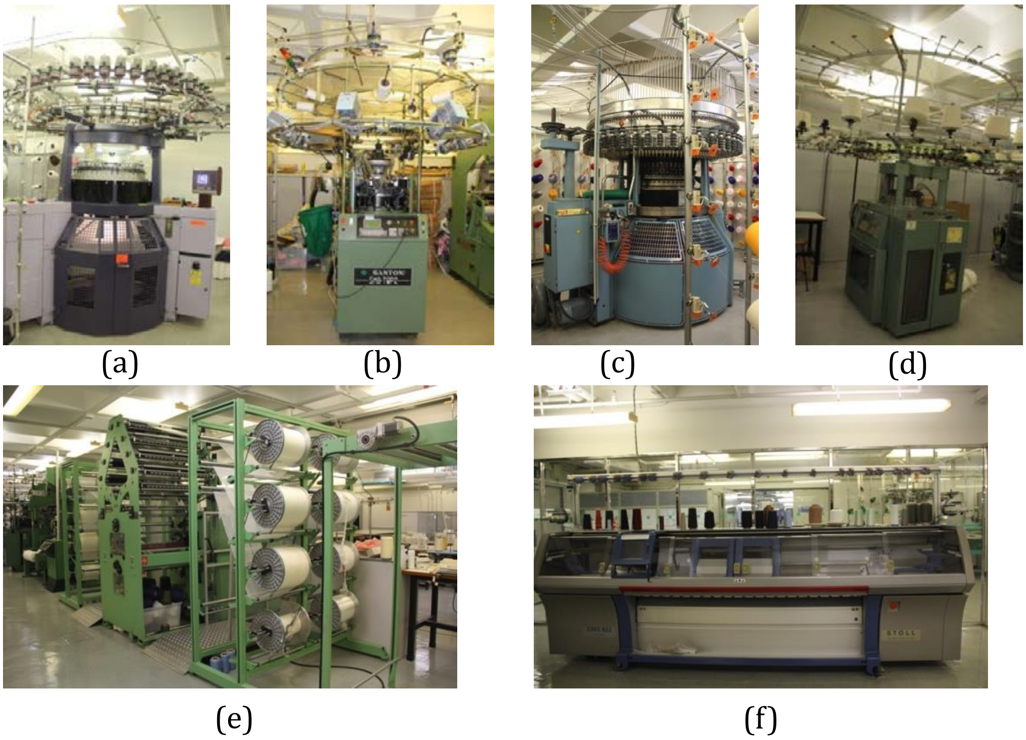

Figure 2.23 Different knitting machines: (a) TERROT double jacquard electronic circular knitting machine, (b) SANTONI seamless circular electronic knitting machine, (c) JUMBERCA computerized single jacquard knitting machine; (d) FUKUHARA rib circular knitting machine, (e) MULLER double electronic warp knitting machine, (f) STOLL computerized flat knitting machine.

In the past few years, the thermal performance of knitted fabric with conductive yarn has been extensively studied. Aside from electrical blankets, heatable textile materials have a great number of applications including for seat heaters in cars (Cherenack & van Pieterson, 2012), heated floors, ceiling and walls, heated mattresses and rugs, heating pads, heatable sportswear, motor bike, winter or cold storage clothing, heatable interior parts in the automotive industry (including door panels, seats, armrests and foot mats), heatable skis, bicycle and riding helmets as well as medical prostheses. Table 2.6 lists some of the prototypes of thermal conductive knitted products developed by various academics.

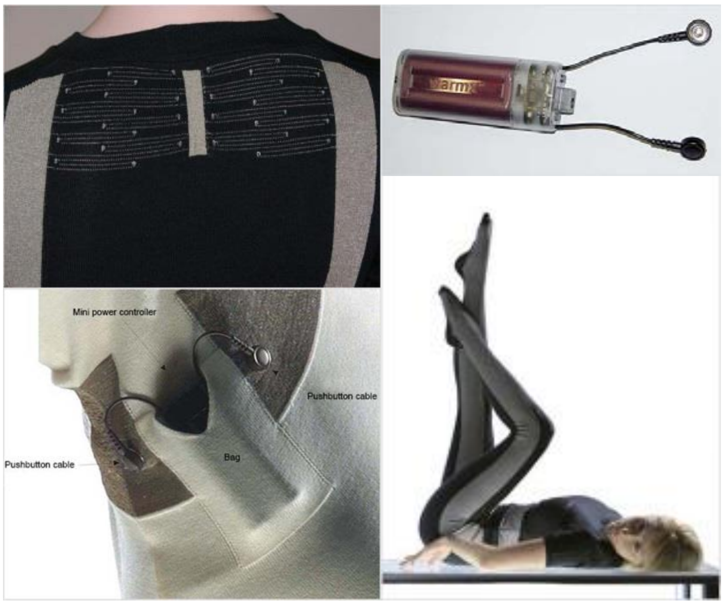

Figure 2.24 Heatable underwear by WarmX GmbH (Knitting industry, 2013).

Aside from academics, the industry also realizes the significant potential of heatable knitted fabrics. The most renowned product is the heatable underwear produced by WarmX GmbH & Co.KG as shown in Figure 2.24. It integrates silver-coated yarn into knitted fabrics by using flat knitting, so that the garment is thin, stretchable and wearable. The side pocket has a portable power supply, to heat the knitted area. The portable power supply can be easily removed for laundering. There are a good number of other applications, such as for winter sportswear and clothing for extreme weather (Knitting industry, 2013).

Table 2.7 Conductive knitted heatable products on market.

Product	Company	Description
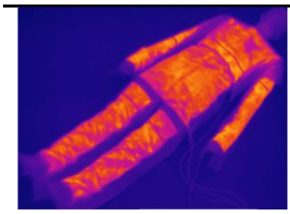	Rolf Mayer GmbH & Co.KG.	**Conductive heatable knitted fabric** (Cluster Technical Textiles Neckar-Alb, 2013) Conductive threads knitted into fabric by using a circular knitting machine with defined interval courses. The distance between two adjacent conductive courses influence the resistance of the fabric, thus, the heating effect can be influenced.
	HTS/Amptek Company (USA)	**The Duo-Tape® heater (HTS/Amptek, 2016)** The Duo-Tape® heater is a flexible electric heating element with high temperature which is cushioned and supported by knitted warp fabric. It can be applied on conductive surfaces as well as ceramic or glass.
	Berghaus Limited	**“Heatcell Mitt” (Jon, 2005)** An electrically-heated winter mitt in which conductive yarn is knitted into the actual fabric of the mitt to form the circuit for heating with a compact battery.

Besides the WarmX heatable underwear, there are also various conductive knitted heatable products as shown in Table 2.7. In addition, conductive knitted fabrics are available at the Sparkfun shop (Sparkfun, 2016), SHIELDEX (SILVERELL, 2016) and online venues with silver-plated nylon jersey.

2.4.3 Heating principle of conductive knitted fabrics

When an electrical current passes through a resistor (a conductive fabric), thermal energy is created and correspondingly the temperature of the resistor will rise. Equation (2.7) describes the relationship between thermal energy and resistance.

$$\frac{dQ_{in}}{dt} = \frac{U^2}{R} \qquad (2.7)$$

where Q_{in} is the amount of created thermal energy, U is the external voltage, R is the resistance of the resistors, and t is the heating time.

Thus, the thermal energy of a conductive fabric generated for a certain amount of time is closely related and inversely proportional to the resistance.

On the other hand, the heat will dissipate in the external environment to a certain degree depending on the thermal diffusivity and temperature increase ratio. Thus, the temperature of the conductive fabric continues to increase under an applied power until the generated and dissipated heat are equal. Equation 2.8 describes this process.

$$\frac{U^2}{R} = \alpha * (T - T_0) \qquad (2.8)$$

where α is the heating dissipation coefficients, T is the fabric temperature, and T_0 is the environment temperature.

From the equation, it is observed that the temperature of a conductive fabric is closely related to its resistance when the outer voltage is fixed (Ding et al., 2014).

In another study (Tong et al., 2014), the temperature of a heating fabric can be predicted by Equation 2.9.

$$T(U) = T_0 + \frac{U^2}{\alpha * R_0 - U * \beta * \sqrt{\alpha * R_0}} \tag{2.9}$$

β is a constant related to the performance of the conductive fabric. When the fabric density, knitted structure and material are known, then the β value will be confirmed.

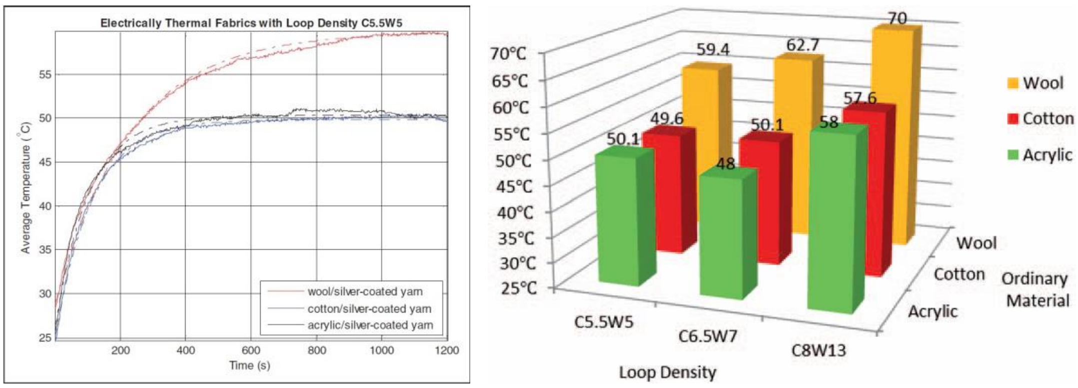

(a) (b)

Figure 2.25 (a) Measured and simulated temperatures of fabric made with different yarns, (b) Average temperature of nine fabrics after heating for 20 minutes [Reprinted from (Li et al., 2013) with permission of SAGE Publications].

The same input power is applied onto nine types of fabrics with three types of loop densities and made with three types of materials (Figure 2.25(a)). The temperature of the nine fabrics after 20 minutes of heating is presented in Figure 2.25(b). It is shown that, from a heat-retention perspective, wool is the best of the three materials (Ding et al., 2014; Li et al., 2013).

It is also found that the resistance of the conductive knitted fabric significantly decreases (maximum 30%) when the temperature increases. After taking the temperature effect on resistance into consideration, the quantitative relationship between the electrical resistance of a conductive knitted fabric and temperature is established.

$$\frac{R_1}{R_0} = 1 + \frac{1}{2}\beta^2(T - T_0) - \frac{1}{2}\sqrt{4\beta^2(T_s - T_0) + \beta^4(T_s - T_0)^2} \qquad (2.10)$$

Figure 2.26 Thermal knitwear with function of transcutaneous electrical nerve stimulation. (Li, 2010)

Based on this relationship, a theoretical model was proposed to control the temperature of conductive knitted fabrics with different courses and different wales. By using the theoretical model, temperature control on the thermal garment can be precisely achieved (Figure 2.26) (Li, 2010).

2.4.4 Problem Statements

Although traditional heatable materials have a variety of advantages, such as robustness, light in weight and are waterproof, there is still inconvenience and reduced esthetics when the devices are embedded into garments. For example, their inability to be extended and inflexibility mean that it is difficult to place them onto uneven surfaces, or else, the resistance wire will break. Their thickness cannot be reduced to form products in which thinness is necessary. They are normally non-washable and have side effects on humans. They are usually fabric-coated electrical products and not really textile products. Therefore, at present, a number of academics and the industry have put forth great efforts to develop heatable knitted fabrics, which could enhance the wearability of heatable materials.

It was found that knit construction which influences the resistive property of conductive knitted fabrics will thus affect the thermal performance. Although some products have been successfully commercialized, there is no information on how the knitted structure impacts the thermal ability and no systematic theoretical analysis based on the knitted loop models. Therefore, if a systematical study is carried out on the properties of knitted fabric that incorporate conductive yarn, the results can be directly applied onto thermal products which will greatly enhance the performance of flexible thermal products in aspects of convenience, comfort, hygiene, controllability and energy cost conservation.

2.5 Summary

Based on the literature review in this chapter, it is evident that wearable electronics have been increasingly examined in recent decades. By reviewing the previous work on wearable electronics, it is found that there is a need for a systematic study of the use of conductive yarn in knitting stitches, since the knit construction which influences the resistive property of conductive knitted fabric will thus affect the thermal performance. There are no explicit instructions on how knitted structures impact thermal ability from the knitted loop models.

When conductive yarns are knitted into fabrics, the performance will be influenced by the conductive paths, which are determined by the different constructions of the knitted structures. Previous studies on the properties of conductive knitted fabrics have mainly focused on the plain knit structure. However, tuck and float are also elements in knitted structures. The lack of relative research will impede the development of wearable electronics. Therefore, the present study will focus on the study of the impact of the knitted structure on the electrical properties of conductive knitted fabrics.

The applications of conductive knitted fabrics are numerous in electrical textiles and functional garments. Heatable knitted garments have elicited academic interest in the possibility of replacing traditional large and bulky thermal garments. From theoretical studies, it is found that adjusting the resistance values of conductive knitted fabrics can control the thermal performance. Therefore, it is necessary to systematically study the relationship between resistance and knitted structures to further the work on electric functional products. The present study will also provide a criterion for adjustment of the heating performance.

CHAPTER 3 METHODOLOGY

3.1 Introduction

In order to address the research gaps in the related literature, systematic research methodology was used in this thesis to investigate the impact of different knitted structures on the properties of conductive knitted fabric.

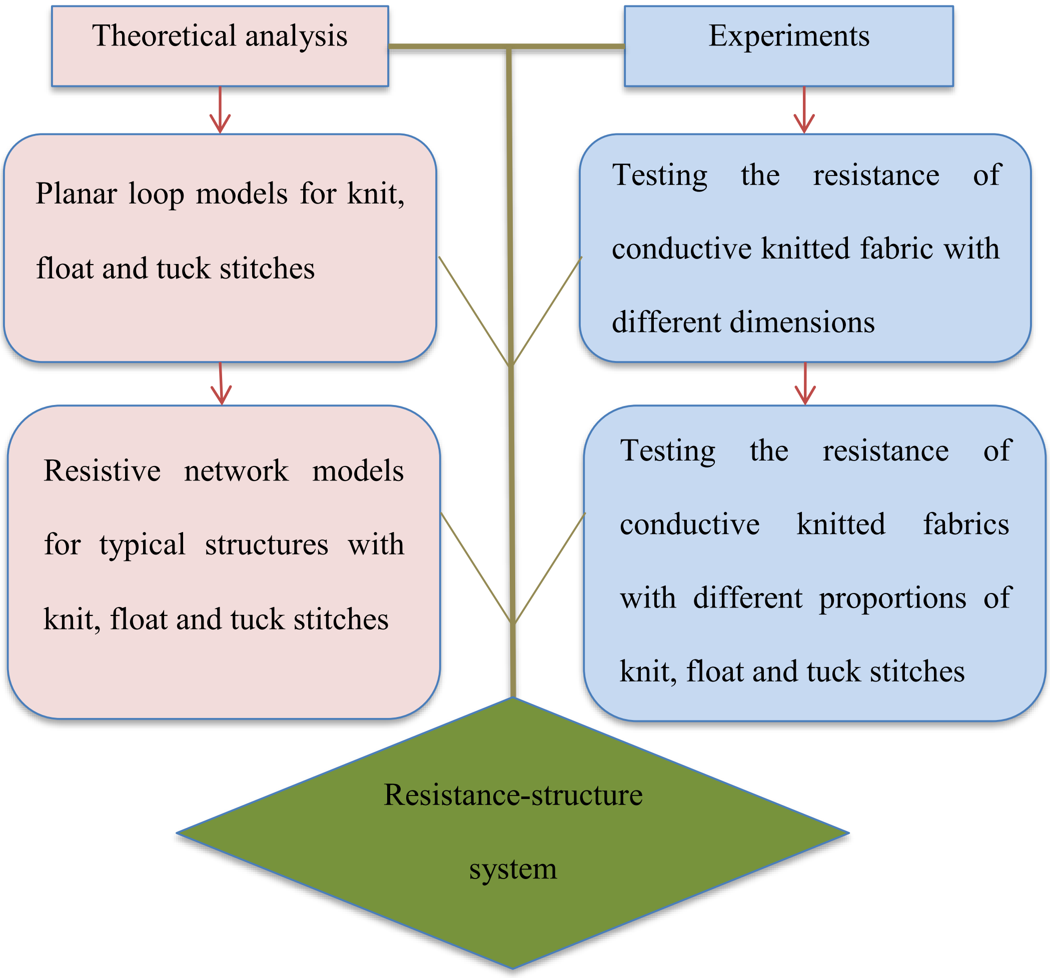

Figure 3.1 Flowchart of process to obtain resistance-structure system for conductive knitted fabrics.

3.2 Methdology

A resistance-structure system is developed in this study by using theoretical analysis and through experimentation as shown in Figure 3.1. The variables used will be discussed in detail in the following.

1) Materials

Table 3.1 Materials used.

<table>
<tr><th colspan="2">Purpose</th><th>Material</th><th>Specification</th></tr>
<tr><td rowspan="2">Conductive fabric</td><td>Conductive section</td><td>Nylon 66 coated with silver yarn</td><td>Yarn count: 47 Tex
Linear resistance: 1 Ω/cm</td></tr>
<tr><td>Non-conductive section</td><td>100% wool yarn</td><td>Yarn count: 30/2 Nm</td></tr>
<tr><td rowspan="5">Thermal garment</td><td rowspan="2">Resistance</td><td>Fine monofilament yarn coated with silver</td><td>Linear resistance: 68.6 Ω/cm</td></tr>
<tr><td>100% merino wool</td><td>Yarn count: 28/2 Nm</td></tr>
<tr><td>Electrode</td><td>Nylon 66 coated with silver yarn</td><td>Yarn count: 47 Tex
Linear resistance: 1 Ω/cm</td></tr>
<tr><td rowspan="2">Non-conductive part</td><td>100% acrylic</td><td>Yarn count: 20/2 Nm</td></tr>
<tr><td>100% wool yarn</td><td>Yarn count: 24/2 Nm</td></tr>
</table>

As mentioned earlier, silver coated yarns are the best choice to fabricate conductive knitted materials. In the present study, the materials used for different purposes, such as resistance, are listed in Table 3.1. When fabricating the thermal garment prototypes, resistance is obtained by knitting with low resistance yarns. Therefore, a fine monofilament yarn coated with silver was adopted. For ease of knitting on the knitting machine, a mixed yarn of 100% wool and Nylon 66 coated with silver is used to obtain the appropriate fiber thickness. To achieve aesthetically pleasing effects, 100% acrylic and 100% wool yarn are used for the three thermal garment prototypes.

2) Structures

In order to establish an overall resistance-structure system, the knitted structures incorporate knit, float and tuck stitches. Since this is a fundamental study, these typical structures are adopted. Table 3.2 lists the knitted structures in the present study.

Table 3.2 Knitted structures.

	Structure	Knitting notation
Knit	Single plain knit	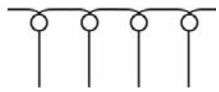
Float	1x n float	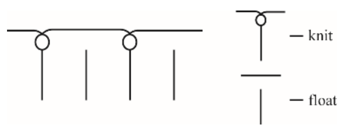
Tuck	Single pique	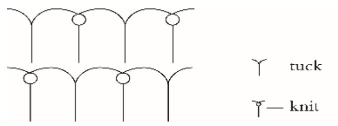

In Table 3.2, the notation of the float structure shows a 1 x 1 float structure. For those 1 x n float structures, the knitting notation is alternatively constituted of one knit stitch and n float stitches. To test the resistance of fabrics with different proportions of stitches, changes to the structures were made and details on the knitting notation are provided in Chapter 6.

3) Sample specifications

All of the swatch samples are uniform with dimensions of 100 wales by 100 courses. To investigate the different resistance values in accordance with the increase in number of courses and wales, the knitted samples, which have different structures, were made with different sized conductive areas, see Table 3.3. To investigate the different resistance values in accordance with the proportion of knit, float and tuck stitches, knitted samples with different structures were made with different proportions of these stitches, see Table 3.4.

Table 3.3 Specifications of conductive area of different structures.

Structure	Fixed 100 wales	Fixed 100 courses
Jersey	1,2,3,4 and 5 courses	10 wales
Float 1x1	1,2,3,4 and 5 courses	20 wales
Float 1x2	1,2,3,4 and 5 courses	30 wales
Float 1x3	1,2,3,4 and 5 courses	40 wales
Float 1x4	1,2,3,4 and 5 courses	50 wales
Float 1x5	1,2,3,4 and 5 courses	60 wales
	Fixed 70,80,90 and 100 wales	**Fixed 70,80,90 and 100 courses**
Single Pique	20,40,60,80 and 100 courses	10,20,30,40 and 50 wales

Table 3.4 Specification of proportions of different stitches.

Structure	Proportion					
Knit	100%					
Float	20%	30%	40%	50%	60%	70%
Tuck	20%	25%	30%	35%	40%	45%

4) Prototype parameters and devices

All of the samples and prototypes were fabricated and finished with constant parameters. The knitting process was conducted by using a flat knitting machine under a temperature of 20°C ±2°C and relative humidity of 65% ±5%. The parameters of the knitting machine are listed in Table 3.5. The NP value is a stitch cam setting on the STOLL knitting machine, which is related to controlling the tightness of the fabric. For the same knitted structure, a higher NP value means a less dense fabric. The WM value is a parameter of the takedown tension and a higher value means a greater tension.

Table 3.5 Knitting machine parameters.

Specimen		NP value	WM
Jersey/Float 1xn/Single Pique		12.0	3.0
Garment prototype	Tuck on both needle beds	Front/back beds:9.0	7.0
	Double jacquard	Front bed:11.0; back bed:10.5	7.0
	Single jacquard/ single knit	12.0	7.0

Table 3.6 Devices.

Device	Name	Company
Knitting machine	STOLL CMS822 Multi-gauge computerized flat knitting machine	H. Stoll GmbH & Co. KG
Multimeter	6 1/2 Digit 34401A Multimeter	Agilent Technologies, Palo Alto, CA
Power Supply	DAXIN digital control DC power supply	DongGuan DAXIN Electronic Co.,Ltd.
Far-infrared camera	FLIR E33 Infrared Thermal Imager	Peiport Scientific Limited

After removing the knitted samples from the knitting machine, they were conditioned at a temperature of 24°C and relative humidity of 65% ±5% for at least 24 hours. Then, all of the measurements to test the resistance were carried out in accordance with the AATCC Test Method 84 – Electrical Resistance of Yarn and AATCC Method 76 – Determination of Surface Electrical Resistivity of Fabrics. The devices employed in this study are listed in Table 3.6.

3.3 Summary

In this chapter, the methodology used to establish a resistance-structure system has been outlined. Conductive knitted samples and garments are made by using different variables, including materials, structures, and knitting parameters and devices. The resistance-structure system can thus be established by using both theoretical analysis and experiments. As well, conductive thermal garments are fabricated to evaluate the newly developed resistance-structure system.

CHAPTER 4 THE FUNDAMENTAL STUDY ON RESISTANCE PROPERTIES OF CONDUCTIVE KNITTED FLOAT STRUCTURES

4.1 Introduction

As reviewed in Chapter 2, the conductive paths could influence the resistance properties. Therefore, to study the resistance properties of conductive knitted fabrics with variable structures systematically, it is better to analysis the conductive paths in individual knitted constructions. In my research, the fundamental knitting elements-float and tuck are studied from a micro-viewpoint. In this chapter, the float element is considered.

Firstly, a geometrical model of float knitted stitch was established based on Munden's model. Semi-circles and sine curves together with a straight line constitute the geometrical model. The model considered the diameter of knitted yarns.

Based on the established model, resistive network of float knitted structures can be developed by treating different parts as linear resistances and contact resistances. By applying electrical theory, the equivalent resistive network was implemented and the resistance value can be derived for the conductive float knitted structures.

To verify the resistive network model, corresponding knitted fabrics with float structures are produced by computerized flat knitting machines. A digital Multimeter conducts the testing of resistance values. The experimental results illustrate the resistive network model is an efficient methodology to predict the resistance values of conductive float knitted fabrics.

4.2 The establishment of geometrical model for float stitch

4.2.1 The formation of geometrical model of knit-element

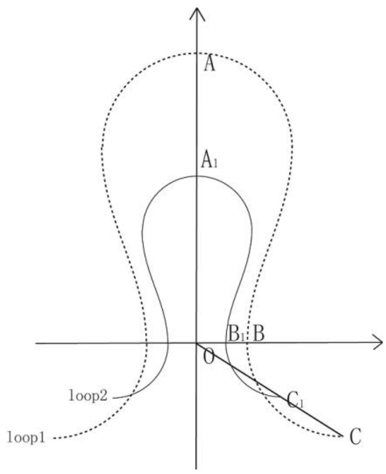

Figure 4.1 The two similar loops in Munden's geometric model.

By now, multiplex mathematical models including purely geometric models, mechanical models, kinematic/dynamic models and thermodynamic models, etc. have been proposed based on planar and spatial spaces. In my research, the knitted fabric is assumed to be in a fully relaxed state, i.e., a configuration of minimum energy. Therefore, to describe such a knitted fabric, a 2 dimensional model is appropriate. Among the previous geometrical model, Munden's model is one of the classical models illustrating the relationship between the length of yarn and the dimension of the knitted loop in plain knitted fabrics. Munden's model assumes the shape of a knitted loop to be fixed and every part of a knitted loop is always proportional to its loop length. As illustrated in Figure 4.1, loop 2 is proportional to loop 1 and the expression $\frac{\mathrm{OA}}{\mathrm{OA_1}} = \frac{\mathrm{OB}}{\mathrm{OB_1}} =$

$\frac{OC}{OC_1} = p$ is established, where p is the ratio of the lengths of loops 1 and 2.

The loop geometric model is set up on the base of Munden's model. It considers the loop pillar as a sine function and the loop arc as a semi-circular function. Figure 4.2(a) is the established geometric model with a negligible diameter of yarn in a Cartesian coordinate system, and Figure 4.2(b) displays the case with consideration of diameter. The midpoint of the shortest straight line drawn within the loop (line $E'E$) is defined as the original point. Figure 4(c) demonstrates the interlocked status of two contact loops in wale direction. It is observed that the sinker loop of the upper loop (in pink color) connects to the needle loop of the lower loop (in green color) tightly. Therefore, it is proposed that the distance of $D_1{}'E'$ is equal to yarn's diameter in the geometrical model. For curve $\widehat{E'D'}$, x can be recognized as a sine function in which the amplitude is half of $D_1{}'E'$, the period is twice of OO_1 and phase shift is $(-O_1D' + \frac{D_1'E'}{2}, \frac{OO_1}{2})$. For easy expression, definitions are given out as shown in Figure 4(c): **r** is the radius of semi-circle $\widehat{D'AD}$, **d** is the diameter of the knitted yarn, **w** is the distance between two adjacent stitches in the wales direction (wale distance), and **h** is the distance between two adjacent stitches in the course direction (courses distance). Therefore, Equation (4.1) is established to describe the relational expression between x and y for curve $E'D'$.

$$-x = \frac{d}{2} sin\left(\frac{\pi}{h} y - \frac{h}{2}\right) - [-\left(r - \frac{d}{2}\right) \tag{4.1}$$

In the same way, the relational expression between x and y for curve $\widehat{DE}$ can be obtained as well.

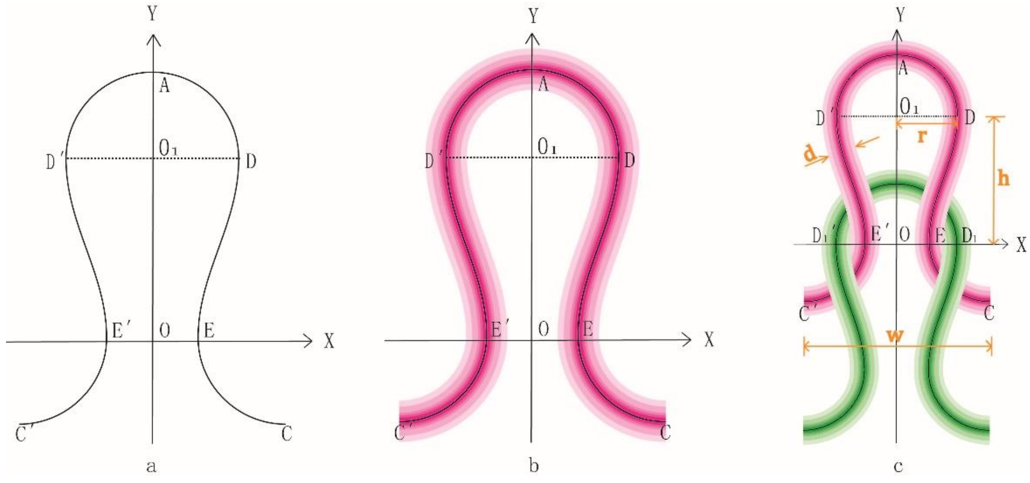

Figure 4.2 The geometric model displayed by the axis line of the yarn, (b) The geometric model displayed by yarn with a certain diameter, (c) Two adjacent loops in wales direction interlocked with each other.

As a result, the loop can be expressed with the following set of Equations:

$$y_1 = -\sqrt{r^2 - (x_1 + \frac{w}{2})^2} \qquad (-\frac{w}{2} \le x_1 \le -\frac{w}{2} + r) \qquad \widehat{C'E'} \tag{4.2}$$

$$y_2 = \frac{h}{\pi}\sin^{-1}\left[1 - \frac{2(x_2+r)}{d}\right] + \frac{h}{2} \quad (-r \le x_2 \le -\frac{w}{2} + r) \qquad \widehat{D'E'} \tag{4.3}$$

$$y_3 = \sqrt{r^2 - {x_3}^2} + h \qquad (-r \le x_3 \le r) \qquad \widehat{D'AD} \tag{4.4}$$

$$y_4 = \frac{h}{\pi}\sin^{-1}\left[1 - \frac{2(r-x_4)}{d}\right] + \frac{h}{2} \quad (\frac{w}{2} - r \le x_4 \le r) \qquad \widehat{DE} \tag{4.5}$$

$$y_5 = -\sqrt{r^2 - (x_5 - \frac{w}{2})^2} \qquad (\frac{w}{2} - r \le x_5 \le \frac{w}{2}) \qquad \widehat{EC} \tag{4.6}$$

Where x_1 and y_1 are x and y coordinate values for curve C′E′ in the Cartesian coordinate system; and in the same way, x_2 and y_2 are for curve E′D′, x_3 and y_3 are for curve D′AD, x_4 and y_4 are for curve DE, x_5 and y_5 are for curve EC, respectively.

4.2.2 The formation of geometrical model for a float element

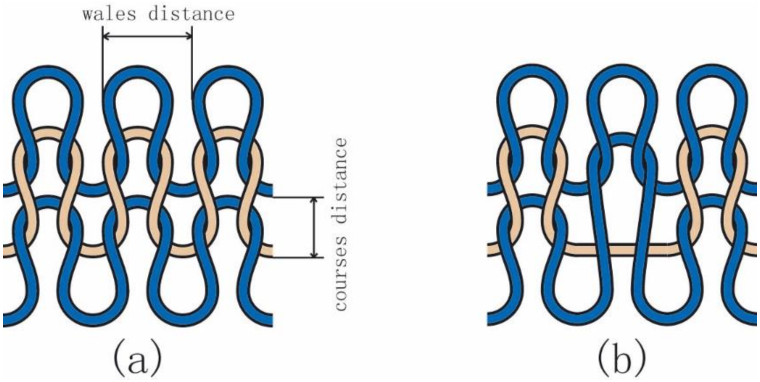

Figure 4.3 (a) the effect formed by knit stitch; (b) the effect formed by float stitch.

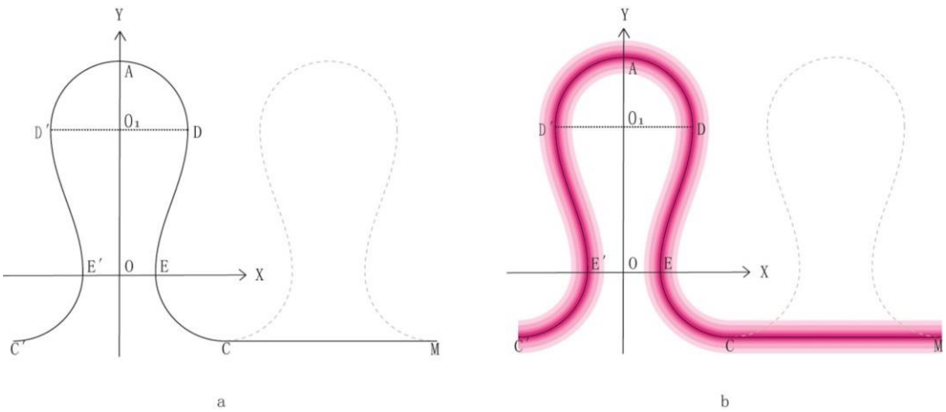

Figure 4.4 (a) The geometric model of a float knitted structure displayed by the axis line of the yarn; (b) The geometric model of a float knitted structure displayed by yarn with a certain diameter.

Figure 4.3 illustrates the effects of knit (a) and float (b) in a weft knitted structure, respectively. From the picture, the float stitch can be recognized as an extension line from the adjacent stitch. The length of the extension line is the wales distance of a knitted fabric. Therefore, the model fit for float stitches can be established by treating the float yarn as an extended line paralleled to the x-axis, as shown in Figure 4.4. In Figure 4.4, the straight-line CM parallels to the x-axis represents the float yarn in a float knitted structure, and the length of CM is n times the wales distance (n is the number of float stitches in a repeatable pattern area determined by the structure of the knitted fabric required). Therefore, CM can be expressed by Equation (4.7) as below:

$$y_6 = -r \qquad \left(\frac{w}{2} \le x_6 \le \left(\frac{1}{2} + n\right) w\right) \tag{4.7}$$

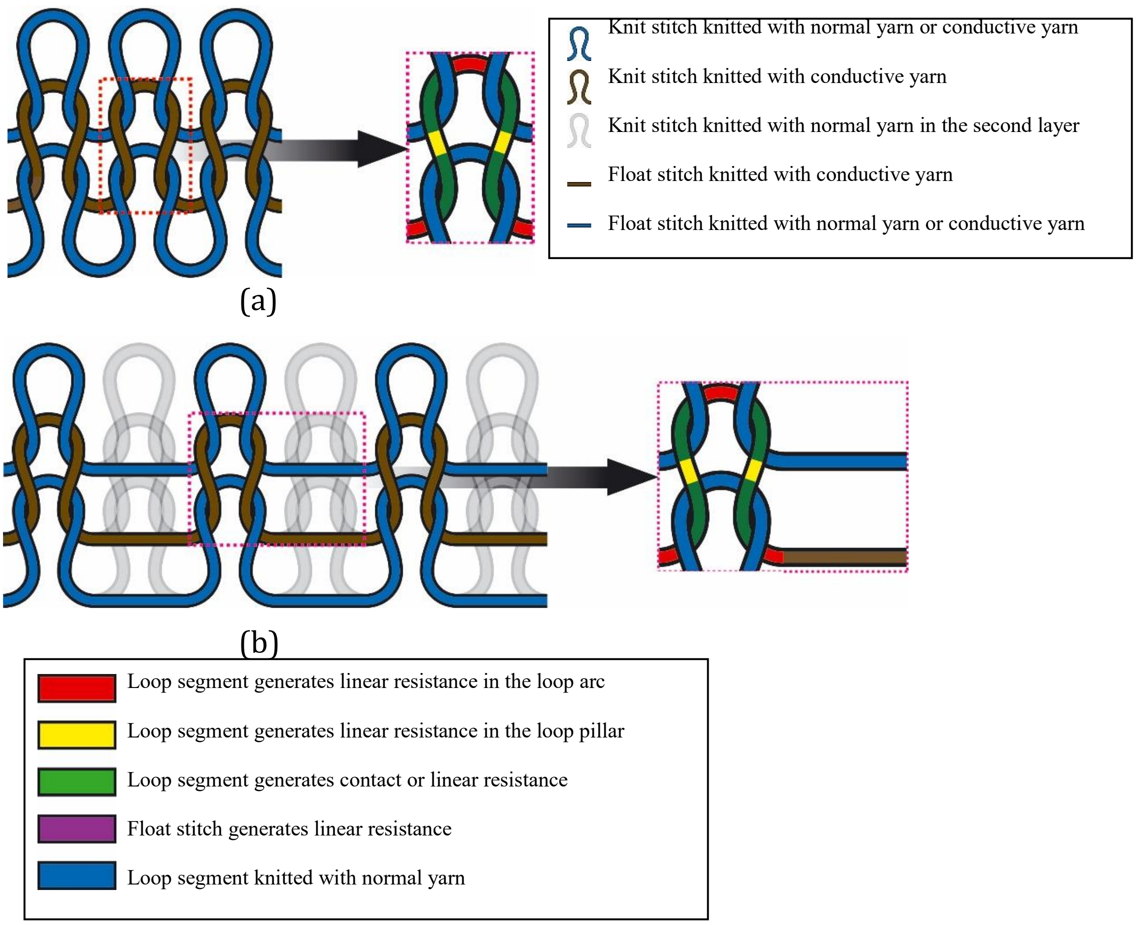

Figure 4.5 (a) Interlocked state of a pattern unit in a plain knitted structure. Interlocked state of a pattern unit in a float knitted structure.

4.3 The establish of resistive network model for float knitted structures

4.3.1 Resistive representation for different parts of geometrical float models

Table 4.1 Resistive network of a single pattern unit in four different situations.

Option	Upper loop	Lower loop	Resistive work
1)	Without conductive yarn	Without conductive yarn	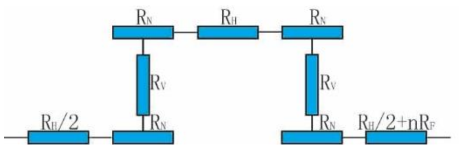
2)	Without conductive yarn	With conductive yarn	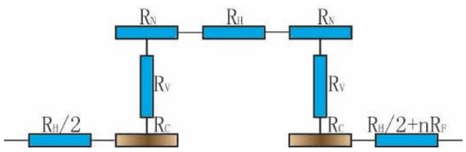
3)	With conductive yarn	Without conductive yarn	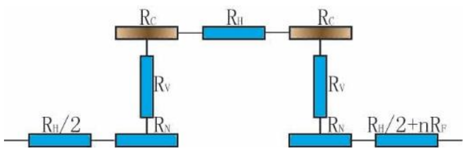
4)	With conductive yarn	With conductive yarn	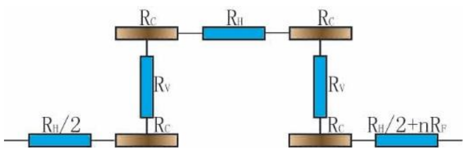

When a single loop is interlocked with two neighbouring loops in the upper and lower sides, it can be divided into nine sections, which are distinguished by different colours in Figure 4.5(a). In these nine sections, the red parts are the linear resistances in the loop arc; the yellow parts are the linear resistances in the loop pillar; and the green parts can generate contact resistance when the upper or lower loop is knitted with conductive yarn, otherwise, the green parts represent the linear resistance in the loop pillar and arc.

In float knitted structures, in addition to the nine different sections in plain knitted structures, there is a linear resistance of the float stitches coloured purple in Figure 4.5(b). It has been observed that a plain knitted structure and a float knitted structure can be distinguished based on whether a float yarn exists in the knitted fabric. For a 1xn float structure, when n=0, the knitted structure is simply the plain knitted structure. Therefore, the model of a plain knitted structure is included in the model of a float knitted structure in the case where n=0, as shown below. As a consequence, the four different resistive networks associated with a single pattern unit are listed in Table 4.1.

In Table 4.1, the grey colour icon represents contact resistance and the blue colour icon represents linear resistance. R_H is the linear resistance in the loop arc between two loop pillars (red parts); R_V is the linear resistance in the loop pillar (yellow parts); R_C is the contact resistance between the linear resistance R_H and R_V (green parts); R_N is the linear resistance between the linear resistance R_H and R_V (green parts); and R_F is the linear resistance generated by one float stitch.

4.3.2 Resistive network model for different distributions of conductive yarn in float knitted fabrics

4.3.2.1 In case of distribution in the course direction

Conductive yarn may be knitted into fabric with different arrangements of wales and courses. For convenience, k is defined as the number of conductive knitting wales, and j is defined as the number of conductive knitting courses. In the sections below, the resistive network of the conductive knitted stitches for different numbers of courses is introduced. Figure 4.6 illustrates the interlocked status of the conductive yarns with normal yarns when it was knitted into fabric with one to five courses. It was observed that: 1) there was no contact resistance if only one course was knitted with conductive yarn; 2) contact resistance needed to be considered when two successive courses were knitted with conductive yarns, as there was an area in overlap between two adjacent loops in the wale direction; and 3) in case of three or more conductive knitted courses, a repeatable area was derived between the first and last course. The corresponding resistive network may be drawn as follows:

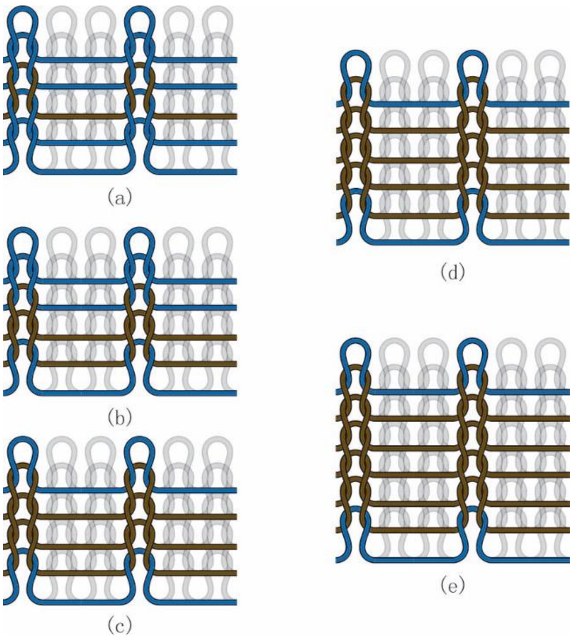

Figure 4.6 (a) Conductive yarn knits in one course, (b) Conductive yarn knits in two courses, (c) Conductive yarn knits in three courses, (d) Conductive yarn knits in four courses, (e) Conductive yarn knits five courses.

1) Conductive yarn knits one course (j=1).

In Figure 4.7, the resistive network outlined by the green square and shaded in grey is a repeating area in the course direction. N is the number of integrated repeating pattern units, i.e., N is the integer part of the result of the wales number (k) divided by n+1, and m can be calculated by Equation (4.8):

$$m = k - N(n+1) - 1 \tag{4.8}$$

Therefore, the resistive value can be represented by Equation (4.9):

$$R = (N+1)(R_H + 2R_V + 4R_N) + (k - N - 1)R_F \tag{4.9}$$

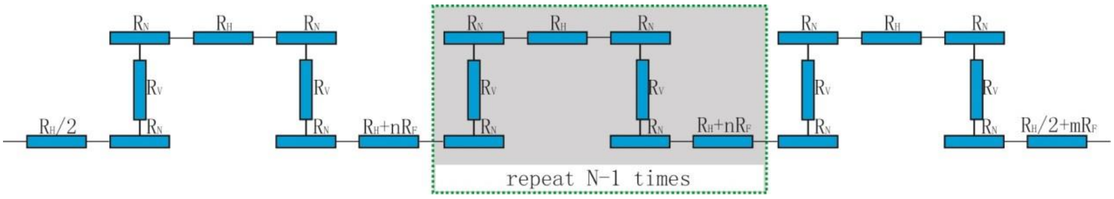

Figure 4.7 The resistive network for one course of conductive yarn knits.

2) Conductive yarn knits two continuous courses (j=2).

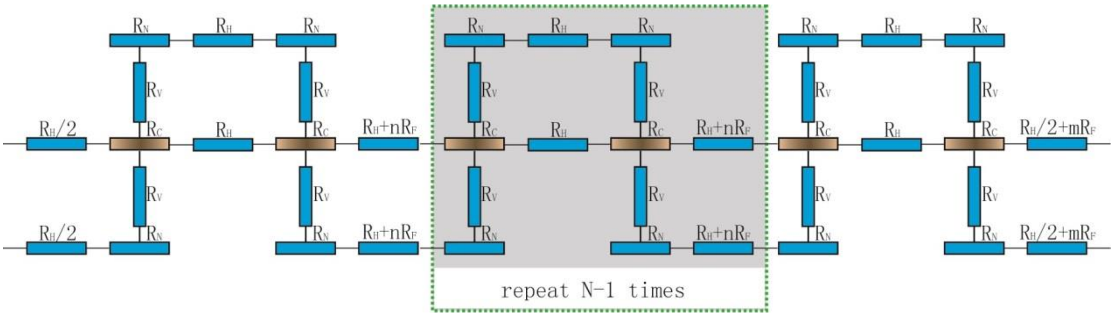

Figure 4.8 The resistive network when j=2.

Figure 4.8 shows the resistive network of conductive knitted stitches with two courses, and the area enclosed by the green square and shaded in grey is the repeating area in the horizontal direction, as in Figure 4.7. As discussed above, four linear resistances in four directions connect the contact resistance RC generated in this case. The computation of the resistance for the resistive network in this case is quite complex. For simplicity, Li et al. treated the contact resistance R_C in the crossover of the two wires as four quarters of the R_C distributed to its four neighbouring branches, as shown in Figure 4.9.

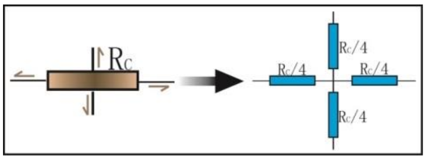

Figure 4.9 The treatment of crossover resistance.

By inserting the modified R_C into the original resistive network, the resistive network is converted to a network without crossover resistances (Figure 4.10).

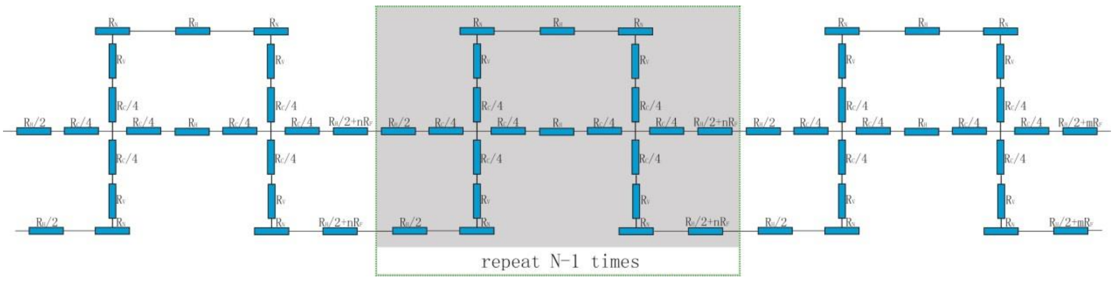

Figure 4.10 The converted resistance network when j=2.

In Figure 4.10, edge resistances may be ignored because they have little influence on the entire network when N is sufficiently large; thus, the resistive network can be further simplified.

To calculate the above resistive network, four combined resistance symbols, namely R_1,

R_2, R_3, and R_4, are used throughout this paper, and they can be calculated by Equations (4.10) to (4.13). R_1 and R_3 may be regarded as the inner resistances generated in the knit and float stitches, respectively. R_2 and R_4 may be regarded as the outer resistances, which are located in the boundary parts of the knit and float stitches and are connected to the non-conductive area, respectively.

$$R_1 = R_H + 0.5R_C \tag{4.10}$$

$$R_2 = R_H + 2R_N + 2R_V + 0.5R_C \tag{4.11}$$

$$R_3 = R_H + nR_F + 0.5R_C \tag{4.12}$$

$$R_4 = 2R_V + 2R_N + R_H + nR_F + 0.5R_C \tag{4.13}$$

By importing R_1, R_2, R_3, and R_4, the resistive network in Figure 4.10 becomes simplified, as shown in Figure 4.11.

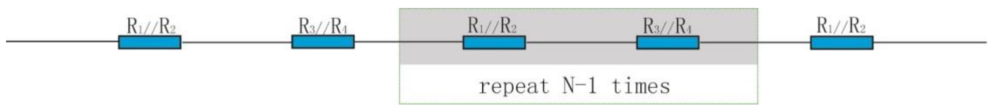

Figure 4.11 The simplified resistive network when j=2.

According to Figure 4.11, the resistance of the overall resistive network can be expressed by Equation (4.14).

$$R = \frac{R_1R_2}{R_1+R_2}(N+1) + \frac{R_3R_4}{R_3+R_4}N \tag{4.14}$$

3) Conductive yarn knits three or more courses (j≥3).

If the conductive yarn knits three or more courses, the repeating area will not only appear in the horizontal but also in the vertical direction. The original resistive network is shown in Figure 4.12.

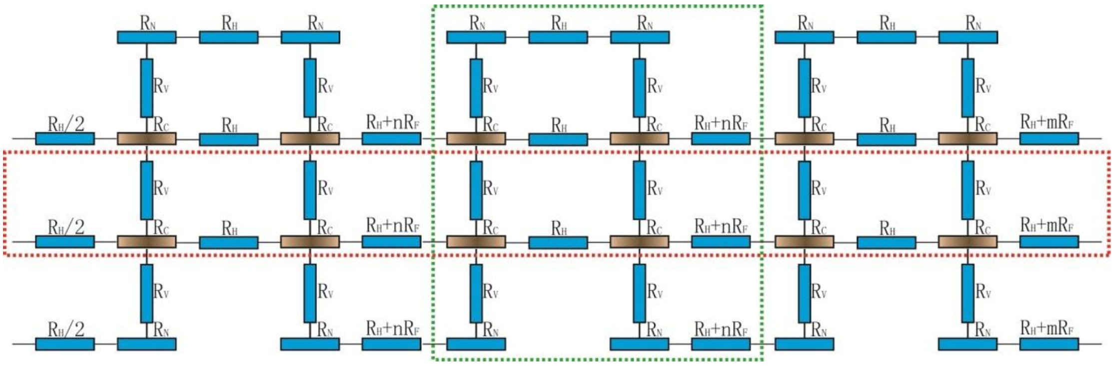

Figure 4.12 The original resistive network when j≥3.

In Figure 4.12, the resistive network enclosed by the green dashed square is the repeated area in the horizontal direction; the resistive network in red is the repeated area in the vertical direction. Similarly, the crossover contact resistance R_C is transferred to its four neighbouring lines, and the original resistive network is transformed to a resistive network without crossover resistances, as shown in Figure 4.13.

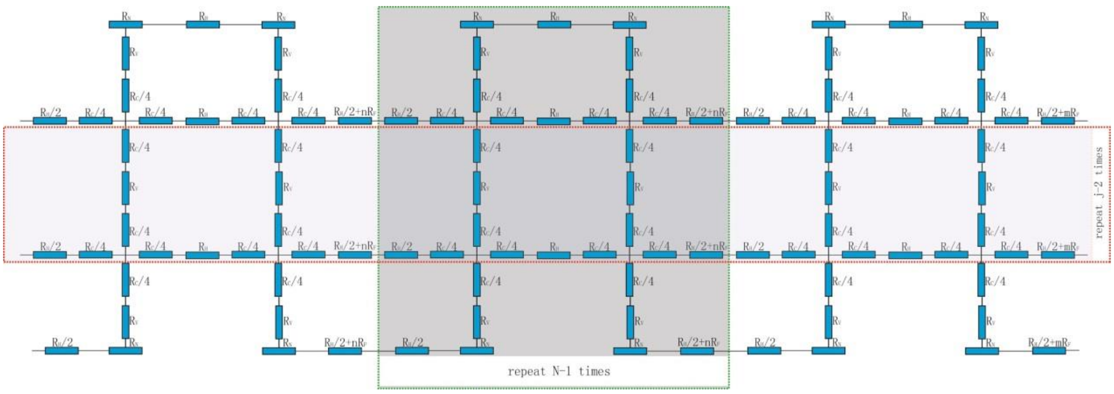

Figure 4.13 The resistive network after transformation when j≥3.

The resistances at the edge are ignored again; then, by importing Equations (4.10) to

(4.13) and using Equation (4.15) to replace the resistors in the vertical direction between the blocks, the resistive network is simplified as shown in Figure 4.14.

$$R_5 = R_V + 0.5R_C \tag{4.15}$$

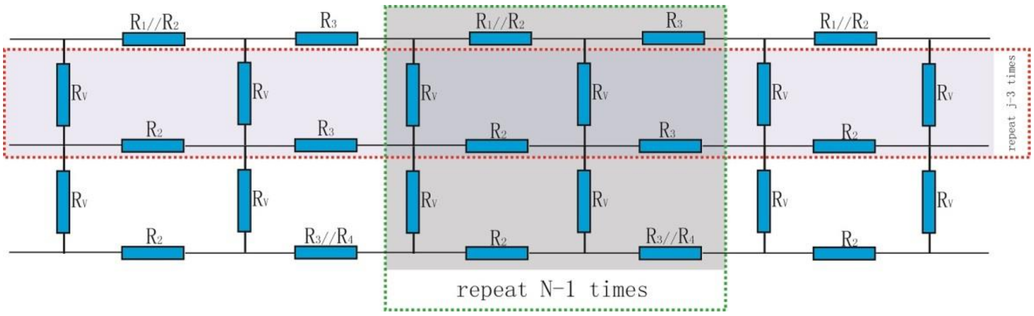

Figure 4.14 The simplified resistive network when j≥3.

Computation of the resulting resistive network based on the resistances that exist in both the horizontal and vertical routes is now too complicated to solve. However, the resistances in the vertical routes may be eliminated by applying the signal flow graph theory. Two additional resistances, Δ_1 and Δ_2, are added to the resistive network to give the overall resistive network an equipotential distribution in the horizontal direction. Therefore, no current will flow in the vertical direction. The expressions of Δ_1 and Δ_2 are represented by Equations (4.16) and (4.17).

$$\Delta_1 = \frac{{R_2}^2 R_3}{(R_1+R_2)(R_2+R_3)} \tag{4.16}$$

$$\Delta_2 = \frac{{R_2}^2 R_3}{(R_3+R_4)(R_2+R_3)} \tag{4.17}$$

According to the signal flow graph theory the simplified resistive network is updated as shown in Figure 4.15.

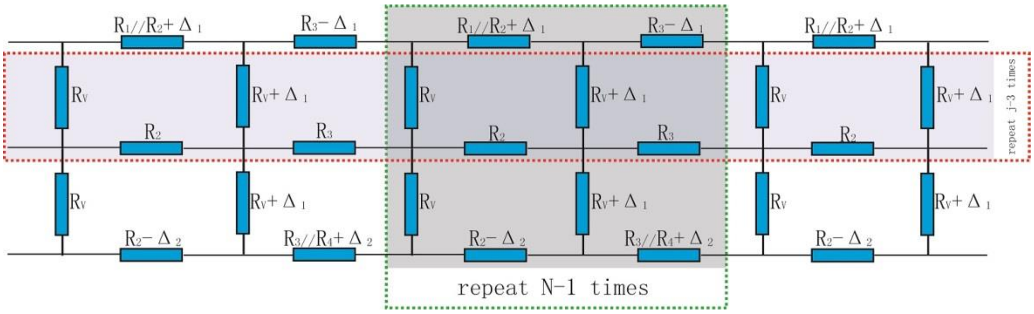

Figure 4.15 The equivalent resistance when j≥3 after applying signal flow graph theory.

In principle, Δ_1 and Δ_2 are introduced to make the ratio of the two adjacent resistances in the horizontal route equal. In Figure 4.15, because

$$\frac{R_1\|R_2+\Delta_1}{R_3-\Delta_1}=\frac{R_2}{R_3}=\frac{R_2-\Delta_2}{R_3\|R_4+\Delta_2},$$

resistors in the vertical routes can be eliminated as illustrated in Figure 4.16.

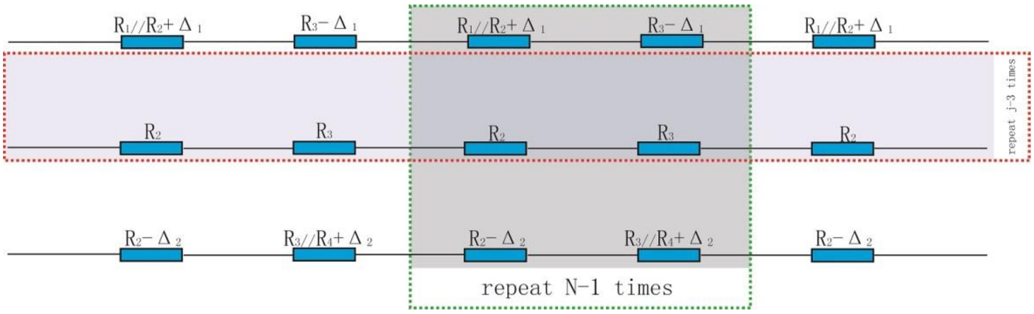

Figure 4.16 The equivalent resistance when j≥3 after eliminating the vertical resistors.

After eliminating the vertical resistors, the resistance of the float knitted structure 1xn with a certain wales number k and course number j is computable and expressed by Equation group (4.18). The resistors R_1, R_2, R_3, and R_4 are again defined by the previous Equations (4.10) to (4.13), and the resistors R_A, R_B, and R_C are defined by Equations

(4.19) to (4.21).

$$R=\begin{cases}(N+1)(R_H+2R_V+4R_N)+(100-N-1)R_F & j=1\\ \frac{R_1R_2}{R_1+R_2}(N+1)+\frac{R_3R_4}{R_3+R_4}N & j=2\\ \frac{1}{\frac{1}{R_A}+\frac{(j-3)}{R_B}+\frac{1}{R_C}} & j\geq 3\end{cases} \tag{4.18}$$

$$R_A=N(R_1\|R_2+R_3)R_1\|R_2 \tag{4.19}$$

$$R_B=N(R_2+R_3)+R_2 \tag{4.20}$$

$$R_C=N(R_3\|R_4+R_2)+R_2 \tag{4.21}$$

4.3.2.2 In case of distribution in the wale direction

Float knitted structures can be designed as illustrated in Figure 4.17, and the pattern unit (framed by green square) repeats partially in the horizontal direction and extends from top to bottom in fabrics to form a vertical distribution. Because there is no additional contact resistance accompanying the increase in the repeated unit in the course direction, Figure 4.12 can be utilised to illustrate the corresponding resistive network when k≥1. If the edge resistances are ignored again, the resistive network is equivalent to that shown in Figure 4.18.

Similarly, because the knitted structure is mainly symmetric, the resistors in the vertical direction in the network form an equipotential state in every block. There is negligible current flow through the horizontal resistors R_2 and R_3. As a consequence, the horizontal resistors R_2 and R_3 may be eliminated, which will simplify the resistive network (Figure 4.19), and the corresponding resistance of the simplified resistance can be expressed by Equation (4.22).

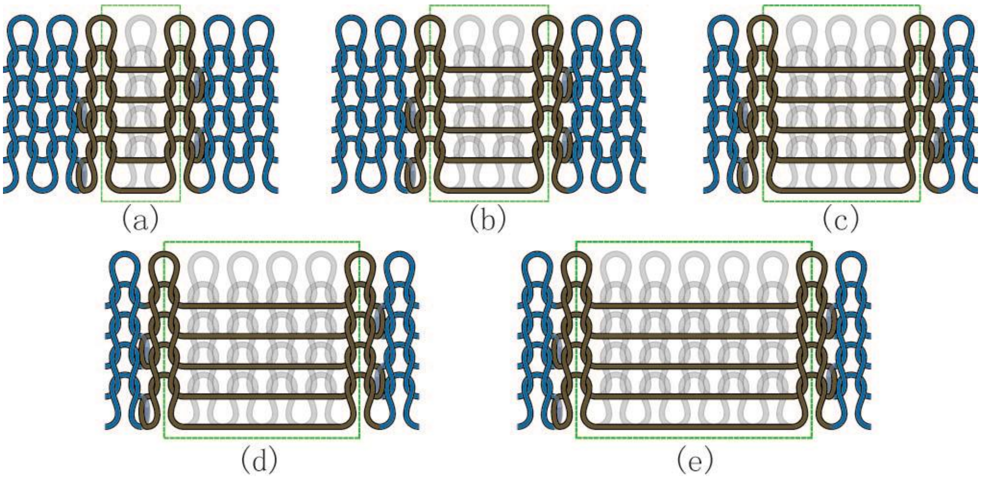

Figure 4.17 Float knitted stitches distributed in the horizontal direction of a knitted fabric: (a) 1x1 float, (b) 1x2 float, (c) 1x3 float, (d) 1x4 float, and (5) 1x5 float.

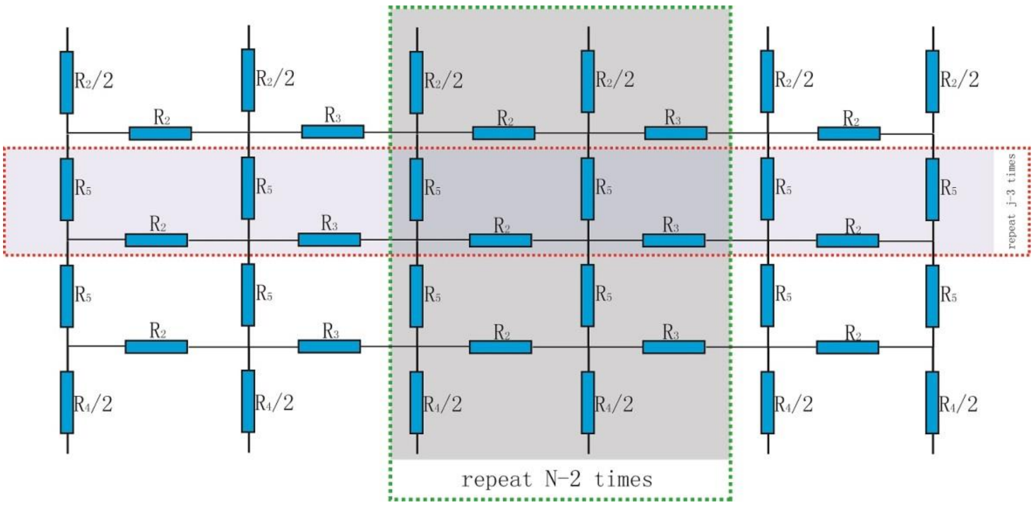

Figure 4.18 The equivalent resistive network for a wales distribution when k≥1.

$$R = \frac{\frac{R_2}{2}+(j-2)R_5+\frac{R_4}{2}}{N} \qquad (k \geq 1) \tag{4.22}$$

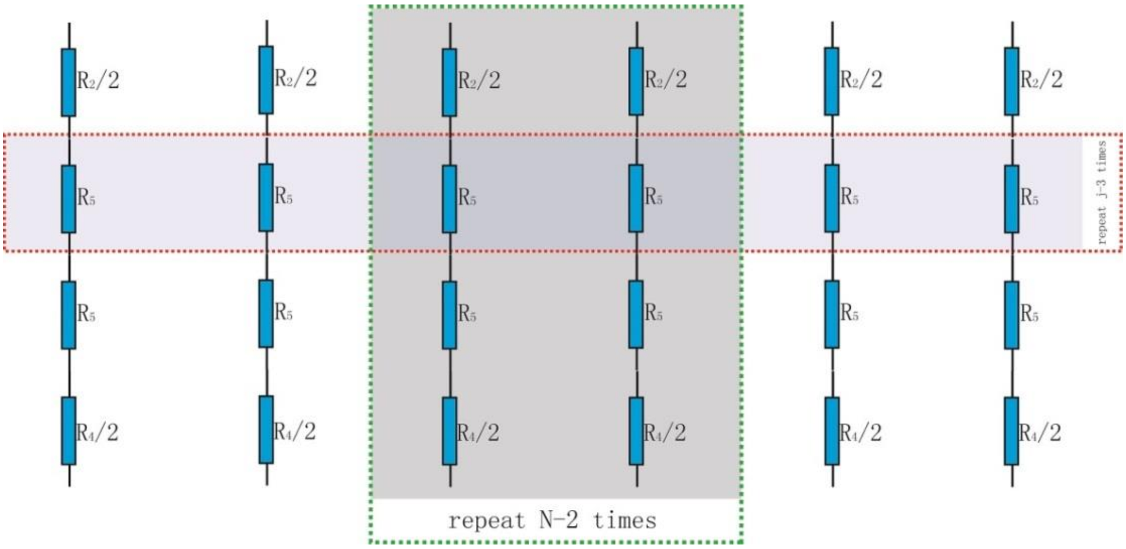

Figure 4.19 The final resistive network for the wales distribution when k≥1.

In summary, so far, the resistive network model for conductive float knitted structures with different wale and course numbers have been set up and corresponding equations to calculate their resistance value have been derived.

4.4 The experimental verification for the resistive network model for conductive float knitted structures

4.4.1 Experimental design

4.4.1.1 Materials and structure

All samples were manufactured on an E7.2 STOLL CMS 822 computerised flat knitting machine because of the powerful pattern design functionality. In the experiments, the samples were knitted with normal and conductive yarn. The materials used include conductive yarn and background yarn, which are shown in the Table 4.2.

Table 4.2 The materials used for conductive part and background part.

Materials	Yarn count	Ingredient	Conductivity
Conductive yarn	47 Tex	Nylon 66 coated with silver	1 Ω/cm
Background yarn	30/2 Nm	100% merino wool	/

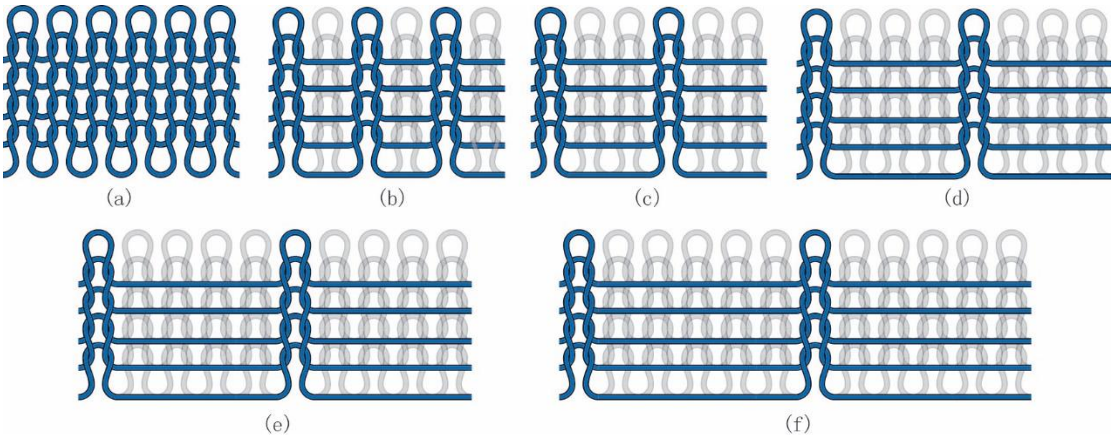

Figure 4.20 (a) Jersey, (b) 1x1 float, (c) 1x2 float, (d) 1x3 float, (e) 1x4 float, (f) 1x5 float.

The float structure was developed by one knitted loop stitch followed by a fixed number of float stitches. For example, the 1xn float structure was composed of one integrated knit loop stitch and n float stitches. Additionally, the jersey structure was knitted to serve as the reference. Six different structures, including the jersey and 1x1, 1x2, 1x3, 1x4, and 1x5 floats, were manufactured as shown in Figure 4.20. The loop diagram of 1x1 float is shown in the Figure 4.21(a), and Figure 4.21(b) shows the fabric image captured with a light microscope (LEICA M165 C).

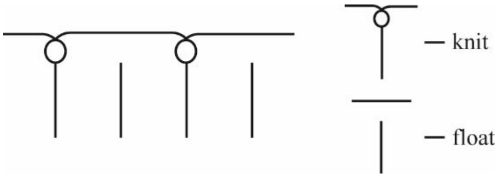

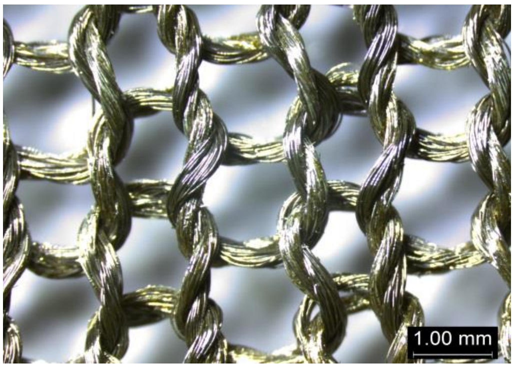

Figure 4.21(a) The loop diagram of 1x1 float knitted structures, (b) The fabric image captured with a light microscope (LEICA M165C).

4.4.1.2 Procedures and specifications

For STOLL (H. Stoll GmbH & Co. KG) computerized flat knitting machine, fabrics' density was mainly controlled by NP value which is a machine parameter to adjust needle's downwards position of loop formation. In the experiment, NP value was adjusted to 12.0, which is a normal value for single face fabric on flat knitting machine. As a result, the density of all the samples was 8.62 courses per cm and 7.14 wales per cm in wales and course direction respectively. The fabric was uniform, with a dimension of 100 courses x 100 wales, and multi-layer knitting technology was employed. For the aim of dimensional stability, the conductive area was knitted with two layers, which were constituted by one conductive layer with float structures and the other one non-conductive layer with the back jersey structure. As shown in Figure2 (a) and (b), the samples were knitted in two series, with the conductive yarn distributed in the courses and wales directions, and three identical swatches of each design were prepared to strengthen the results.

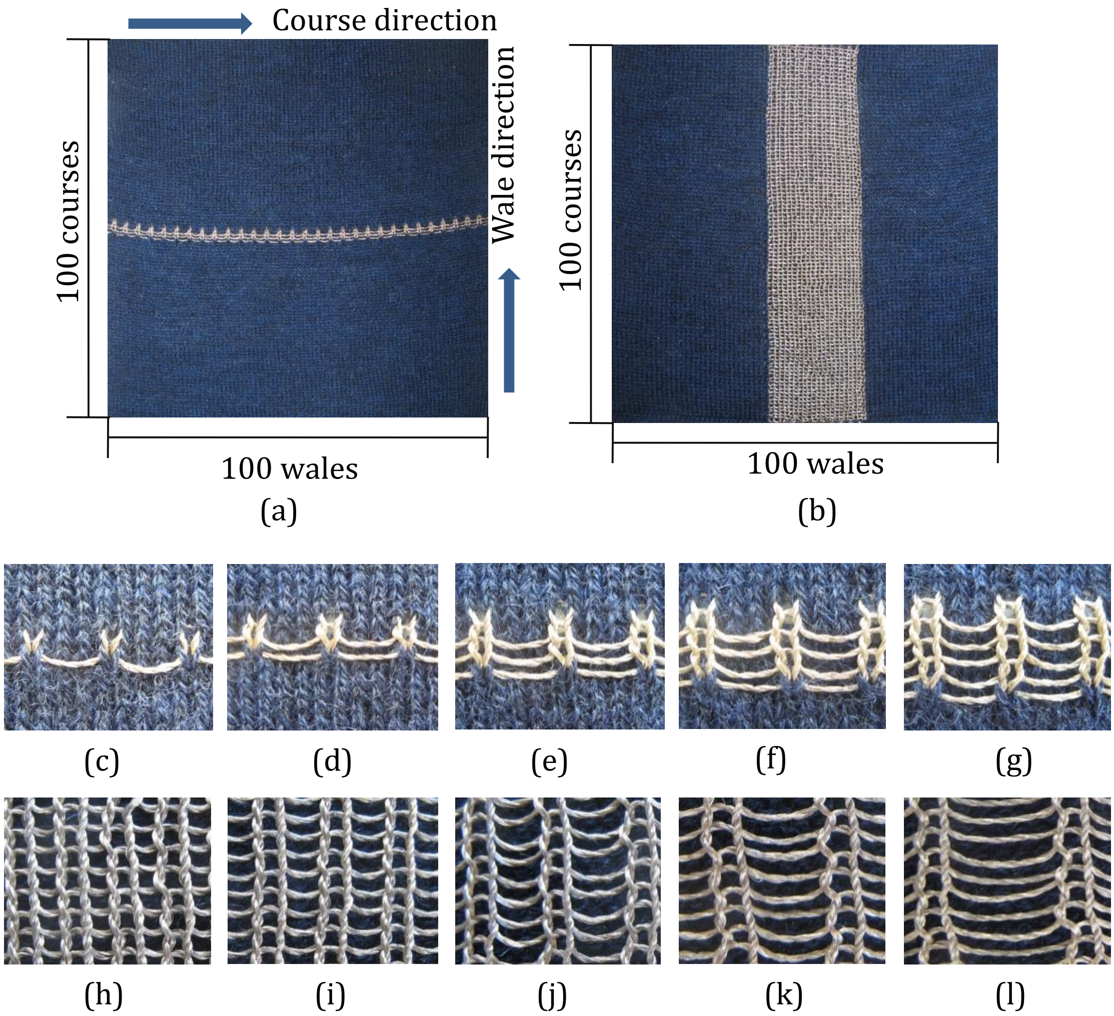

Figure 4.22 Sample pieces of (a) Series 1, (b) Series 2, In series 1, partial images of structure 1x3 float knitted with (c) one course, (d) two courses, (e) three courses, (f) four courses, (g) five courses, In series 2, partial images of structure (h) 1x1 float, (i) 1x2 float, (j) 1x3 float, (k) 1x4 float, (l) 1x5 float.

Due to the different influences of the float stitches in the courses and wales directions, series 1 was designed to determine the relationship between the resistance and the different float structures with variable course numbers, and series 2 was designed to determine the relationship between the resistance and variable float length in the float structures. Therefore, in series 1, the samples were prepared by knitting the conductive yarn fixed within 100 wales for six different structures, and the number of courses was varied from 1 to 5. Figure 4.22 (c) to (g) shows the fabric images for 1x3 float structure knitted with one course to five courses. To effectively investigate the influence of the float stitch with a varied number of wales, samples with too few repeat pattern units were not considered in our study. Therefore, in series 2, the samples were prepared by knitting the conductive yarn using 100 fixed courses in six different structures, and 10 horizontal repeat pattern units were included in every structure, i.e., the number of wales was varied to be 10 courses for the jersey, 20 courses for the 1x1 float, 30 courses for the 1x2 float, 40 courses for the 1x3 float, 50 courses for the 1x4 float, and 60 courses for the 1x5 float structures. Figure 4.22 (h) to (l) illustrates the fabric images of series 2 knitted with 1x1 float, 1x2 float, 1x3 float, 1x4 float and 1x5 float structures, respectively. After leaving the machine, the samples were laid out on a platform for 24 hours without ironing or laundering.

4.4.2 Experimental results and discussion

4.4.2.1 The measurement of resistance values of knitted fabrics

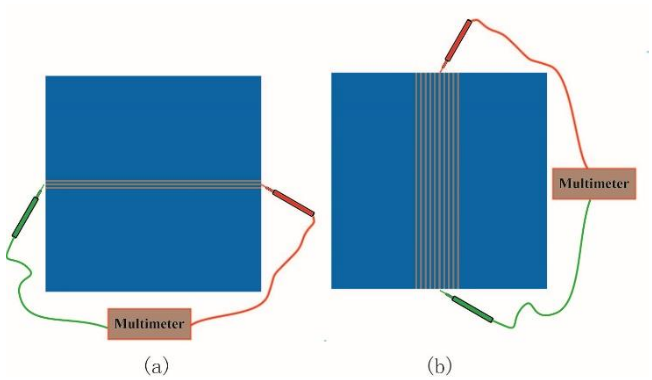

Figure 4.23 The testing illustration for measuring resistances by Multimeater in case of (a) series1, (b) series 2.

Table 4.3 The resistance values of different conductive fabrics with 100 wales and variable course numbers (Unit: Ω).

structure	jersey			float 1x1			float 1x2			float 1x3			float 1x4			float 1x5		
sample Code	S1	S2	S3	S1	S2	S3	S1	S2	S3	S1	S2	S3	S1	S2	S3	S1	S2	S3
course 1	78.9	79.7	79.7	50.4	51.3	51.0	38.2	40.4	39.9	36.3	36.1	37	33.8	32.5	32.8	28.5	29.8	29.7
course 2	34.9	35.5	35.1	22.4	22.8	23.1	18.5	18.2	18.1	15.9	16	16.2	14.8	15.5	15.1	13.9	14.2	14.0
course 3	22.2	22.0	22.7	13.9	13.6	13.4	11.3	11.2	11.3	9.8	9.6	10.0	9.0	9.3	9.2	8.8	8.7	8.6
course 4	15.2	15.3	16.0	10.0	10.7	10.5	8.6	8.7	9.3	8.1	7.7	8.2	7.2	6.9	7.1	6.6	6.3	6.7
course 5	12.8	12.4	12.9	7.9	7.8	8.0	6.9	7.9	7.1	6.2	6.3	6.3	5.5	5.4	5.8	5.3	5.4	5.5

The resistances were measured using a 6 1/2 Digit 34401A Multimeter (Agilent Technologies, Palo Alto, CA). The test was conducted under external force 0.5N. The testing points on the fabric samples for series 1 and 2 between which the resistance has been measured were illustrated in Figure 4.23 (a) and (b), respectively. The resistance values measured for series 1 and 2 are listed in Tables 4.2 and 4.3, respectively. The average measured values with error bars and simulated values are shown in Figures 4.24 and 4.25, respectively.

Table 4.4 The resistive values of different conductive fabrics with 100 courses and variable wale numbers (Unit: Ω).

structure	**jersey**			**float 1x1**			**float 1x2**			**float 1x3**			**float 1x4**			**float 1x5**		
Sample Code	**S1**	**S2**	**S3**	**S1**	**S2**	**S3**	**S1**	**S2**	**S3**	**S1**	**S2**	**S3**	**S1**	**S2**	**S3**	**S1**	**S2**	**S3**
course 10	1.62	1.63	1.61	-	-	-	-	-	-	-	-	-	-	-	-	-	-	-
course 20	-	-	-	1.67	1.71	1.58	-	-	-	-	-	-	-	-	-	-	-	-
course 30	-	-	-	-	-	-	1.67	1.83	1.72	-	-	-	-	-	-	-	-	-
course 40	-	-	-	-	-	-	-	-	-	1.79	1.75	1.82	-	-	-	-	-	-
course 50	-	-	-	-	-	-	-	-	-	-	-	-	1.79	1.77	1.82	-	-	-
course 60	-	-	-	-	-	-	-	-	-	-	-	-	-	-	-	1.77	1.82	1.86

4.4.2.2 The measurement of the geometrical model-related parameters d, w, h, and r

Table 4.5 Experimental values of the loop model-related parameters d, w, and h.

Parameter	Diameter of yarn(d)			Width of a loop (w)			Height of a loop (h)		
Times	1	2	3	1	2	3	1	2	3
Experimental Value(mm)	0.34	0.29	0.37	1.37	1.51	1.36	0.92	1.03	0.90
Mean(mm)		0.33			1.41			0.95	
Standard deviation		0.04041			0.08386			0.07	

From the knitted swatches, the loop-related parameters d, w, and h were measured. As shown in Table 4.5 each parameter was tested three times and the experimental data, as well as their average value and standard deviation (SD), were also listed. According to the previous geometric model, r can be calculated as $r = \frac{1}{4}(w + 2d)$, which was approximately 0.52 mm.

4.4.2.3 The calculation of resistance values based on the resistive network model

By importing the experimental data from Table 4.5 into Equation group (4.2) to (4.6), the updated Equation group (4.23) to (4.27) was derived as follows:

$$y_1 = -\sqrt{0.52^2 - (x_1 + \frac{1.41}{2})^2} \qquad (-0.705 \le x_1 \le -0.185) \quad \widehat{C'E'} \tag{4.23}$$

$$y_2 = \frac{0.95}{\pi}\sin^{-1}\left[1 - \frac{2(x_2+0.52)}{0.33}\right] + \frac{0.95}{2} \qquad (-0.52 \le x_2 \le -0.185) \quad \widehat{D'E'} \tag{4.24}$$

$$y_3 = \sqrt{0.52^2 - {x_3}^2} + 0.95 \qquad (-0.52 \le x_3 \le -0.52) \quad \widehat{D'AD} \tag{4.25}$$

$$y_4 = \frac{0.95}{\pi}\sin^{-1}\left[1 - \frac{2(0.52-x_4)}{d}\right] + \frac{0.95}{2} \qquad (0.185 \le x_4 \le 0.52) \quad \widehat{DE} \tag{4.26}$$

$$y_5 = -\sqrt{0.52^2 - (x_5 - \frac{1.41}{2})^2} \qquad (0.185 \le x_5 \le 0.705) \qquad \widehat{EC} \qquad (4.27)$$

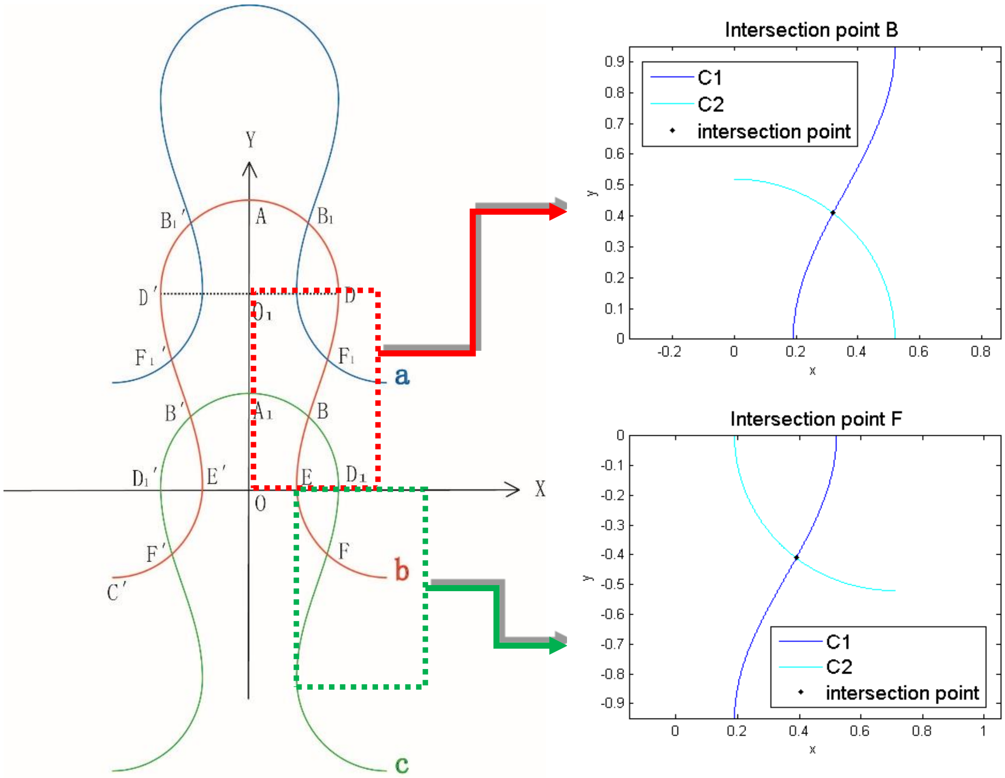

Figure 4.24 Three interlocking loops in the vertical direction.

The model of three loops interlocked one by one in the vertical direction is shown in Figure 4.24. In Figure 4.24, compared with loop **b**, loop **a** was considered to shift “h” on the y axis, and loop **c** was considered to shift “–h” on the y axis. The point of intersection B can be determined by Equations (4.26) and (4.28):

$$y = \sqrt{0.52^2 - x^2} \qquad (0 \le x \le 0.52) \qquad \widehat{A_1D_1} \qquad (4.28)$$

MATLAB 2007a calculated point B (x_B, y_B), and its x and y coordinate values were computed to be approximately 0.3198 and 0.4100, respectively. Similarly, another important intersection point, F (x_F, y_F), was calculated, and the x and y coordinate values were computed to be approximately 0.3902 and -0.4100, respectively.

A parametric Equation (4.30) used to demonstrate the Curve $\widehat{DE}$ was established on the basis of Equation (4.29).

$$t = \frac{\pi}{0.95}y - \frac{\pi}{2} \tag{4.29}$$

$$\begin{cases} x = \frac{0.33}{2}\text{sint} + 0.52 - \frac{0.33}{2} \\ y = \frac{0.95}{\pi}t + \frac{0.95}{2} \end{cases} \tag{4.30}$$

According with the theory of Definite Integral, the length of a curve can be calculated by Equation (4.31):

$$s = \int_a^b \sqrt{\left(\emptyset'(t)\right)^2 + \left(\varphi'(t)\right)^2}\ dt \tag{4.31}$$

Thus, the length of curve $\widehat{BE}$ was computed by Equation (4.32):

$$s_{BE} = \int_{-\frac{\pi}{2}}^{\frac{0.31980}{0.95}\pi - \frac{\pi}{2}} \sqrt{\left(\frac{0.33}{2}\text{cost}\right)^2 + \left(\frac{0.95}{\pi}\right)^2}\ dt \tag{4.32}$$

The length of curve $\widehat{BD}$ was computed by Equation (4.33):

$$s_{BD} = \int_{\frac{0.31980}{0.95}\pi - \frac{\pi}{2}}^{\frac{\pi}{2}} \sqrt{\left(\frac{0.33}{2}\text{cost}\right)^2 + \left(\frac{0.95}{\pi}\right)^2}\ dt \tag{4.33}$$

By utilising MATLAB 2007a, the approximate value of the curve length can be derived as:

$$s_{BE} = 0.3333\ ;\ s_{BD} = 0.6836.$$

The curve $\widehat{D_1F}$ can be defined as a definite integral by the following integral Equation (4.34):

$$s_{D_1F} = \int_{-\frac{0.4100t}{0.95}+\frac{\pi}{2}}^{\frac{\pi}{2}} \sqrt{\left(\frac{0.33}{2}\text{cost}\right)^2 + \left(\frac{0.95}{\pi}\right)^2}\ dt \tag{4.34}$$

The curve $\widehat{FE_1}$ can be defined as a definite integral by the following integral Equation (4.35):

$$s_{FE_1} = \int_{-\frac{\pi}{2}}^{-\frac{0.4100t}{0.95}+\frac{\pi}{2}} \pi\sqrt{\left(\frac{0.33}{2}\cos t\right)^2 + \left(\frac{0.95}{\pi}\right)^2}\, dt \tag{4.35}$$

The approximate value of a curve length can be derived by MATLAB:

$s_{D_1F} = 0.4347$; $s_{FE_1} = 0.5825.$

Similarly, by inserting intersection point F (0.3902, -0.4100) into Equation (4.28), the curve length can be defined as a definite integral with the following results:

$s_{EF} = 0.4724$; $s_{FC} = 0.3444.$

Due to the circular symmetry of curve $\widehat{EC}$ and curve $\widehat{AD}$, it can be concluded that:

$s_{B_1D} = 0.4724$; $s_{AB_1} = 0.3444.$

So far, the curve lengths of the nine sections divided by the interlocking of the loops in an integrate loop can all be derived from the computed curve length and the experimental data. The linear resistances related to the curve lengths are displayed below:

$s_{B_1'B_1} = 2s_{AB_1} = 0.6888\text{mm};$

$s_{BF_1} = s_{BD} - s_{D_1F} = 0.2468\text{mm};$

$s_{B_1F_1} = s_{B_1D} + s_{DF_1} = 0.9071\text{mm};$

$s_{CM} = w = 1.41\text{mm}.$

Because the linear resistance changes in proportion to the length of yarn, based on the above computation, the proportional relationship of the linear resistances R_H, R_V, R_N, and R_F was 0.6888: 0.2468: 0.9071: 1.410.

4.4.2.4 The simulation results

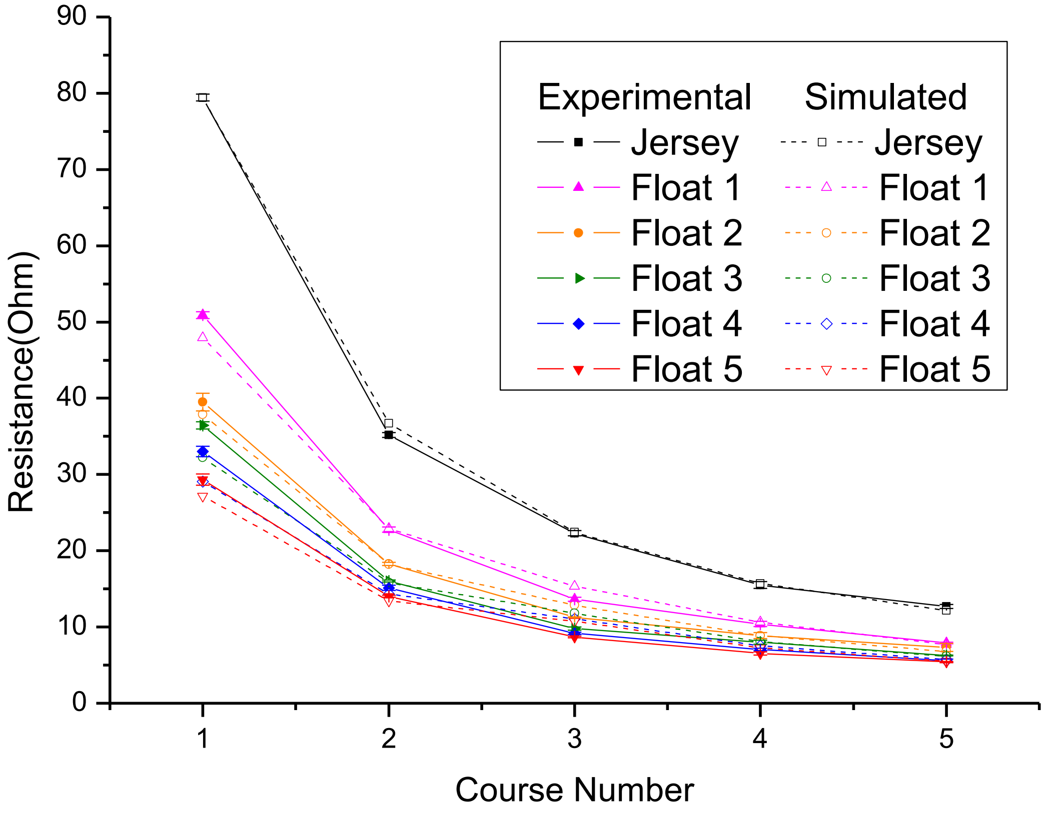

Figure 4.25 The simulated and experimental resistance results for different structures with 100 fixed wales and variable course numbers.

By inserting the ratio of the four linear resistances into Equations (4.18) and (4.22), the simulated and experimental results of the resistances for different structures with 100 fixed wales and variable course numbers were obtained and are shown in Figure 4.25; the simulated and experimental results of the resistances of different structures with 100 fixed courses and 10 pattern repeat units are shown in Figure 4.26. The reason for the collection of different data in the course and wales directions was explained in the preceding sample preparation section. The data points connected by solid lines are the simulation results, and those connected by dashed lines are the experiment results. It is evident that the trend of the two data sets is generally identical. It can also be observed that the experimental results coincide with the theoretical results within an acceptable degree of error in cases in which the conductive yarns are embedded in both the horizontal and vertical directions.

4.4.2.5 Discussion

As shown in Figure 4.25, the resistance value is inversely proportional to the course number of the conductive fabric. This result can be explained by Ohm's law, which states that a parallel connection will reduce the resistance of a circuit.

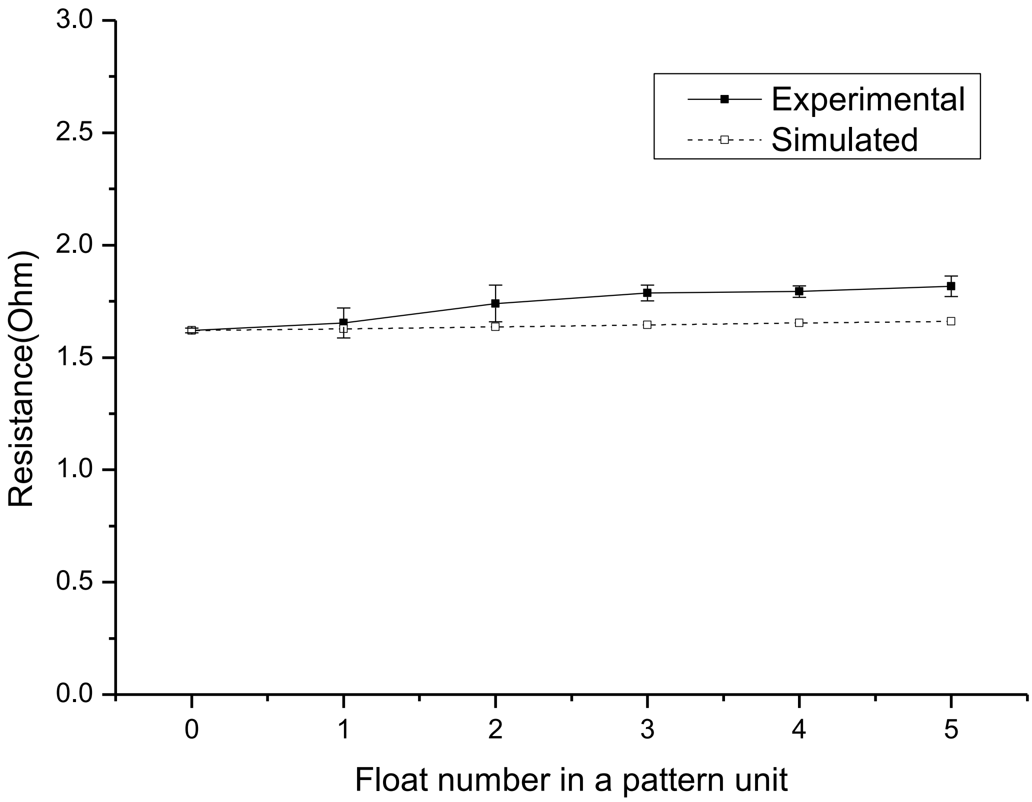

Figure 4.26 The simulated and experimental resistance results for different structures with 100 fixed courses and variable wale numbers.

It can be seen from Figure 4.25 that the jersey structure has the largest resistance, followed by the 1x1, 1x2, 1x3, 1x4 and 1x5 float structures in descending order. The highest value recorded in the experiment was approximately 80 Ω and was associated with one course of conductive yarn knitted in the jersey structure. However, when the conductive yarn was knitted in five courses, the measured resistance value was very low, especially with float structures, which were all approximately 10 Ω. With an increase in the number of float stitches in a float structure unit, the resistance values tended to decrease because an increase in float stitches will generally increase the number of parallel conductive yarns in the structure, which helps to decrease the resistance. The resistance values will finally approach a marginal value as the float stitch number approaches infinity. This result occurs because the number of loop stitches is dramatically reduced because these stitches are replaced by float stitches when there is an increase in float stitches. In addition, when there is an increase in knitting courses in a knitted fabric, the resistive effect will be diminished and, thus, the resistance value of the conductive knitted fabric with various numbers of knitting courses become similar. The reason is still that an increase in the number of parallel connections in a circuit reduces the overall resistance value.

The discrepancy illustrated in Figure 4.25 between the experimental and theoretical values can be explained by the instability of the knitted fabric. It can be seen that the experimental results are very close to the theoretical results for the jersey structure (i.e., when n=0). Consistent with the increasing number of float stitches, the difference between the experimental and simulated results becomes more noticeable. The relatively large difference in the two sets of results occurs for the structures of the 1x4 and 1x5 floats. In the jersey fabric, the loop is arranged one by one tightly, the deformation of the loop is very limited, and the theoretical model fits the loop status well. Therefore, the variation between the experimental data and the simulated results is small. However, regarding the float structure, although the float yarn stitches are knitted under the same machine parameters as those used for the jersey structure, the loop shape has been changed under the influence of the float stitch in the fabrics because the embedded float yarn can make the knit stitch slightly looser than the knit stitch in the jersey structure. Because the embedded float yarn can make the knit stitch slightly looser than the knit stitch in the jersey structure. Because the model of the float stitch is established based on the knit stitch in the jersey structure, there should be some deviation between the practical and theoretical results. However, the discrepancy is small and, thus, acceptable. An improved method could be developed by considering the loop deformation when establishing the model for float structures or when developing new knitting techniques to make the float structures as stable as the jersey structure.

In Figure 4.26, when repeat times and course numbers were both fixed, although the wale number varied among the different structures, the resistance value remained constant because the length of the float yarn did not influence the resistance values, according to Equation (4.22). However, the experimental values trended slightly upward, which was due to the existence of the electric current in the horizontal direction during the measurement of the resistance. The electric current in the horizontal direction was ignored in the calculations; however, such a current will indeed be generated when loading a voltage source due to the slight asymmetry at the edge of the resistive work. As the resistance of the float yarn increased, the resistance in the horizontal direction increased, which restrained the conduction of the electric current in the horizontal direction. Therefore, the final resistance was approximately constant with a slight increase.

4.5 Conclusion

This chapter presented a reasonable theoretical description of the resistance values of different knitted structures based on float stitches. The theoretical conclusions were well verified by the experimental values, and the deviation between the experimental and theoretical values can be explained reasonably well with the related electrical knowledge. The deviation may own to the slightly shape discrepancy between loops knitted with different yarns, the deformation properties of the It may be concluded that float stitches can definitely decrease the overall resistance of a conductive fabric compared with the resistance of a fabric with only knit stitches when the wales number is fixed. However, the changes in the float structure have little influence on the resistance of a knitted fabric when the course number is fixed. Considering these rules, when designing a conductive knitted fabric with specific resistance values, increasing the number of float stitches in one pattern unit could reduce the resistance of the overall fabric, and keeping the repeat number of pattern units unchanged could enlarge the fabric size with constant fabric resistance.

Generally, there is a slightly shape discrepancy between loops knitted with different yarns, however, the same models for the same structures with conductive yarns and non-conductive yarns are adopted in this paper because the research purpose does not focus on it.

Therefore, this study provides an effective method for the computation of resistance values in a conductive knitted fabric. Simultaneously, it demonstrates the possibility of controlling the resistance values of a conductive knitted fabric of fixed dimensions and density. Moreover, the research provides a scientific method for a further research on contact resistance and length-related resistance in conductive knitted fabrics, which can also be adopted for the study of tuck structures in the future.

CHAPTER 5 THE FUNDAMENTAL STUDY ON RESISTANCE PROPERTIES OF CONDUCTIVE KNITTED TUCK STRUCTURES

5.1 Introduction

In previous chapter, the float knitted structures are studied systematically, thus, further contribution to development of conductive yarn by variable knitted structures, such as the basic loops element of tuck stitch is in needed. Since tuck structures are more complicated structure than knit and float, the present research will firstly study the resistance properties of conductive Single Pique structure which is a typical tuck structure in knitting technology.

In this chapter, based on a geometrical model established for Single Pique, the resistive network models for variable course and wale number are deduced. Therefore, the resistance values for conductive Single Pique fabric will be predicted if course and wale number are given.

To verify the resistive network model, experimental design is conducted and it is found that the experimental results can cohere with the simulated results deduced by the resistive network model. It can be concluded that the resistive network models are effective in the prediction of resistance values in advance. The method will contribute to the study of resistance impact of variable knitwear structure design. Furthermore, it can be a useful illustration for the design of conductive thermal knitted garments.

5.2 The establishment of geometrical model for float stitch

5.2.1 The deformation of geometrical model for a tuck cell in Single Pique structures

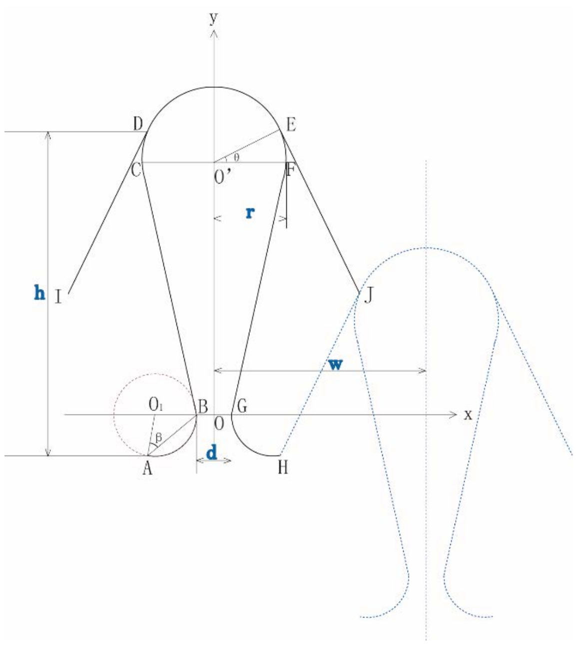

Figure 5.1 The geometrical model for a tuck cell in Single Pique structure.

Firstly, a planar geometrical model was established as shown in Figure 5.1. A tuck cell ($I\widehat{DE}J$) and a loop cell ($ABC\widehat{DEF}GH$) construct the geometrical model. To simplify the calculation process, the loop pillars (BC and GF) can be represented by straight lines and the loop arcs ($\widehat{AB}$, $\widehat{CF}$ and $\widehat{GH}$) can be represented by partial circles. As defined in the model, h is the distance between two adjacent stitches in the wale direction (course distance); w is the distance between two adjacent stitches in course direction (wale distance); d is the diameter of the conductive yarn; r is the supposed radius of circle arc $\widehat{CF}$; and r' is the supposed radius of circle arc $\widehat{AB}$. It is assumed that two conductive yarns connect together at the bottom of two loop pillars (BC and GF). Therefore, the distance between B and G is equal to d as shown in Figure 5.1. E is assumed to be the point of tangency between line EJ and semi-circle $\widehat{CF}$. θ is denoted to be $\angle EO'F$ and β is denoted to be $\angle O_1AB$. To obtain the expression of radio r', L_{AB} (the length for Line AB) can be firstly represented by Equation (5.1), then r' can be calculated by Equation (5.2).

$$L_{AB} = \sqrt{\left(rcos\beta - \frac{d}{2}\right)^2 + \left[\sqrt{r^2 - \left(\frac{d}{2}\right)^2} - rsin\beta\right]^2} \tag{5.1}$$

$$r' = \frac{L_{AB}}{2cos\beta} \tag{5.2}$$

Based on the above definition, the different parts, $\widehat{AB}$, BC, $\widehat{CF}$, FG, ID, $\widehat{DE}$ and EJ of the geometrical model can be represented by corresponding Equations (5.3) to (5.10) as shown in below.

$$\widehat{AB}: y = -\sqrt{r'^2 - \left(x + r' + \frac{d}{2}\right)^2} \quad \left(-rcos\theta \le x \le -\frac{d}{2}\right) \tag{5.3}$$

$$\widehat{GH}: y = -\sqrt{r'^2 - \left(x - r' - \frac{d}{2}\right)^2} \quad \left(\frac{d}{2} \le x \le rcos\theta\right) \tag{5.4}$$

$$BC: y = \frac{h - \sqrt{r^2 - \left(\frac{d}{2}\right)^2}}{\frac{d}{2} - r}\left(x + \frac{d}{2}\right) \quad \left(-r \le x \le -\frac{d}{2}\right) \tag{5.5}$$

$$\widehat{CF}: y = \sqrt{r^2 - x^2} + h - \sqrt{r^2 - \left(\frac{d}{2}\right)^2} \quad \left(-r \le x \le -\frac{d}{2}\right) \tag{5.6}$$

$$FG: y = -\frac{h - \sqrt{r^2 - \left(\frac{d}{2}\right)^2}}{\frac{d}{2} - r}\left(x - \frac{d}{2}\right) \quad \left(\frac{d}{2} \le x \le r\right) \tag{5.7}$$

$$ID: \quad y = -\frac{h}{4rcos\theta - 2w}x + \frac{h}{2} + \frac{h(rcos\theta - w)}{4rcos\theta - 2w} - \sqrt{r^2 - \left(\frac{d}{2}\right)^2} + rsin\theta \quad (-w + rcos\theta \le x \le -rcos\theta) \tag{5.8}$$

$$\widehat{DE}: y = \sqrt{r^2 - x^2} + h - \sqrt{r^2 - \left(\frac{d}{2}\right)^2} \quad (-rcos\theta \le x \le rcos\theta) \tag{5.9}$$

$$EJ: y = \frac{h}{4rcos\theta - 2w}x - \frac{h}{2} - \frac{h(rcos\theta - w)}{4rcos\theta - 2w} + \sqrt{r^2 - \left(\frac{d}{2}\right)^2} - rsin\theta \qquad (rcos\theta \le x \le w - rcos\theta) \tag{5.10}$$

5.2.2 The 3D simulation of Single Pique structure by Mathematics

By the Mathematics drawing software, the tuck cell can be simulated in 3D effects as shown in Figure 5.2 (a), and the Single Pique knitted structure can be also simulated by the repeatable tuck cells as shown in Figure 5.2(b). The program statement in Mathematics is listed in the Appendix.

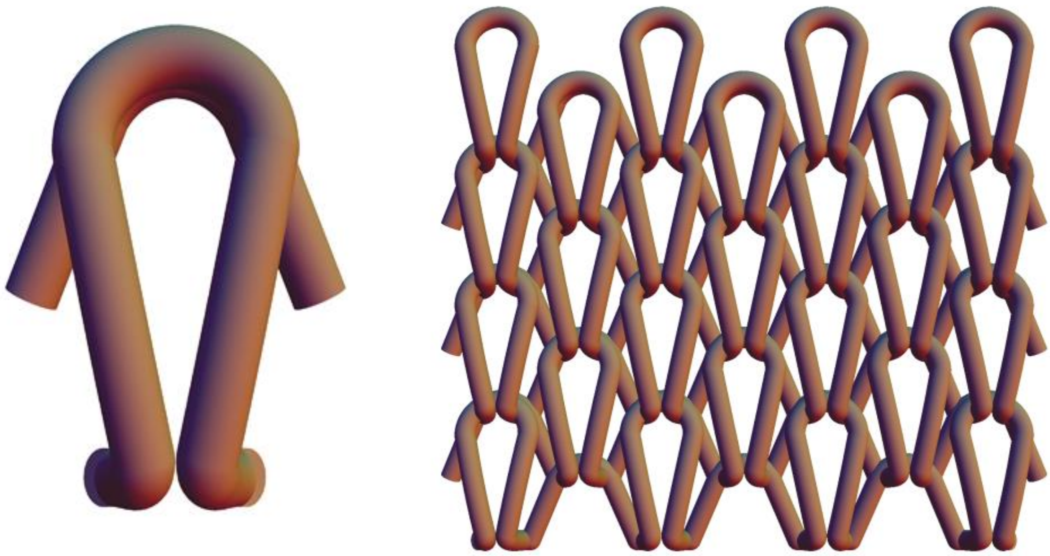

(a) (b)

Figure 5.2 The 3D simulation effect of (a) a tuck cell; (b) Single Pique structure.

5.3 The establishment of the resistive network models for Single Pique structures

5.3.1 The original resistive network model based on the Single Pique configuration

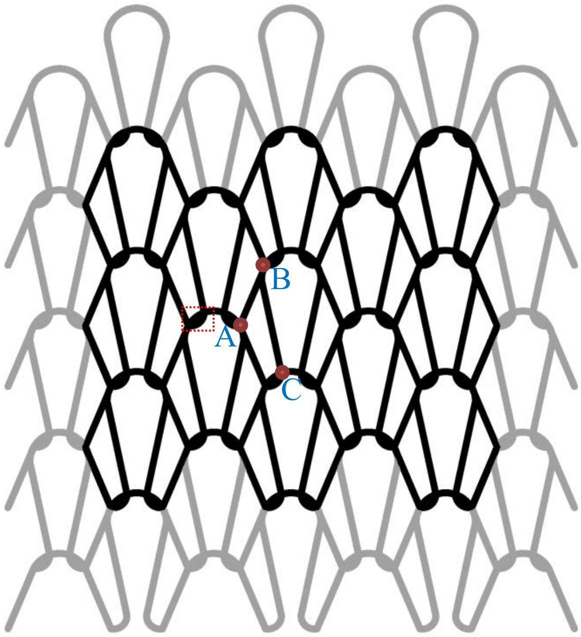

Figure 5.3 The structure configuration of Single Pique knitted structure.

As the same as conductive float knitted fabrics, the resistive network of conductive Single Pique fabrics is composited by contact resistance and linear resistance. As introduced before, linear resistance R_L and contact resistance R_C both contribute to the whole resistance of knitted fabric. As shown in Figure 5.3, R_C is generated in the areas which are framed by red square; R_A is supposed to be the linear resistance which is generated by the length of conductive yarn from Point A to B and R_B is supposed to be the linear resistance which is generated by the length of conductive yarn from Point B to C. According with the structure configuration shown in Figure 5.3, the original resistive network model with N courses and M wales is developed as shown in Figure 5.4.

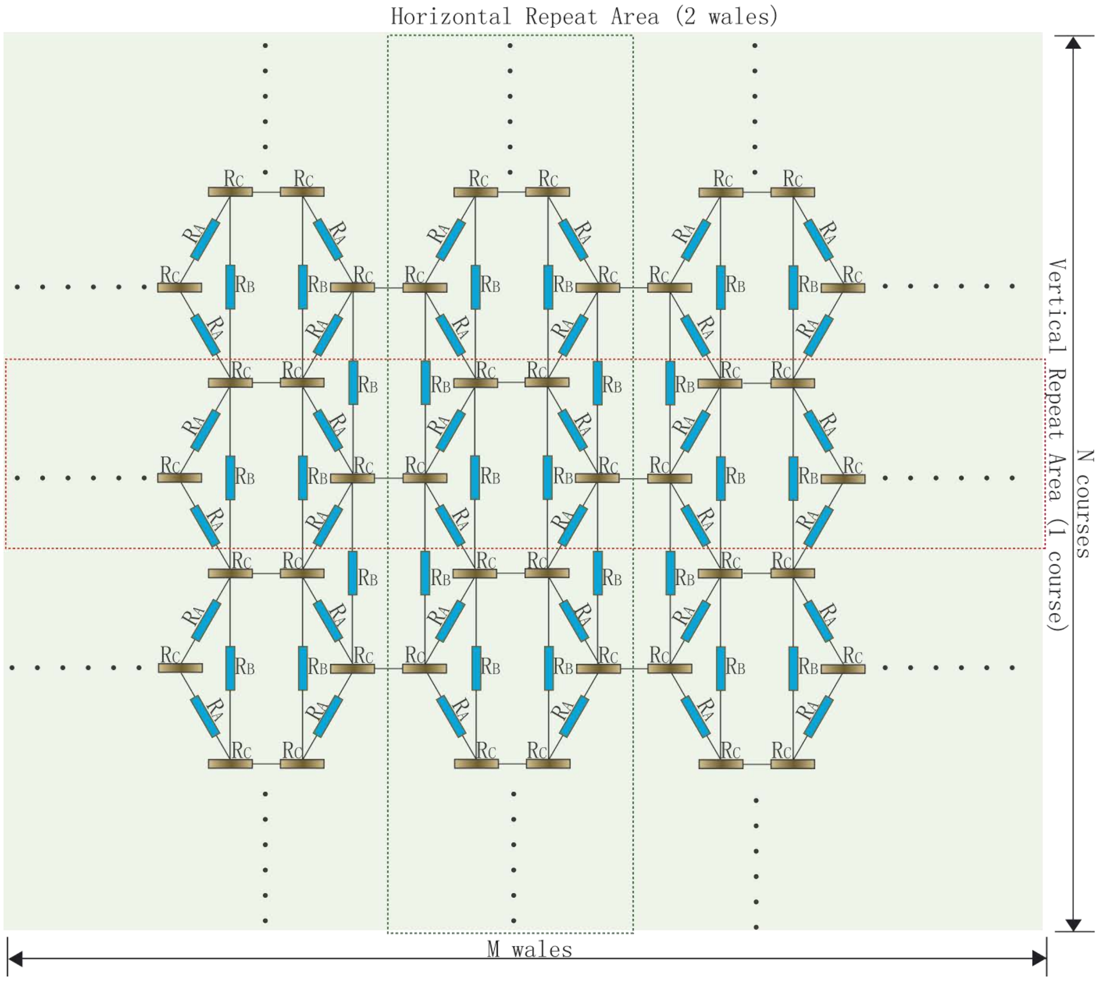

Figure 5.4 The original resistive network model of Single Pique knitted structure.

It can be seen that all the $\mathrm{R_C}$ are located in the crossover of the resistive network. To simplify the resistive network, $\mathrm{R_C}$ can be divided into five equal small resisters Δr to distribute to the five branches which connect to $\mathrm{R_C}$ as shown in Figure 5.5.

To further develop the simplified resistive network, resistive network modeling was carried out by using the two following relationships.

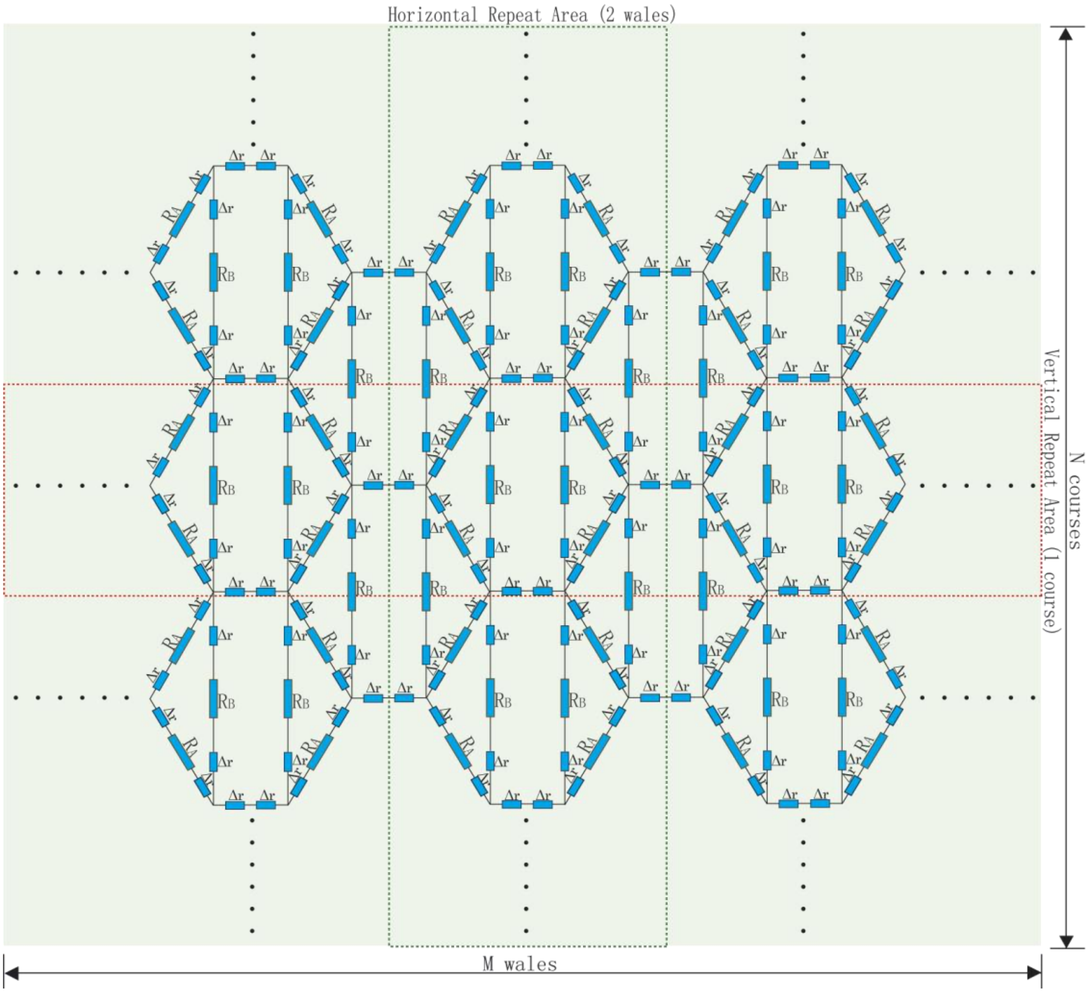

Figure 5.5 The simplified resistive network after eliminating R_C.

5.3.2 Resistive network model for different distributions of conductive yarn in Single Pique fabrics

5.3.2.1 In case of distribution in wale direction

In this case, the external voltage is located in vertical direction as show in Figure 5.6. The resistance in the horizontal direction may be removed because the voltage potential is evenly reduced in the vertical direction. Thus, the potential difference in horizontal direction is so tiny to be ignored which cause the electrical current can be ignored.

Therefore, the resistance in horizontal direction is negligible. As a consequence, the resistive network can be simplified as shown in Figure 5.7, in which $R_1 = R_A + 2\Delta r$; $R_3 = R_B + 2\Delta r$.

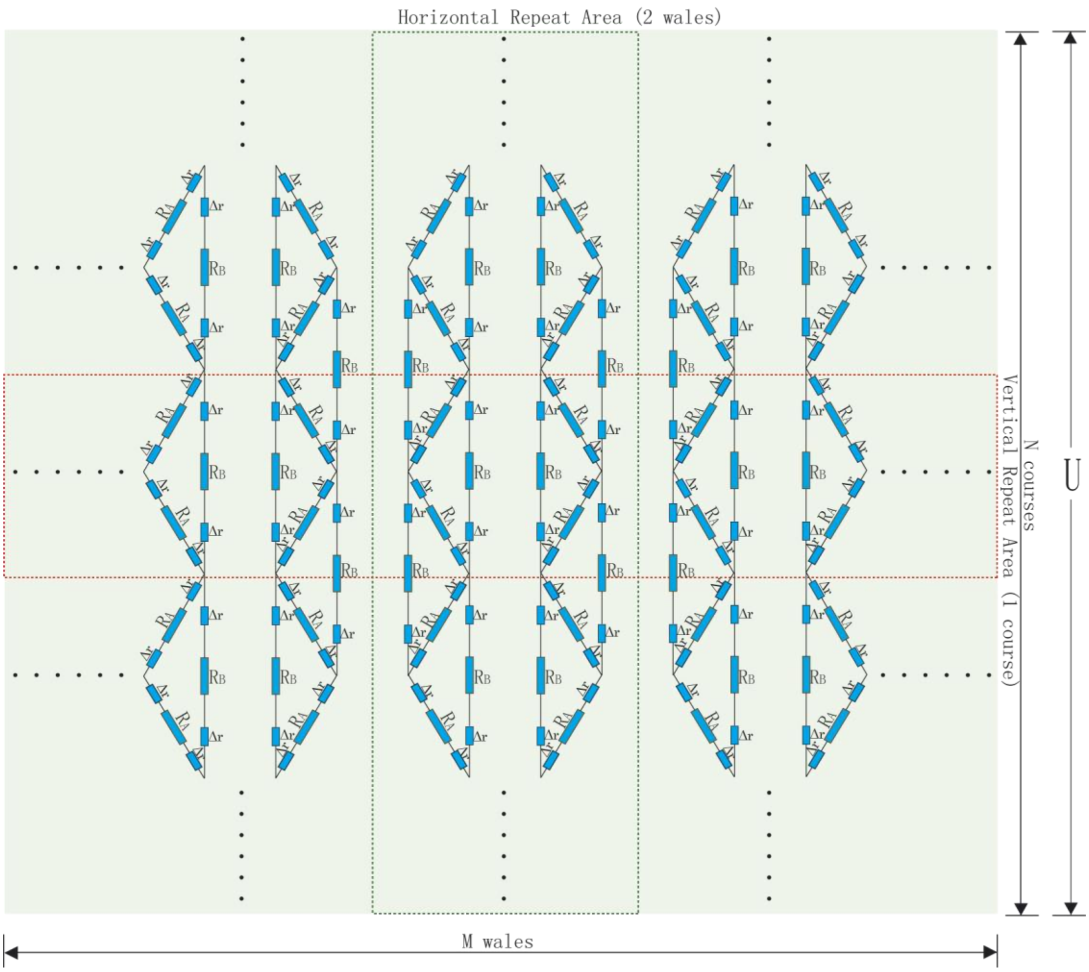

Figure 5.6 Further simplified resistive network after eliminating the resistances in the horizontal routes.

The electric current from nodal point A to nodal point C is equal to the electric current from nodal point C to nodal point B. It is assumed that the electric current from A to C is I_1 and the electric current from A to B is I_2.

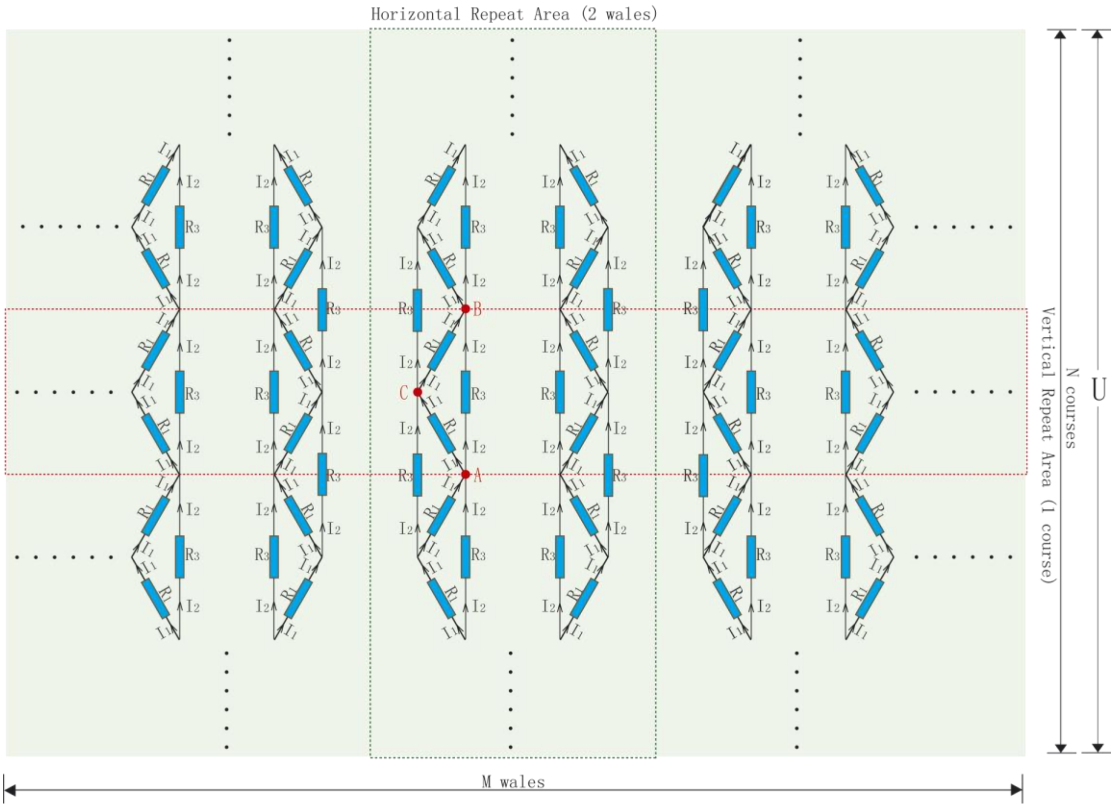

Figure 5.7 Equivalent resistive networks for the case of external voltage located in vertical direction.

The voltage from A to B (1 course) can be calculated by Equation (5.11).

$$\Delta U = \frac{U}{N} \tag{5.11}$$

At the same time, based on the Kirchhoff voltage law, the voltage ΔU from A to B in the electrical route can be deduced by Equation (5.12) and (5.13).

$$\Delta U = 2I_1 \cdot R_1 \tag{5.12}$$

$$\Delta U = I_2 \cdot R_3 \tag{5.13}$$

Therefore, I_1 and I_2 can be calculated as Equation (5.14) and (5.15).

$$I_1 = \frac{\Delta U}{2R_1} \tag{5.14}$$

$$I_2 = \frac{\Delta U}{R_3} \tag{5.15}$$

Therefore, the total electric current I_T can be derived by Equation (5.16)

$$I_T = (2I_2 + I_1) \cdot M = (\frac{2U}{R_3N} + \frac{U}{2R_1N}) \cdot M \tag{5.16}$$

Lastly, the total resistance value R of the conductive Single Pique knitted fabric with N courses and M wales can be computed by Equation (5.17) (The computation is conducted in vertical direction):

$$R = \frac{U}{I_T} = \frac{N}{M}(\frac{1}{\frac{2}{R_3}+\frac{1}{2R_1}}) \tag{5.17}$$

5.3.2.2 In case of distribution in course direction

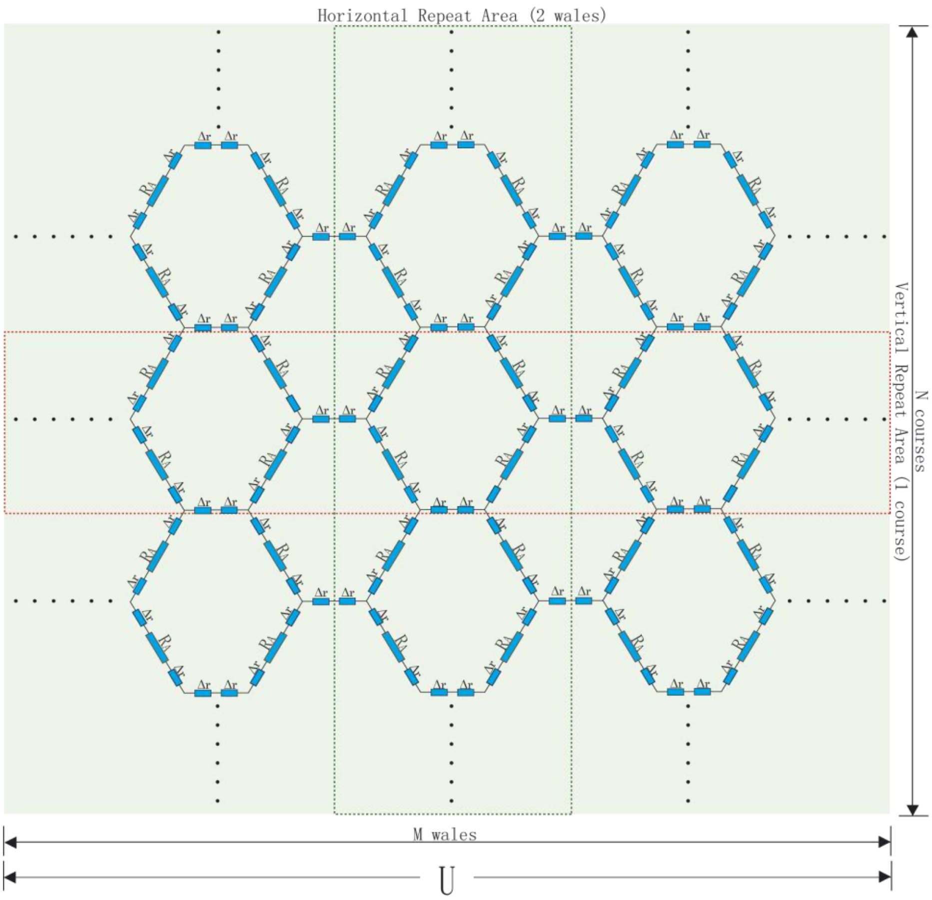

Figure 5.8 Further simplified resistive network after eliminating the resistances in the vertical routes.

As with the analysis in the previous case, the resistance in the vertical direction may be neglected since the voltage is evenly reduced in the horizontal direction. Then, the simplified resistive network can be further simplified as shown in Figure 5.8, in which $R_1 = R_A + 2\Delta r$; $R_2 = 2\Delta r$. The equivalent resistive network for the case of external voltage located in horizontal direction can be derived as shown in Figure 5.9.

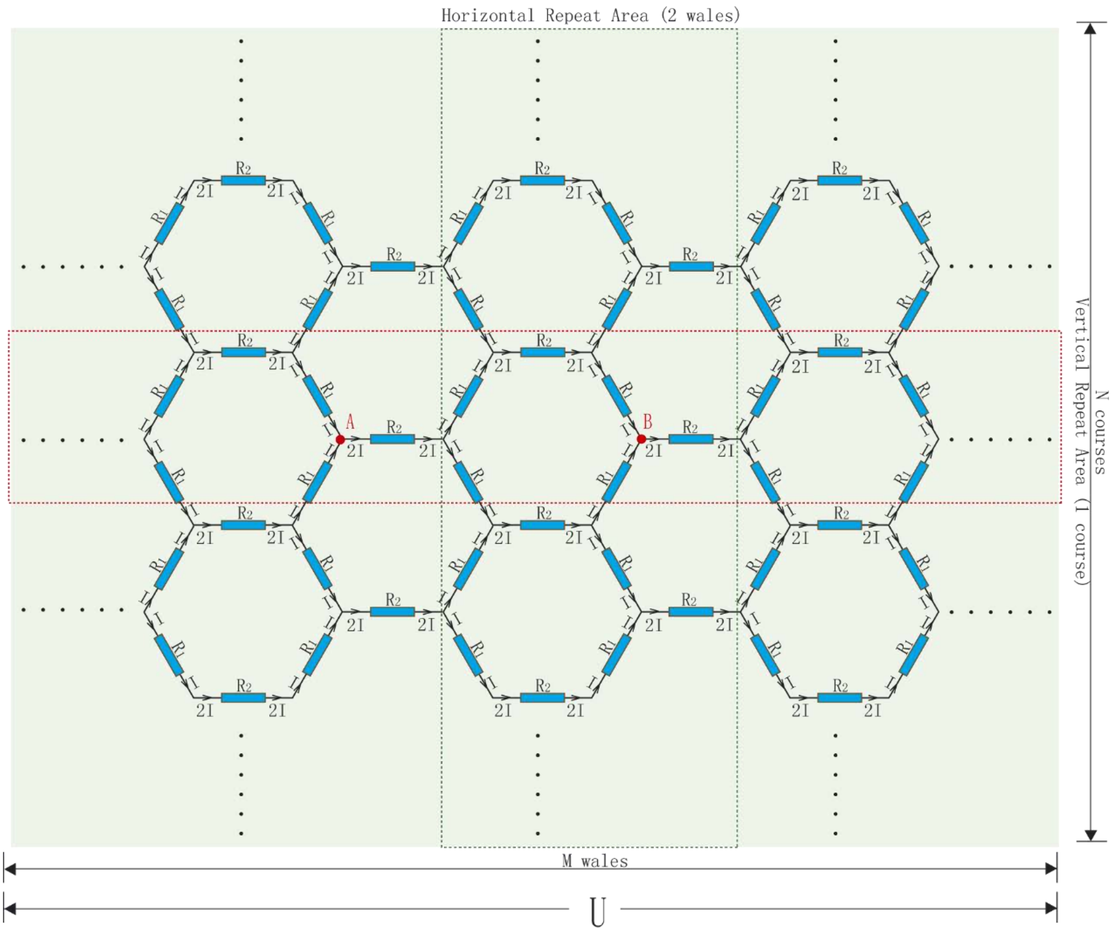

Figure 5.9 Equivalent resistive network for the case of external voltage located in horizontal direction.

Because the distance from nodal point A to nodal point B is 2 wales in Figure 5.9, the voltage ΔU from A to B (2 wales) can be calculated by Equation (5.18).

$$\Delta U = \frac{U}{\frac{M}{2}} = \frac{2U}{M} \tag{5.18}$$

Based on the Kirchhoff voltage law, the voltage ΔU from A to B in the electrical route can be deduced by Equation (5.19).

$$\Delta U = 2I \cdot R_2 + I \cdot R_1 + 2I \cdot R_2 + I \cdot R_1 = 2I \cdot R_1 + 4I \cdot R_2 \tag{5.19}$$

From Equation (5.18) and (5.19), Equation (5.20) can be derived.

$$\frac{2U}{M} = 2I \cdot R_1 + 4I \cdot R_2 \tag{5.20}$$

Then, the electric current I can be concluded by Equation (5.21).

$$I = \frac{U}{M(R_1+2R_2)} \tag{5.21}$$

Therefore, the total electric current I_T can be derived by Equation (5.22).

$$I_T = 2I \cdot N = \frac{2NU}{M(R_1+2R_2)} \tag{5.22}$$

In conclusion, the resistance value of the conductive Single Pique knitted fabric R with N courses and M wales can be computed by Equation (5.23) (The computation is conducted in horizontal direction):

$$R = \frac{U}{I_T} = \frac{M}{N}\left(\frac{R_1}{2} + R_2\right) \tag{5.23}$$

5.4 The experimental verification for the resistive network model of conductive Single Pique structures

5.4.1 Experimental design

5.4.1.1Materials and structure

The experimental samples are knitted on a STOLL CMS 822 computerized flat knitting machine (H. Stoll GmbH & Co.KG). Table 5.1 lists the specifications of the employed conductive and ground yarns. The conductive area used to measure the resistance properties were knitted by a conductive yarn; and the other area were knitted by a wool yarn as the background to make the conductive area stable.

Table 5.1 Conductive and background yarns.

Material	Yarn count	Composition	Linear resistance
Conductive yarn	47 Tex	Nylon 66 coated with silver	1 Ω/cm
Background yarn	30/2 Nm	100% merino wool	/

Single Pique is a typical knitted structure with tuck stitches. It is a good reference to study the influence of tuck stitches on the resistance properties of knitted fabrics. The loop diagram of the Single Pique structure is shown in Figure 5.10 (a), and the surface of Single Pique fabric is shown in Figure 5.10 (b) viewed under a light microscope (LEICA M165 C).

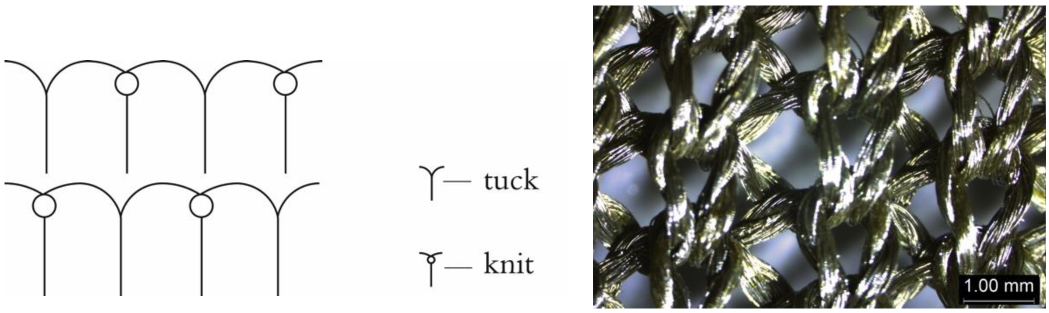

(a) (b)

Figure 5.10(a) Loop diagram of Single Pique structure (b) Surface of Single Pique fabric viewed under a light microscope (LEICA M165 C).

5.4.1.2 Procedures and specifications

The experiments are designed to test the resistance properties of conductive Single

Pique fabrics with different wale number and course number. Therefore, samples with fixed course number and variable wale number and samples with fixed wale number and variable course number are manufactured, respectively. Details specifications for the size of fabrics are listed in Table 5.2 and Table 5.3. Figure 5.11 shows the image of partial knitted samples.

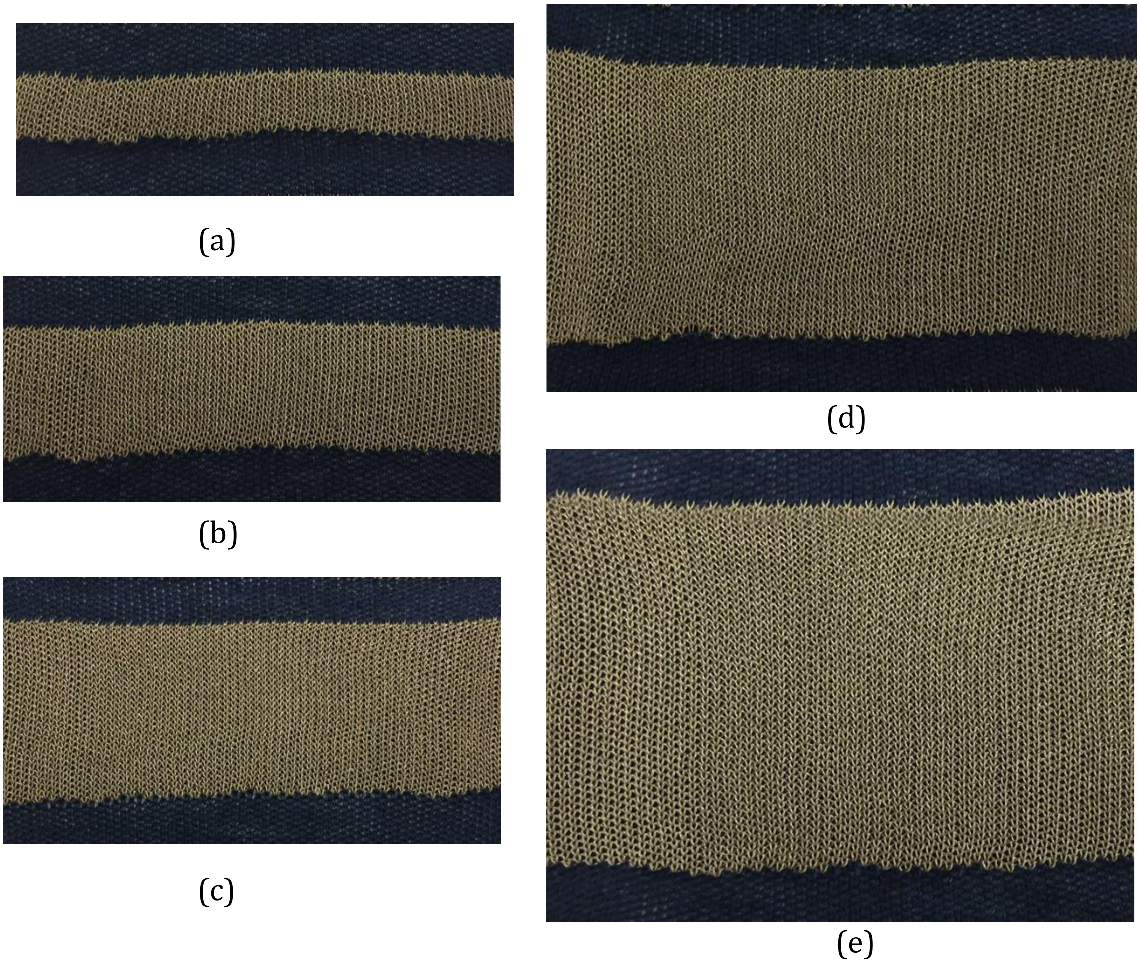

Figure 5.11 Image of knitted samples with 100 wales and different number of courses: (a) 20 courses, (b) 40 courses, (c) 60 courses, (d) 80 courses, (e) 100 courses.

Table 5.2 Sample specifications with fixed course number and variable wale number.

Different wales number	Fixed 70 courses	Fixed 80 courses	Fixed 90 courses	Fixed 100 courses
10 wales	3 samples	3 samples	3 samples	3 samples
20 wales	3 samples	3 samples	3 samples	3 samples
30 wales	3 samples	3 samples	3 samples	3 samples
40 wales	3 samples	3 samples	3 samples	3 samples
50 wales	3 samples	3 samples	3 samples	3 samples

Table 5.3 Sample specifications with fixed wale number and variable course number.

Different courses number	Fixed 70 wales	Fixed 80 wales	Fixed 90 wales	Fixed 100 wales
20 courses	3 samples	3 samples	3 samples	3 samples
40 courses	3 samples	3 samples	3 samples	3 samples
60 courses	3 samples	3 samples	3 samples	3 samples
80 courses	3 samples	3 samples	3 samples	3 samples
100 courses	3 samples	3 samples	3 samples	3 samples

5.4.2 Experimental results and discussion

5.4.2.1 The measurement of resistance values

All of the samples shown in Tables 5.2 and 5.3 are tested by using a 34401A 6 1/2 Digit Multimeter (Agilent Technologies, Palo Alto, CA). Figure 5.12 illustrates how the Multimeter test leads connect to the selvages of the knitted samples. The test was conducted under external force 0.5N. The testing results for each sample with a fixed number of courses and different number of wales are shown in Table 5.4 and those with a fixed number of wales and different number of courses in Table 5.5, respectively.

Figure 5.12 Multimeter test leads connect to the selvages of the knitted samples.

Table 5.4 Experimental results of resistance values for samples with fixed number of courses and different number of wales (unit: Ω)

	Fixed 70 courses			**Fixed 80 courses**			**Fixed 90 courses**			**Fixed 100 courses**		
Sample number	1	2	3	1	2	3	1	2	3	1	2	3
10 wales	0.56	0.57	0.57	0.68	0.63	0.69	1.12	1.06	1.07	1.35	1.51	1.33
Mean		0.57			0.67			1.08			1.40	
Standard Deviation		0.00577			0.03214			0.03214			0.09866	
20 wales	0.41	0.43	0.45	0.46	0.56	0.58	0.61	0.68	0.64	0.72	0.76	0.82
Mean		0.43			0.54			0.64			0.77	
Standard Deviation		0.02			0.06429			0.03511			0.05033	
30 wales	0.35	0.37	0.36	0.43	0.41	0.4	0.44	0.48	0.5	0.5	0.58	0.59
Mean		0.36			0.41			0.47			0.56	
Standard Deviation		0.01			0.01528			0.03056			0.04933	
40 wales	0.28	0.27	0.35	0.3	0.33	0.38	0.4	0.39	0.44	0.47	0.48	0.43
Mean		0.3			0.34			0.41			0.46	
Standard Deviation		0.04359			0.04041			0.02646			0.02646	
50 wales	0.33	0.27	0.28	0.34	0.3	0.31	0.35	0.33	0.34	0.38	0.42	0.43
Mean		0.29			0.32			0.34			0.41	
Standard Deviation		0.03215			0.02082			0.01			0.02646	

Table 5.5 Experimental results of resistance values for samples with fixed number of wales and different number of courses (unit: Ω).

No. of courses	**Fixed 70 wales**			**Fixed 80 wales**			**Fixed 90 wales**			**Fixed 100 wales**		
Sample number	1	2	3	1	2	3	1	2	3	1	2	3
20 courses	0.92	0.96	0.98	1.05	1.04	1.12	1.4	1.39	1.42	1.47	1.44	1.48
Mean	0.95			1.07			1.40			1.46		
Standard Deviation	0.03055			0.04359			0.01528			0.02082		
40 courses	0.44	0.5	0.53	0.5	0.56	0.54	0.7	0.71	0.67	0.8	0.73	0.72
Mean	0.49			0.53			0.69			0.75		
Standard Deviation	0.04583			0.03055			0.02082			0.04359		
60 courses	0.43	0.37	0.4	0.4	0.4	0.39	0.57	0.59	0.52	0.68	0.66	0.65
Mean	0.4			0.40			0.56			0.66		
Standard Deviation	0.03			0.00577			0.03606			0.01528		
80 courses	0.32	0.3	0.31	0.37	0.34	0.33	0.42	0.37	0.38	0.59	0.55	0.57
Mean	0.31			0.35			0.39			0.57		
Standard Deviation	0.01			0.02082			0.02646			0.02		
100 courses	0.24	0.26	0.27	0.27	0.26	0.27	0.33	0.33	0.31	0.53	0.55	0.54
Mean	0.26			0.27			0.32			0.54		
Standard Deviation	0.01528			0.00577			0.01155			0.01		

5.4.2.2 The measurement of geometrical model related parameters

Table 5.6 Parameters related to geometric modeling.

Parameter	**d(mm)**			**w(mm)**			**h(mm)**			**r(mm)**			**θ(°)**	**β(°)**
Times	1	2	3	1	2	3	1	2	3	1	2	3	-	-
Value	0.34	0.29	0.37	1.34	1.30	1.25	2.01	2.09	2.03	0.48	0.49	0.54	30	20
Mean	0.33			1.30			2.04			0.5			-	-
Standard deviation	0.04041			0.04509			0.04163			0.03214			-	-

The parameters related to the geometric modeling of the knitted samples are evaluated, and listed in Table 5.6, where d, w, h, r, θ and β are already defined in the theoretical modeling section of this paper.

By importing the parameters related to the geometric modeling above into the established geometric model, the length of Points I to D, $\mathbf{L_{ID}}$, and Points D to F, $\mathbf{L_{DF}}$, in Figure 4 are computed. Consequently, $\mathbf{L_{ID}} \approx 1.10$ mm and $\mathbf{L_{DF}} \approx 1.60$ mm. Since the linear resistance of the conductive yarn is 1 Ω/cm, the resistance value $R_A \approx 0.11\Omega$ and $R_B \approx 0.16\Omega$.

5.4.2.3 The comparison between simulation results and experimental results

The data points connected by dashed lines are the simulated results and those connected with solid lines are the experimental data. It can be seen that the simulated results agree with the experimental data within an acceptable range of error. The following discussion is on the base of present construction (Single Pique) and normal fabric tightness.

From Figure 5.13(a), it can be observed that when the number of courses is fixed, the resistance value of the fabric is reduced in accordance with the increase in the number of wales. The reason is that when the number of wales is increased, it is the same as if the number of parallel resistors is also increased. Thus, the total resistance of the fabric is reduced. It can be seen that the resistance is drastically reduced in accordance with an increase in the number of wales, and becomes more obvious when the number of courses increase. Also evident from the figure is that when the number of courses is fixed at 100, the resistance of the fabric with 10 wales is around 1.4 Ω and with 50 wales, is markedly reduced to around 0.4 Ω. This phenomenon is because when the number of wales increase, the amount of contact resistance also increases, which result in the reduction of the total resistance. It can also be observed that when the number of wales increases to 50, the data points are very close to each other with different fixed number of courses. This phenomenon is because when the number of wales is increased to a certain number, which was supposed to be 50, the impact of the number of courses becomes irrelevant in terms of the resistance of conductive knitted fabrics. Therefore, when a relatively high resistance is required, fabrics that have more than 50 wales are not a good consideration.

From Figure 5.13(b), it can also be seen that when the number of wales are fixed, the resistance value of the fabric is reduced in accordance with the increase in the number of courses. The reason can also be due to the parallel connection of the resistors, which is the same as the situation when there are a fixed number of courses but different number of wales. From the figure, it can also be observed that in accordance with the increase in the number of courses, there is a difference in the resistances, which is similar to the situation with a fixed number of courses and different number of wales. This could be because the impact of the number of wales is greater than that of the number of courses for the resistance of fabrics. In comparing the fitting curves in Figures 5.13(a) and 5.13(b), it is evident that the experimental data in the case with a fixed number of courses are in better agreement with the simulated results than those with a fixed number of wales. It can be concluded that the fabrics were more stable when the course number is fixed. In comparing the resistance data in our previous research, it was found that the knitted structure of the Single Pique has a slightly lower resistance when the number of courses and wales are the same. Therefore, when a low amount of resistance is required, tuck stitches are more suitable for thermal knitwear designs.

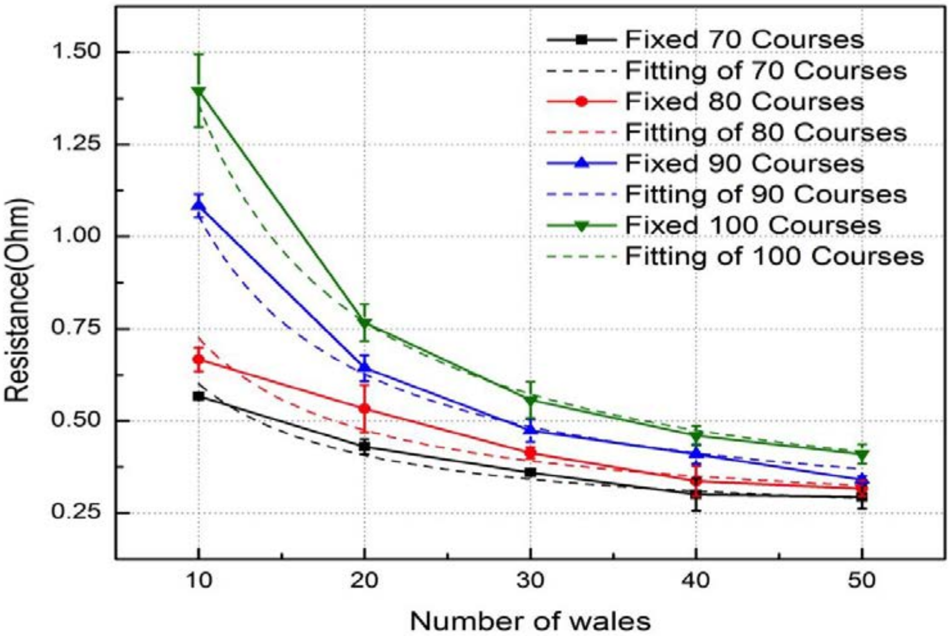

(a)

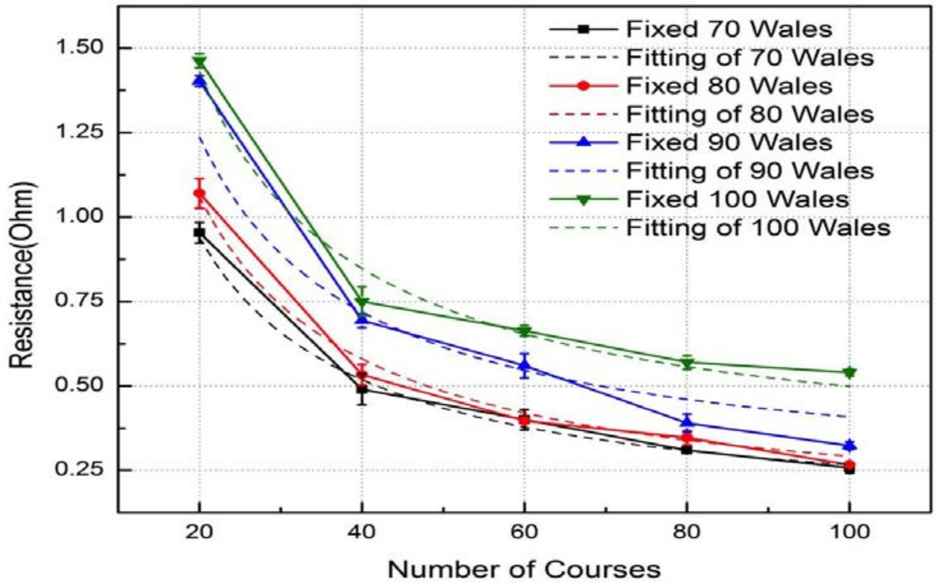

(b)

Figure 5.13 Simulated results and experimental data of resistance values for samples with (a) fixed number of courses and different number of wales, (b) fixed number of wales and different number of courses.

5.5 Conclusions

In this chapter, the resistive impact of tuck structures is systematically studied based on Single Pique structures as the research object. With the support from empirical results, it is verified that the proposed resistive network models can be very powerful method to help in the prediction of resistance values. It can be concluded that when the course number is fixed, the resistance value of the fabric will decrease according to the increase of wale number. As well, when the wale number is fixed, the resistance value of the fabric will decrease according to the increase of course number. The proposed geometrical model may be used to predict the resistive value by applying electrical theory. The developed resistive network model based on the geometrical model is verified to be an effective method to calculate the resistance properties of the conductive Single Pique knitted fabrics. It was found that tuck stitch can contribute to the decrease of whole resistance.

Up to now, knit, float and tuck stitches with conductive yarn have been systematically studied. By the new form of the resistance model, the development may bring great benefits to the industrialization of wearable electronic textile and to apparel industry by creating aesthetic, multi-functional, and high-value-added commercial apparel products. It will also be very helpful in accelerating the innovative development of smart garments. It may be useful to design conductive thermal garments with variable knitted structures to realize controllable temperature effects.

CHAPTER 6 APPLICATION OF RESISTIVITY WITH RESISTIVE NETWORK MODELS

6.1 Introduction

In previous research work, an effective system has been established for the resistive impact of different knitted structures. In this chapter, the system will be further applied and applied to the thermal function.

First, 7 samples of conductive knitted fabrics with float stitches and 7 with tuck stitches are fabricated by considering the proportions of float and tuck stitches in the entire fabric. Corresponding swatches with different structures are prepared. Then, the resistance values are measured to further add to work on resistive network models.

Then, the resistive properties of the 14 samples of conductive knitted fabrics with different structures are examined. Lastly, the impact of the different structures on the electrical properties of conductive knits is discussed.

6.2 Sample fabrication

6.2.1 Material specifications

The experimental samples were still knitted on a STOLL CMS 822 computerized flat knitting machine (H. Stoll GmbH & Co.KG). The yarns used are the same as those used in Chapter 4, which are shown in the Table 4.2 in Chapter 4. The yarn core and appearance of both types of yarns (conductive and wool) are shown in Figure 6.1.

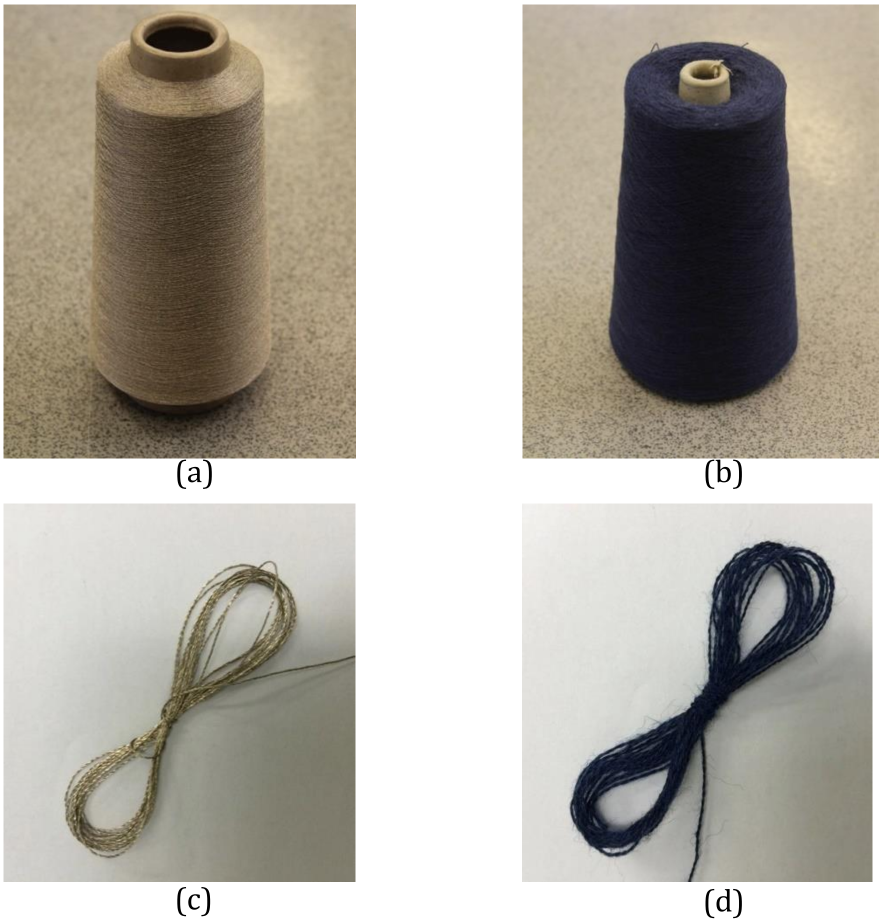

Figure 6.1 Yarn core and sample: (a) core of conductive yarn, (b) core of wool yarn, (c) sample of conductive yarn, (d) sample of wool yarn.

6.2.2 Experimental design

To further develop the resistive network models established in the present study, 7 fabric samples knitted with different proportions of float stitches are fabricated. The fabric samples are uniform in size, with a dimension of 100 courses and 100 wales, and Table 6.1 shows the knitting notations. Float knitted structures can be knitted by using the float jacquard technique for an esthetically pleasing appearance and dimensional stability. In the table, the symbols and represent the knit and float stitches respectively.

Table 6.1 Knitting notations of knitted structures with different proportions of float stitches.

Fabric with different proportions of float stitches (percentage)	**Knitting notation**
20%	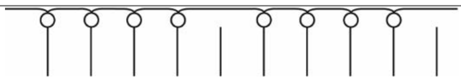
30%	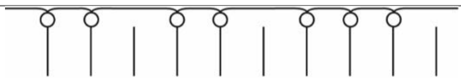
40%	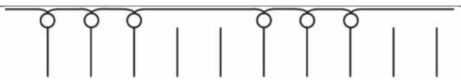
50%	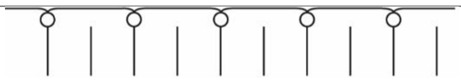
60%	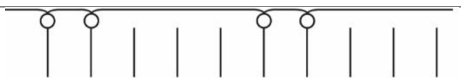
70%	

As well, 7 samples of knitted fabrics with different proportions of tuck stitches are fabricated that have the same dimensions as the fabric samples with float stitches, and Table 6.2 provides the knitting notations. For a more esthetically pleasing appearance, a double layer structure was adopted and a fine lycra yarn was used to sew the two layers together with tuck stitches. In the table, the symbols and denote the knit and float stitches, respectively.

Table 6.2 Knitting notations for knitted structures with different proportions of tuck stitches.

Fabric with different proportions of tuck stitches(percentage)	Knitting notation
20%	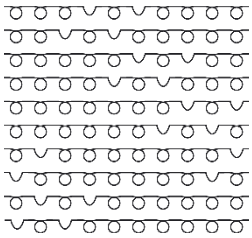
25%	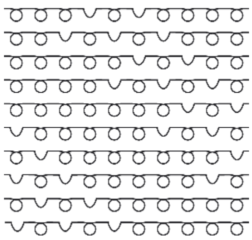
30%	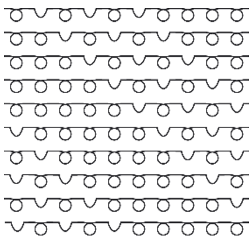
35%	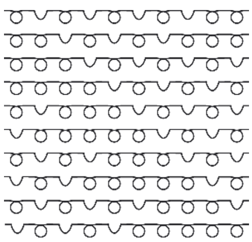
40%	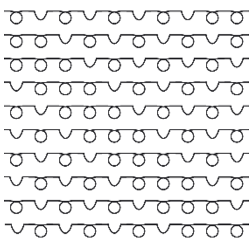
45%	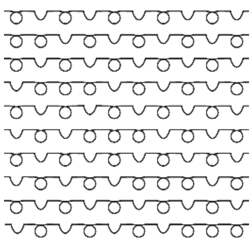

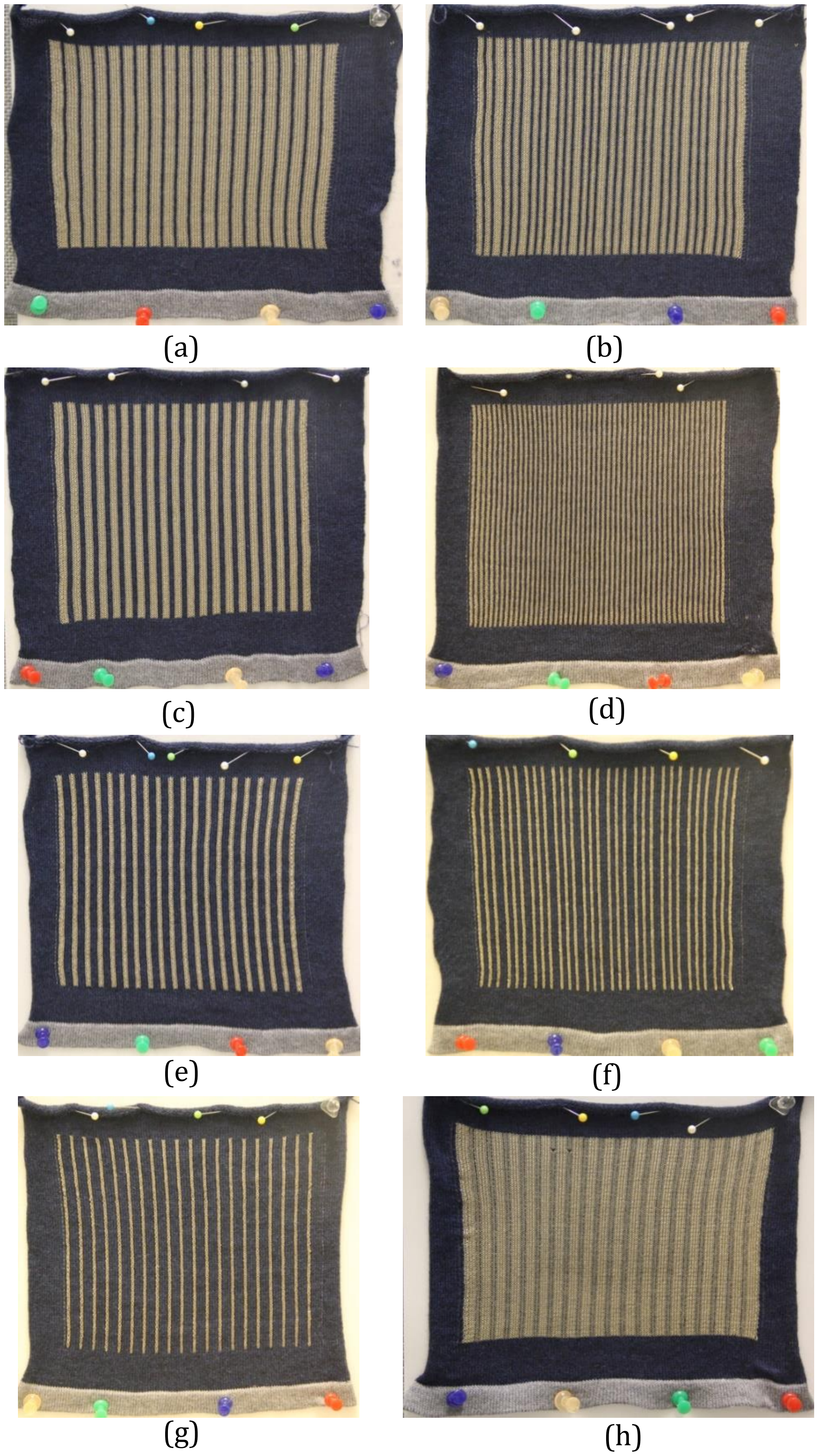

Figure 6.2 Conductive fabric samples knitted with float stitches with different proportions of float stitches: (a) 20%; (b) 30% ; (c) 40%; (d) 50%; (e) 60%; (f) 70%; and (g) 80% float stitches; and (h) 100% knit stitches.

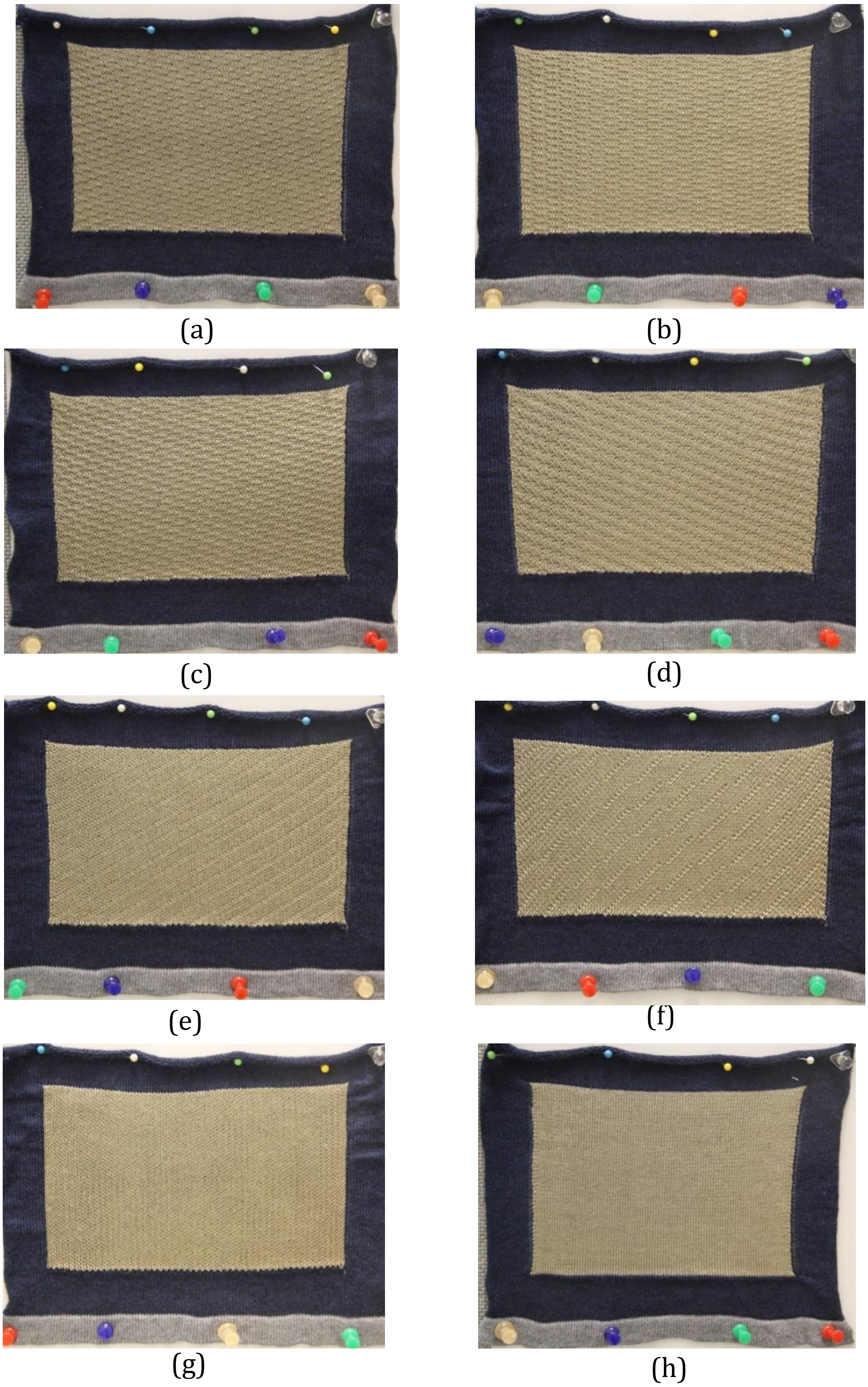

Figure 6.3 Conductive knitted fabric samples with tuck stitches with different proportions of tuck stitches: (a) 20%, (b) 25% , (c) 30%, (d) 35%, (e) 40%, (f) 45%, (g) 50% tuck stitches, and (h) 100% knit stitches.

The fabric views of the different float and tuck knitted structures with different proportions of knit, float and tuck stitches are shown in Figures 6.2 and 6.3, respectively. It can be observed that the different structures can provide a multitude of fabric surface appearances, which contribute to different thermal knitwear designs. All of the different samples were fabricated with the same 3 pieces of fabric for reproducibility.

6. 3 Experimental results

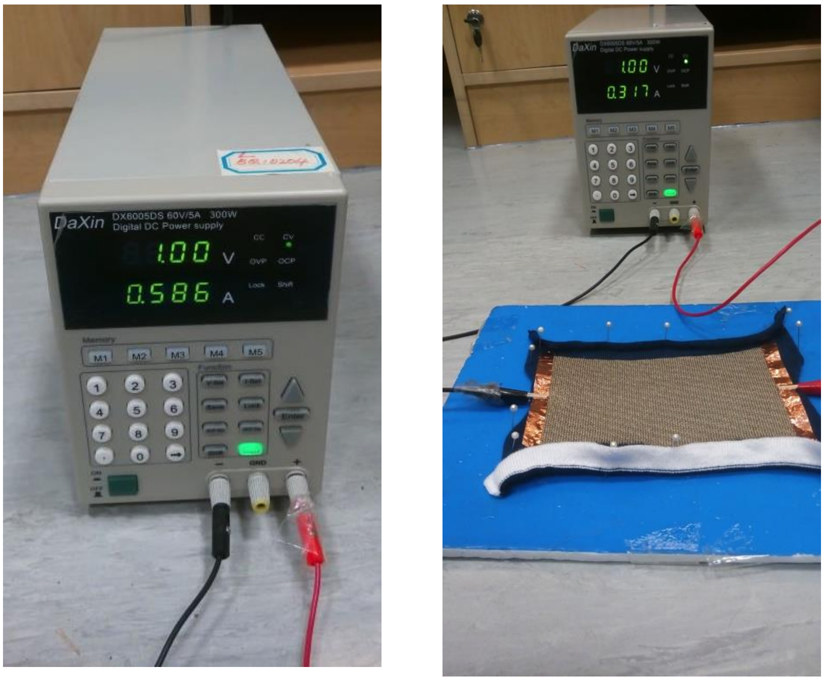

(a) (b)

Figure 6.4 (a) DAXIN digital control DC power supply, (b) Testing of conductive knitted fabric.

All the knitted samples were placed into a constant temperature and humidity chamber for 24 hours after they were removed from the knitting machine. The resistance of the individual fabric samples was measured with a DAXIN digital control DC power supply as shown in Figure 6.4(a). The electrical circuit that went through the conductive fabric samples was measured when an output of 1 V was loaded. To obtain stable and effective data, conductive paper was glued onto the edge of each sample as shown in Figure 6.4(b). The tested resistance values for the samples are listed in Tables 6.3 and 6.4.

Table 6.3 Resistance values of conductive fabrics with different proportions of float stitches (unit: Ω).

Proportion of float stitches (percentage)	Sample 1	Sample 2	Sample 3	Average
0%	1.51	1.46	1.47	1.48
20%	1.46	1.41	1.40	1.42
30%	1.43	1.38	1.40	1.40
40%	1.36	1.41	1.41	1.39
50%	1.40	1.35	1.36	1.37
60%	1.36	1.35	1.28	1.33
70%	1.31	1.26	1.32	1.30
80%	1.45	1.43	1.47	1.45

Table 6.4 Resistance values of conductive knitted fabrics with different proportions of tuck stitches (unit: Ω).

Proportion of tuck stitches (percentage)	Sample 1	Sample 2	Sample 3	Average
0%	1.51	1.46	1.47	1.48
20%	1.24	1.25	1.21	1.23
25%	1.19	1.18	1.14	1.17
30%	1.14	1.15	1.08	1.12
35%	1.05	1.06	1.11	1.07
40%	1.04	1.04	1.07	1.05
45%	1.01	0.98	0.99	0.99
50%	0.95	0.94	0.94	0.94

6.4 Discussion

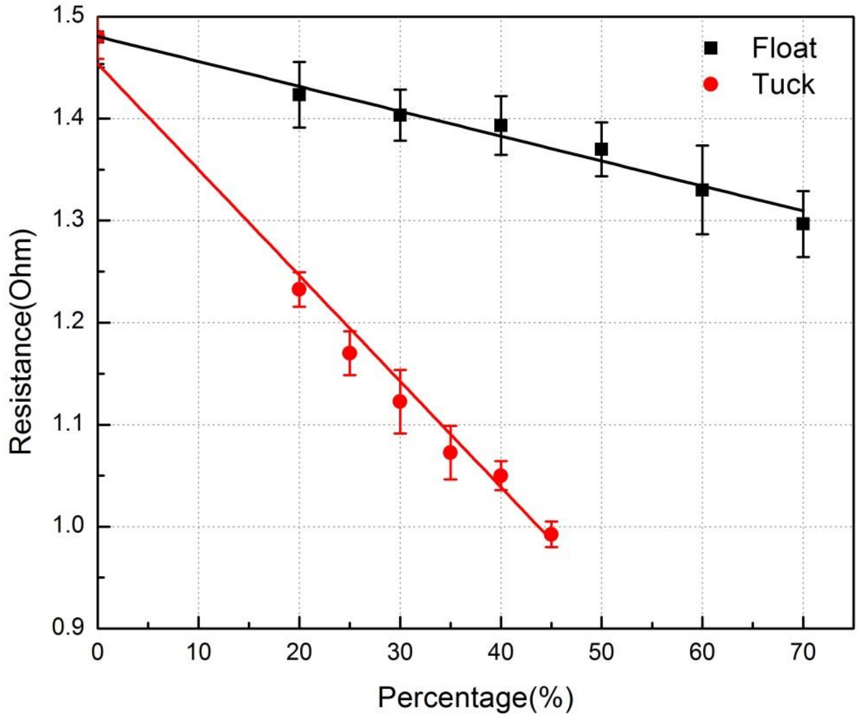

Figure 6.5 Relationship between resistance and proportion (percentage) of tuck and float stitches in conductive knitted fabrics.

The relationship between the resistance value and proportion of float and tuck stitches in the knitted fabrics is plotted in Figure 6.5. It is observed from Table 6.3 that when the proportion of float stitches exceed a certain degree (70%), the resistance value will grow up rather than decline. It is because the long float stitches will destroy the connectivity points. Therefore, in Figure 6.5, the data point is ignored. In the figure, the black squares symbolize the data from the fabric with float stitches, and red circles denote the data from the fabric with tuck stitches. From the plot, it can be seen that the relationship is linear and the fitting equation is provided in Equations (6.1) and (6.2).

$$y = -0.00255x + 1.481 \tag{6.1}$$

$$y = -0.0113x + 1.486 \tag{6.2}$$

It can also be observed in Figure 6.5 that the resistance value significantly declines with increasing number of tuck and float stitches. Therefore, this is further evidence to support the conclusions in the previous chapters. However, the experiments discussed in this chapter compare the tuck and float structures. It was found that tuck stitches are more effective in reducing the total resistance of conductive knitted fabrics. However, float stitches are also effective in reducing the resistance of conductive knitted fabrics if the cost of conductive yarns is reduced because the loop length is much shorter than that of the knit and tuck stitches, as observed from the geometrical models established in the Chapter 4. Related work on the optimal design of knitted fabrics that takes into consideration commercial appeal will be conducted in future research by this author because it is beyond the scope of this work.

From the experimental results, the resistance value of 100% knit fabric is 1.48 Ω. However, when the proportion of float stitches in the knitted fabric is 50%, the resistance value is reduced to around 1.37 Ω, and with tuck stitches, 0.99 Ω. A limitation of tuck structures is that the proportion of tuck stitches cannot exceed 50%. As for float structures, the proportion of float stitches could possibly not even exceed 70%. When the proportion of float stitches is 70%, the resistance is reduced to about 1.32 Ω. If the proportion of float stitches continues to increase, the resistance then increases instead of decreasing as the connectivity points are destroyed by the long float stitches.

6.5 Conclusion

The present chapter mainly provides experimental evidence for the two previous chapters. The chapter shows powerful macroscopic evidence that different knitwear structures could impact the resistivity of conductive knitted fabrics. That is, with an increase in the proportion of tuck and float stitches, the resistance appears to obviously follow a trend of decrease.

The relationship between conductive resistance and proportion of tuck and float stitches is plotted in Figure 6.5, in which a linear relationship is observed. Compared to float stitches, tuck stitches can reduce the total resistance to a larger degree. However, float stitches are the optimal means of reducing the resistance of knitted fabrics when less yarn is necessary or used.

In additional, for knitted structures that use float stitches, the proportion of stitches should not exceed 70%, so that stable connectivity or an optimal structure can be obtained.

CHAPTER 7 PROTOTYPES OF THERMAL GARMENTS WITH DIFFERENT KNITTED STRUCTURES IN HEATING AREAS

7.1 Introduction

Conductive knitted fabrics can be applied many ways and one of the most important applications is as heating textile materials as discussed in Chapter 2. After reviewing previous research work, resistance is found to be the main factor that influences the heating effects under external voltages. Thus, it can be concluded that the changes in knitted structures will consequently change the thermal properties of garments made from conductive thermal materials.

In this chapter, the design and fabrication of three thermal garment samples are discussed, which have different knitted structures in the heating areas. To achieve the latter, different knitting techniques are adopted which will be outlined in detail in the following sections. The heating effects are tested and presented with far – infrared images.

Different knitted structures in the heating areas can provide different heating performances. The heating temperatures can be adjusted by changing the knitted structures when the heating area has the same dimensions. This can be applied towards the design of thermal knitwear and garments in the future.

7.2 Preparation of yarn and knitted structures

With an external voltage load, the temperature of conductive knitted fabric can be calculated by using Equation (7.1):

$$\mathrm{T_s} = \mathrm{T_0} + \frac{\mathrm{U}^2}{\alpha\mathrm{R(U)}}\left(1 - e^{-\frac{\alpha t}{C_v \cdot m}}\right) \quad (7.1)$$

where $\mathrm{T_s}$ denotes the steady-state temperature, U denotes the applied voltage, α is the heat dissipation coefficient and R (U) denotes a function in which the resistance varies with U, The term $1 - e^{-\frac{\alpha t}{C_v \cdot m}} \rightarrow 1$ where the rate of energy input equals the rate of energy loss; the maximum temperature is achieved at the corresponding input power (Li et al., 2013).

For safety purposes, a low voltage of 7.4 V~12V was applied. Correspondingly, the resistance of the conductive yarn was higher, which ranged between 30 Ω ~ 80 Ω.

7.2.1 Yarn selection

In the experiment, a monofilament yarn coated with silver with a resistance of 68.6 Ω/cm was knitted together with 100% wool yarn, where the heating area was 28/2 Nm. In this way, the conductive knitted fabric could reach a temperature that would be comfortable for the human body. To avoid an unaesthetic appearance and silver oxidation, the conductive yarn was covered with regular yarn. Electrodes knitted by using conductive yarns are also necessary for connecting to the external electrical source. Table 7.1 lists the yarns used for the three prototypes.

Table 7.1 Yarns used in prototypes.

Yarn	Heating area		Electrode	Surface		
	Conductive yarn	Blended yarn		Sweater1	Sweater2	Sweater3
Appearance				 	 	  
Yarn type	Monofilament yarn coated with silver	100% wool yarn	Multifilament yarn coated with silver	100% wool yarn	100% acrylic	100% wool yarn
Other	Conductivity: 68.6 Ω/cm	28/2 Nm	Conductivity: 1Ω/cm	24/2 Nm	20/2 Nm	24/2Nm

7.2.2 Selection of fabric structure

To compare the impact of fabric structure on the heating performance of garments made of conductive thermal materials, three different structures were selected, including knit, float and tuck. For the knit structure, plain jersey is the most common; for the float structure, float 1x1 is selected; and for the tuck structure, as discussed in Chapter 5, Single Pique is selected. Their knitting notations have already been provided in the previous chapter, and therefore will not be provided again here.

7.3 Thermal knitwear design

Three sets of knitwear for men were designed in the first stage. All of the knitwear are pullovers with heatable areas in the back as shown in Figure 7.1.

(a) (b) (c)

Figure 7.1 (a) Sweater 1, (b) Sweater 2, and (c) Sweater 3.

7.3.1 Sweater 1

Sweater 1 was designed by using bold horizontal and vertical black stripes against a grey colour background, so that the pattern provided a grid effect. There were two-rectangular areas (15 cm x 15 cm) that were knitted with conductive (high resistance) and wool yarns in the back piece. Therefore, when worn, the back (dorsal) and lumbar region can be heated with the thermal function of the conductive yarn to alleviate back pain from loads. To connect the heating mechanism with an external source of power, two conductive panels adjacent to the heating areas were knitted by using conductive yarn with a much lower resistance, see Figure 7.2. Metallic dual-lock buttons were sewn onto the conductive panel area which allows a portable power supply to be stored in a small pocket underneath on the back. The small portable power supply provides 12 V of power and can be carried around. Also, this design allows ease of disassembly prior to laundering.

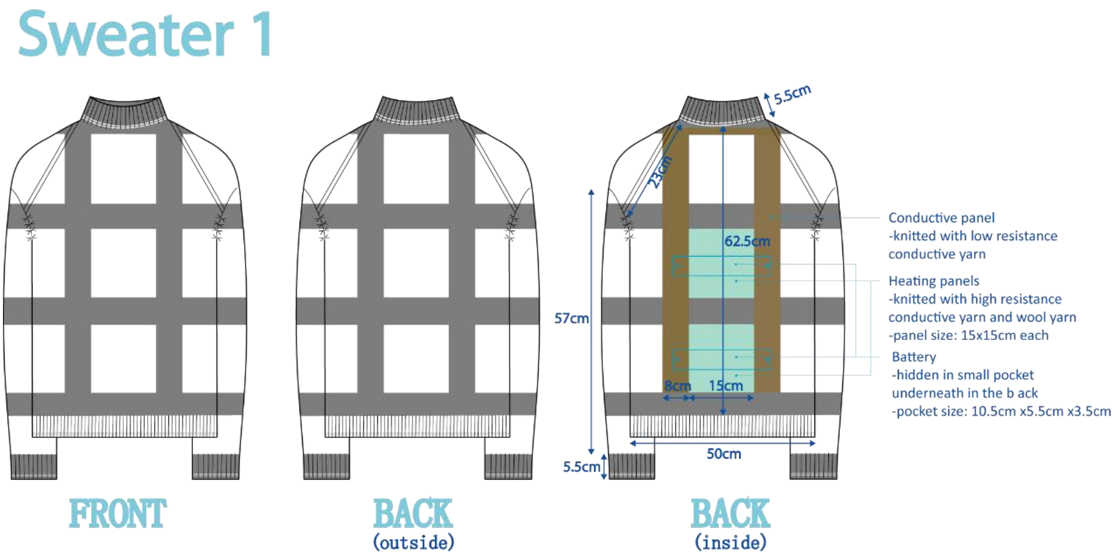

Figure 7.2 Sweater 1 sketch.

7.3.2 Sweater 2

For Sweater 2, a continuous rhombus pattern was created with a twill backing by using the jacquard technique. The technical face and back effects are different due to the pattern design and heating requirements. The heating area was placed in the back piece, which is the same as Sweater 1, and has dimensions of 15 cm x 30 cm as shown in

Figure 7.3. Near the heating area, two parallel conductive panels were extended until they reached the top of the back, which were separated with a zipper. In this way, the two conductive panels could be insulated from each other. An external power source was attached in the same way as Sweater 1. When the power source was in operation, the conductive panels, heating area, and power source together constitute a closed circuit and the heating area with relatively high resistance will generate heat.

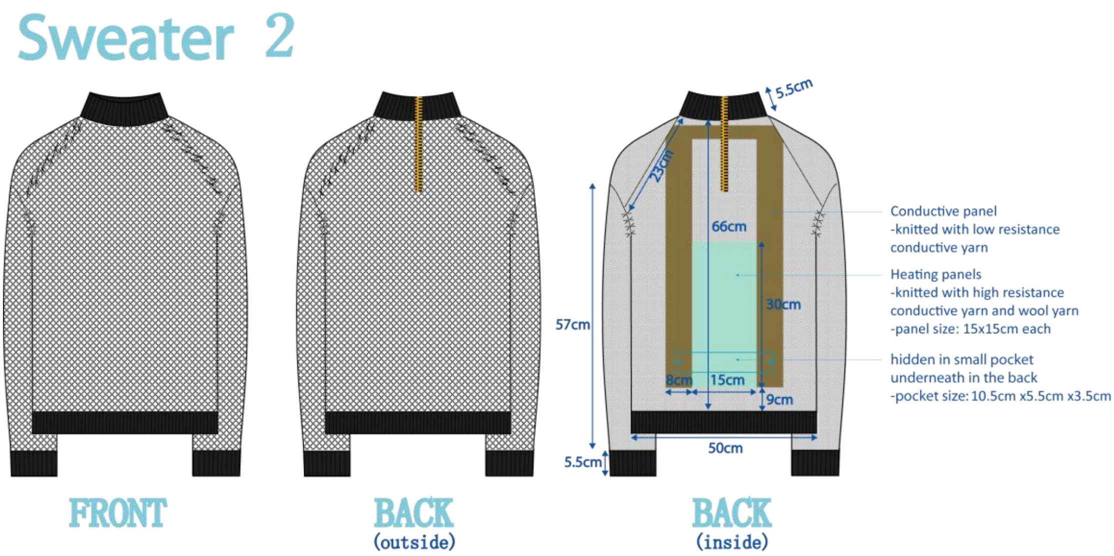

Figure7.3 Sweater 2 sketch.

7.3.3 Sweater 3

For Sweater 3, a black-grey-colour camouflage pattern was obtained by using the single jacquard technique. To realize an irregular colored pattern with single knitting, tuck stitches were used to separate the long float stitches, which can prevent the long float yarns from affecting the knitting process. As with the two previous sweaters, the heating area is 15 cm x 30 cm and placed in the back inside as shown in Figure 7.4. The sweater was designed to address back pain as a medical aid. The two belt-shaped areas inside the back piece were knitted by using high conductivity yarns to act as electrodes for contact with the battery. The heating area was knitted with low conductivity yarn mixed with wool yarn as a resistor to generate heat. Both the resistor and electrodes can be created at the same time when the garment pieces were knitted. As shown in Figure 7.4, the appearance of Sweater 3 is no different from an ordinary sweater.

Figure 7.4 Sweater 3 sketch.

All three thermal garments were designed to conceal the conductive yarn inside so that they are fashionable and practical and the heating area is near the human body to provide a good thermal effect.

7.4 Thermal knitwear fabrication

7.4.1 Sweater 1

The garment was created by first using the STOLL M1 Plus pattern software. The front, back and sleeve pieces are shown in Figure 7.5. Fully fashion technology is adopted here so that the knitted panels are individually shaped by using a linking operation.

To increase the aesthetics, all of the conductive yarns were knitted on the technical back of the fabrics, which was carried out by using the three-layer knitting on flat knitting machines.

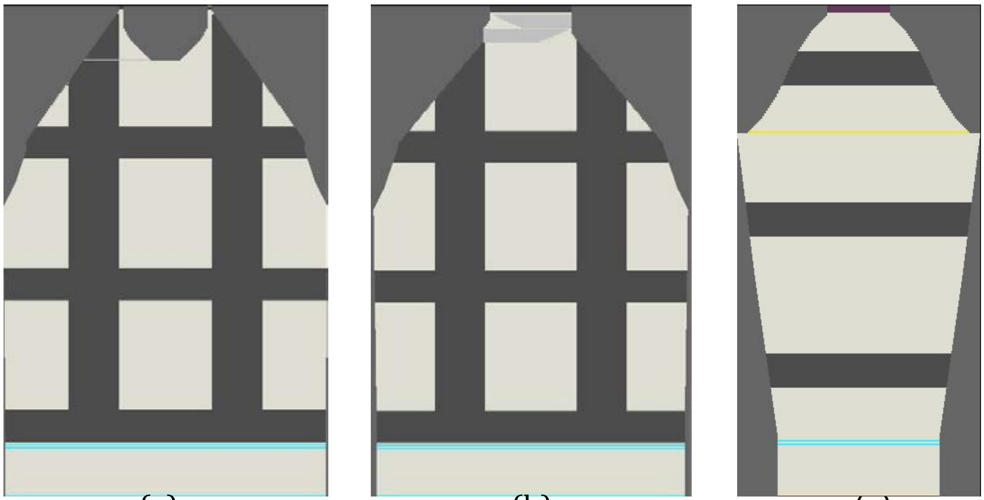
(a) (b) (c)

Figure 7.5 (a) Front, (b) Back, (c) Sleeve pieces of sweater produced with STOLL M1 Plus software

As shown in Figure 7.6(a), the front layer was knitted with normal yarn in accordance with the design pattern, and back layer is partially knitted with conductive yarns for generating heat when an electrical current passes through. For a smooth fabric surface, a middle layer knitted with fine spandex yarn was placed between the front and back layers as shown in Figure 7.6(a). It can be seen that the fabric that has a middle layer has a superior appearance. Besides, another advantage is dimensional stability, i.e., the

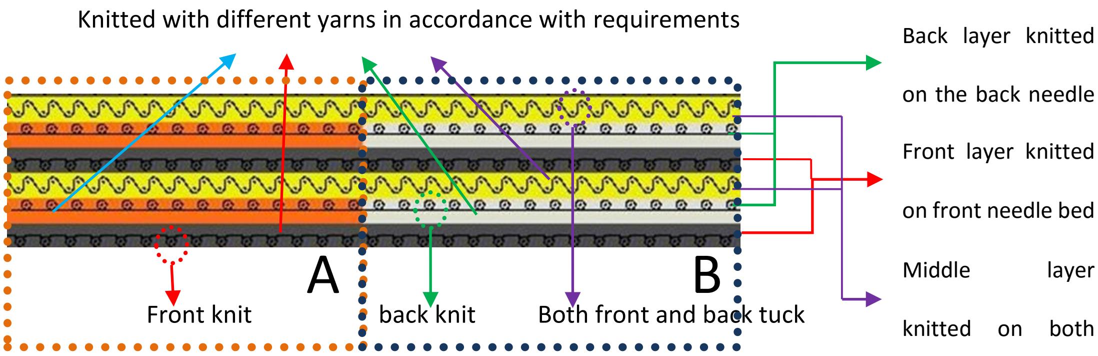

(a)

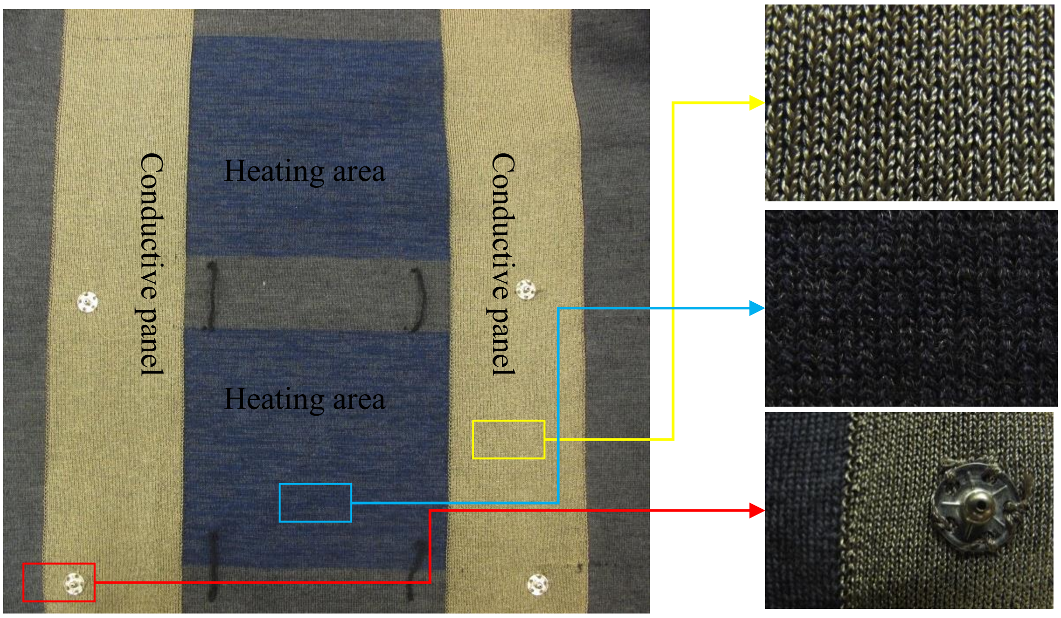

(b)

Figure 7.6 (a) Three-layer knitting with STOLL M1 Plus software, (b) Conductive panels and heating areas - partially enlarged views.

three-layer fabric has better dimensional stability compared to ordinary knitted fabrics. Different yarns were used to knit the three layers as well as different colour sections individually. The front layer was knitted with wool yarn in a grey or black colour. The middle layer connects both the front and back layers with tuck stitches on both sides by using elastic yarn (1 x 20/70 Lycra/Nylon DuPont). As shown in Figure 7.6(b), the elastic yarn cannot be seen from the outside due to the use of tuck stitches. The back layer was knitted with both wool and conductive yarns. In the technical row, different yarn feeders were used, for example, in Figure 7.6(a), two different yarns are used to knit the back layers in Sections A and B so that there are different colours in the back side.

Figure 7.7 Portable external power source.

The front, back and sleeve pieces were produced on a STOLL CMS 822 E7.2 computerized flat knitting machine. Figure 7.6(b) shows the heating area inside the back piece. A metallic dual-lock button is sewn onto the conductive panel with conductive yarn. A portable power source (Figure 7.7) was attached to the conductive panels with the metallic dual-lock buttons on the two ends, the size of which was 10.5 cm (length) x 5.5 cm (width) x 3.5 cm (height).

After the fabrics were removed from the knitting machine, a linking machine was used to connect them together with smooth edges. The front and rear views of Sweater 1 are shown in Figure 7.8. From the figure, the thermal garment appears to be the same as an ordinary garment, which will not cause embarrassment or draw attention to the user.

(a) (b)

Figure 7.8 (a) Front view and (b) Rear view of Sweater 1.

7.4.2 Sweater 2

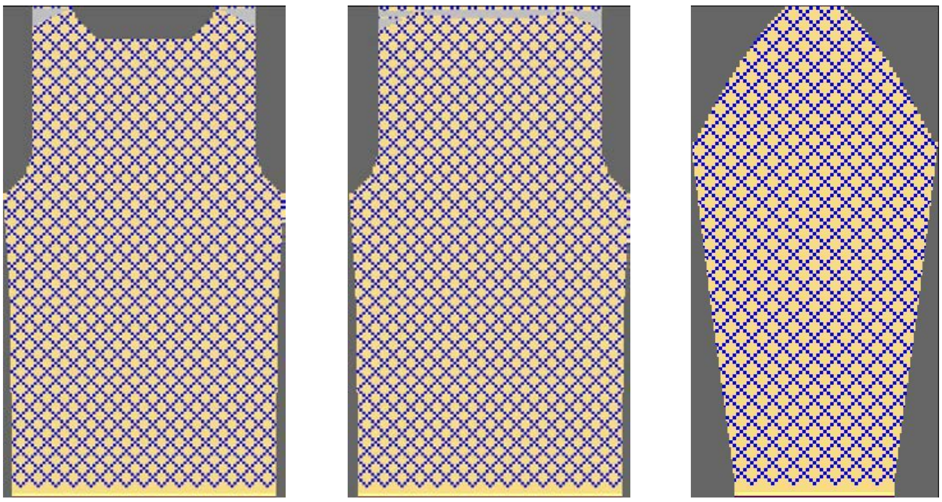

(a) (b) (c)

Figure 7.9 (a) Front, (b) Back, and (c) Sleeve pieces of Sweater 2 by using STOLL M1 Plus software.

As with Sweater 1, Sweater 2 was also knitted by using a STOLL computerized flat knitting machine. Therefore, the M1 Plus System was used to make the individual pieces first and the front, back and sleeve pieces are shown in Figure 7.9.

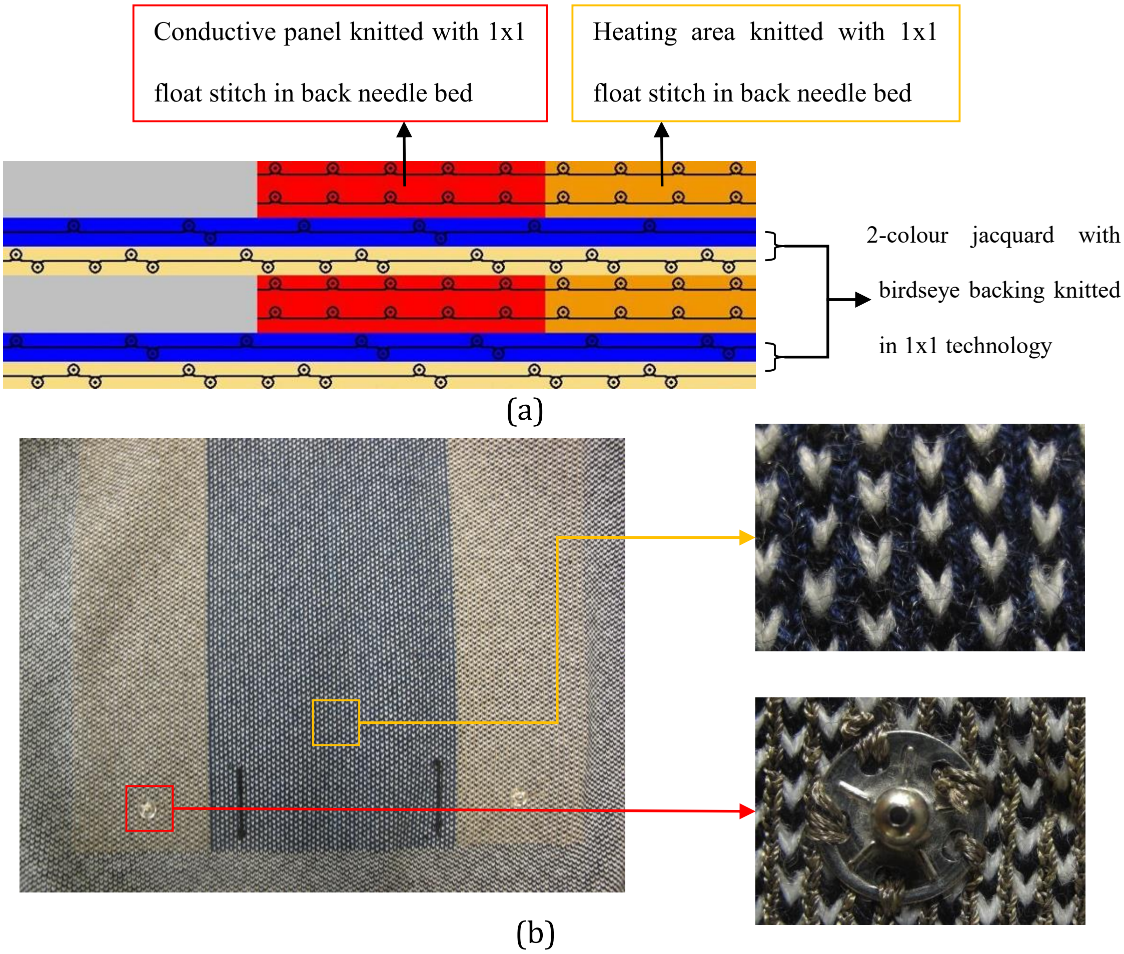

Figure 7.10 Sweater 2: (a) 1x1 structure with Stoll M1 Plus software, and (b) Conductive panels and heating areas - partially enlarged views.

1x1 technology in flat knitting was used to conceal the conductive yarns in the backside of double-jacquard knitted fabric. 1x1 technology in flat knitting means that one needle is used and alternated with another needle out-of-used during knitting, i.e., in the knitting area, only one of the two needles are used for knitting. As shown in Figure 7.10(a), a 2-colour jacquard is knitted in a 1x1 structure and empty needles are used to knit the conductive panels and heating areas into a 1x1 float knitted structure. It can be seen from Figure 7.10(b) that the conductive and normal yarns are knitted in alternate wales. In this way, the conductive yarns are all concealed in the rear of the sweater.

After programming, the sweater was fabricated by using the same machine as Sweater 1 and the front and rear views are shown in Figure 7.11. It can be observed that the electronic components are not evident and thus cannot be distinguished as a thermal garment.

(a)

(b)

Figure 7.11 (a) Front and 2 (b) Rear views of Sweater 2.

7.4.3 Sweater 3

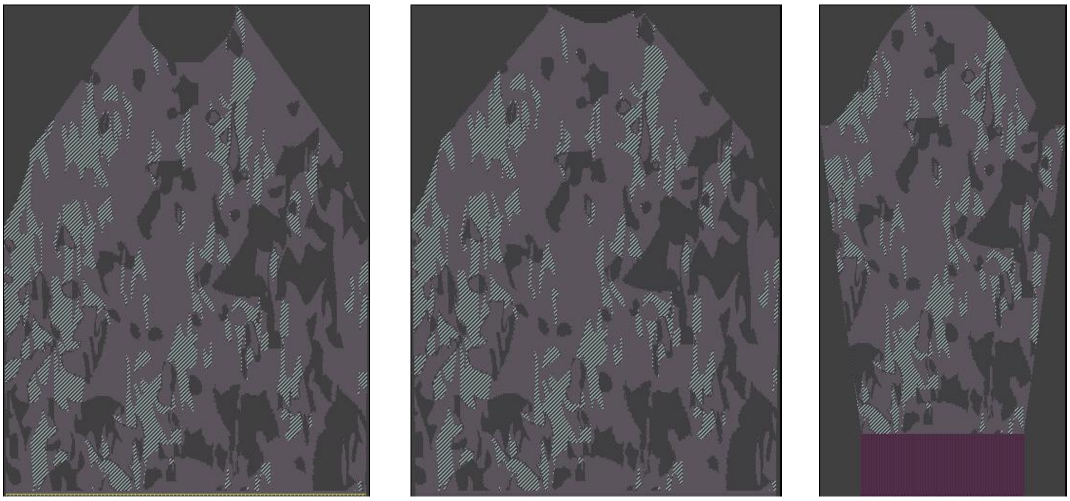

(a) (b) (c)

Figure 7.12 (a) Front, (b) Back, and (c) Sleeve pieces with use of STOLL M1 Plus software.

Sweater 3 was also made by using a STOLL computerized flat knitting machine; thus, the pieces of the front, back and sleeve were first generated by using STOLL M1 Plus software. The pieces are shown in Figure 7.12.

To achieve a colorful effect with a thin handfeel, a structure of a single-jacquard combined with 3-layers was adopted. The 3-layer structure was discussed in Section 7.4.1. Single-jacquard is usually used for small patterned areas which cannot be knitted with long float stitches. To knit a single jacquard pattern with long float stitches, tuck stitches can be knitted into every fourth float stitch. This is the most effective way for knitting single jacquard fabric with unlimited patterns. Figure 7.13(a) illustrates the 3-layer fabric with a single-jacquard pattern. It can be seen that the single jacquard which uses alternate tuck stitches is knitted on a front needle bed and conductive yarns are knitted on the back needle bed for the conductive panels and heating area, which does not affect the aesthetics. Between the two layers, spandex yarns were tuck stitched on both needle beds to knit the middle layer. Figure 7.13(b) shows the conductive panel and heating area.

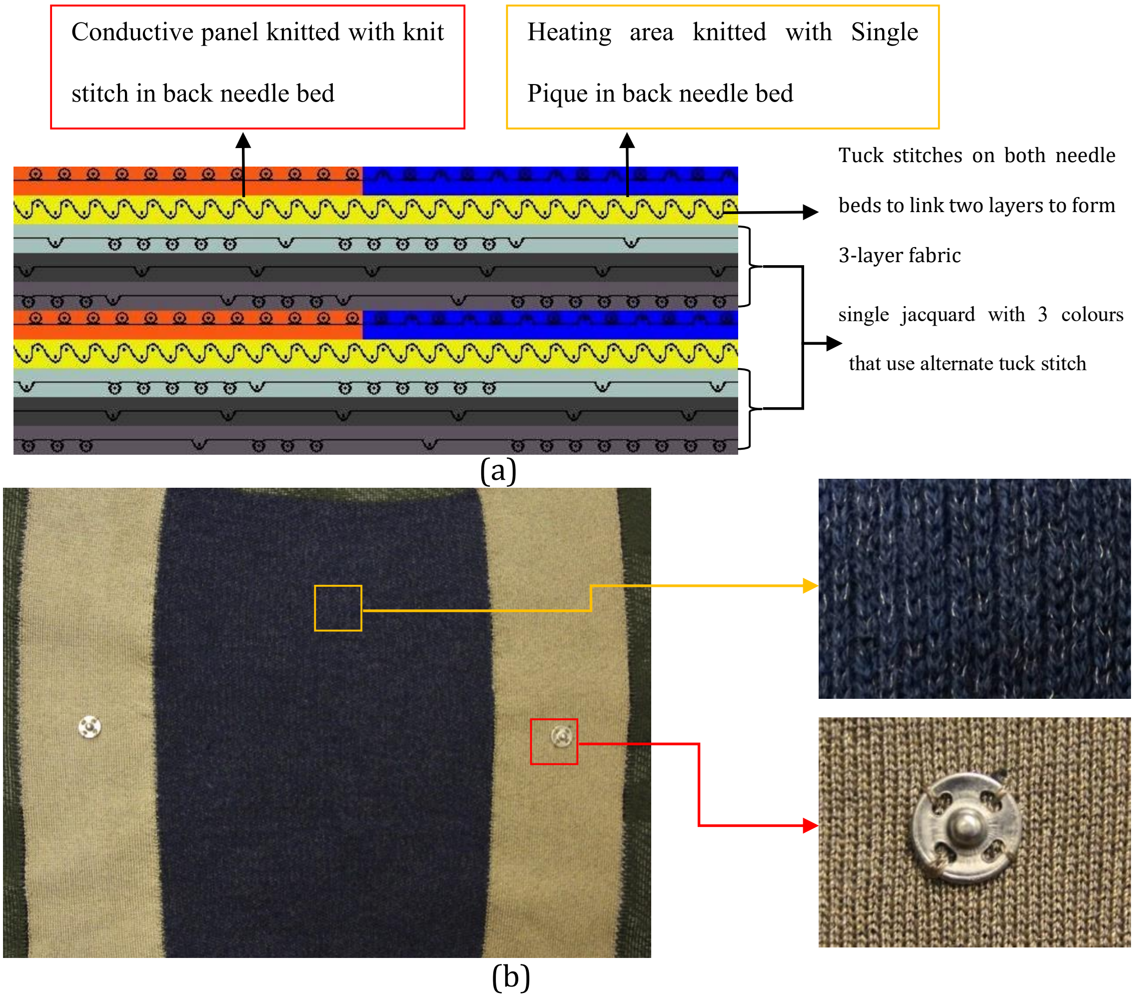

Figure 7.13 Sweater 3: (a) Single jacquard with 3 colours and 3 layers with use of STOLL M1 Plus software, and (b) Conductive panels and heating areas- partially enlarged views.

By linking the front, back and sleeve pieces together, Sweater 3 was produced as shown in Figure 7.14.

(a) (b)

Figure 7.14 (a) Front and (b) Rear views of Sweater 3.

7. 5 Thermal properties of developed garments

7.5.1 The measurement of thermal properties of developed garments

To observe the thermal properties of the thermal garments with different knitted structures of the heating area, an external power source of 12 V was used on the conductive panels, and the temperature in the heating area was recorded by using a far-infrared camera (FLIR E33 Infrared Thermal Imager) for 5, 10, 15 and 20 minutes, respectively. The recorded photographs are shown as Figures 7.15(a) to 7.15(f).

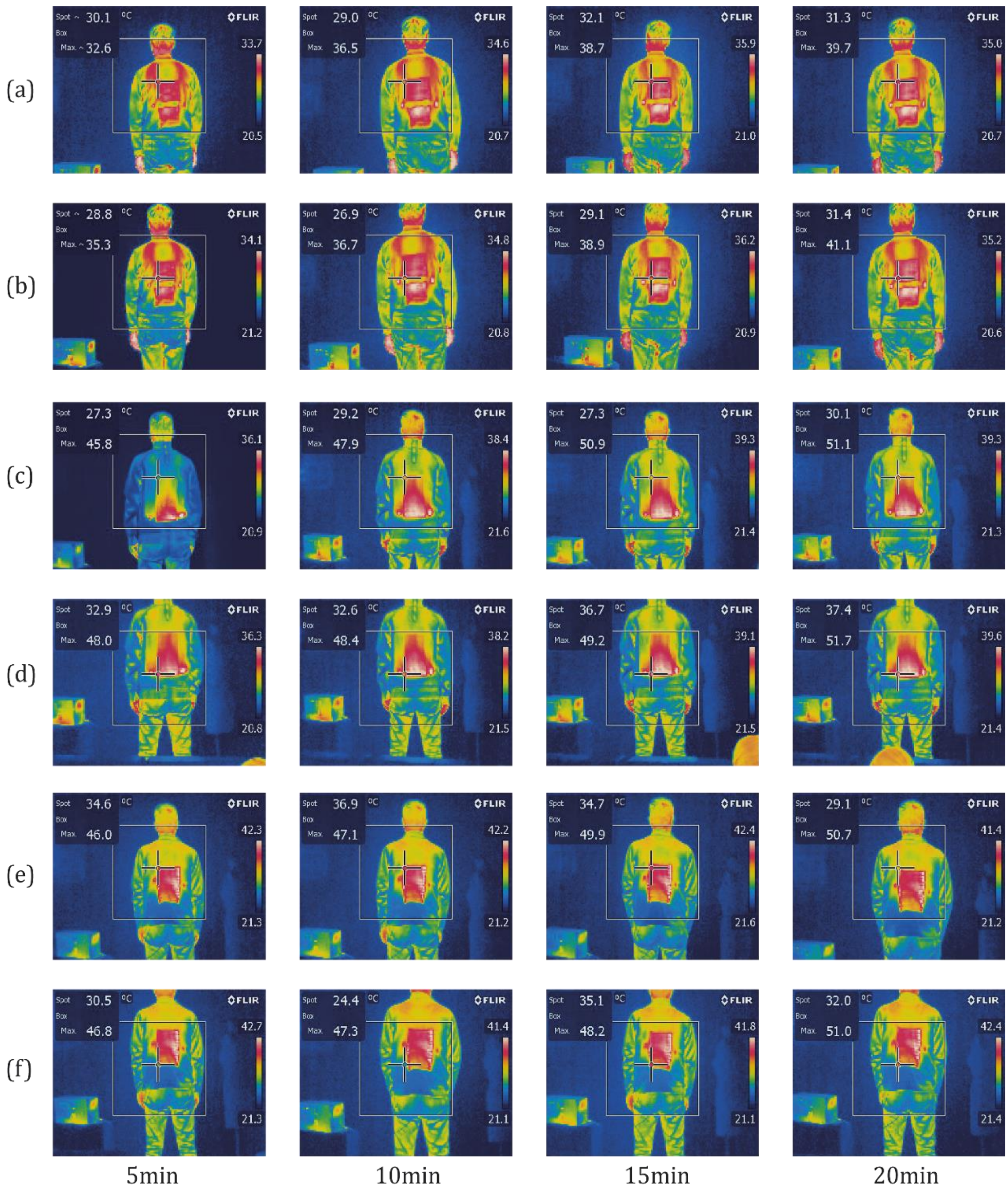

Figure 7.15 Far-infrared images after loading voltage for 5, 10, 15 and 20 minutes in different spots for (a) and (b) Sweater 1, (c) and (d) Sweater 2 and (e) and (f) Sweater 3.

It can be observed that the heating temperature is different in the three sweaters when the external voltage was loaded at the same time. Therefore, it can be concluded that the structure design of the thermal garment is an effective way to improve the thermal properties.

7.5.2 Discussion

From Equation (7.1), the steady-state temperature T_s is a variable which is changed with time t. When t is long enough, T_s will keep in a relatively fixed value, which is linearly proportional to the input power and inversely proportional to the thermal conductively coefficient, which is determined by the fabric parameter.

For the present thermal garments, due to that external power source is uniformed to be 12V, the temperature difference to illustrate the different thermal properties is actually inversely proportional to the thermal conductively coefficient. As concluded in the resistance-structure system, the resistance values are variable with the different knitted structures which has been deeply discussed in Chapter 4 and 5, respectively. As well, the situations are different in case of external power are loaded in wales direction and that in course direction. The corresponding resistance value can be derived by Equation (4.18), Equation (4.22), Equation (5.17) and Equation (5.23).

Due to that wales number and course number in the heating area are not very small, which means that the course number $M \gg 1$ and wales number $N \gg 1$. The Equation (4.18) can be simplified into Equation (7.2) and Equation (5.23) can be simplified into Equation (7.3).

$$R \approx (R_2 + R_3)\frac{N}{M} \tag{7.2}$$

In which R_2 and R_3 is calculated by Equation (4.11) and Equation (4.12). The simplification stands on the principle that $a + b \approx a$ when $a \gg b$. And the real value for R_2 and R_3 can be derived by the experimental data as described in Chapter 4.

$$R = (\frac{R_1}{2} + R_2)\frac{N}{M} \tag{7.3}$$

In which $R_1 = R_A + 2\Delta r$; $R_2 = 2\Delta r$. The real value for R_1 and R_2 can be derived by the experimental data as described in Chapter 5.

Thus, the resistance value for a knitted fabric can be summarized to be Equation (7.4).

$$R = \rho\frac{N}{M} \tag{7.4}$$

In which, ρ is a coefficient which varies with the knitted structure. The value can be measured by experimental data. Therefore, the temperature of conductive knitted fabric can be calculated by Equation (7.5).

$$\mathrm{T_s} = \mathrm{T_0} + \frac{\mathrm{U}^2 M}{\alpha\rho\mathrm{N}}(1 - e^{-\frac{\alpha t}{C_v \cdot m}}) \tag{7.5}$$

Based on the above discussion, a system used to demonstrate the predictability and guidance of the proposed simulation models for designing the knitting structures of thermal knitwear to meet the desired heating temperature can be developed as shown in Figure 7.16.

It can be investigated that according with the demand of appearance and function, the proposed simulation models for designing the knitting structures of thermal knitwear to meet the desired heating temperature can be developed. The garment style and selected knitted structures can be preliminarily designed by the demand appearance and thermal effect and target temperature can be preliminarily confirmed by the thermal effect. Then, according with the garment style and selected structure, the test piece to simulate the real heating area can be knitted. Thus, according with the sample piece, the conductivity coefficient ρ and the heat dissipation coefficient α can be evaluated. Together with target temperature, the resistance value R of heating area under a known external voltage can be calculated, thus, the ratio between M and N can be evaluated. According with the designed heating area which is developed from the garment design, the size of the heating area (i.e. course number and wale number) can be confirmed. If the calculated size is not meet the demand of designed garment. A substitutional structure will be used according with the principle developed from the resistance – structure system which is developed in the present study.

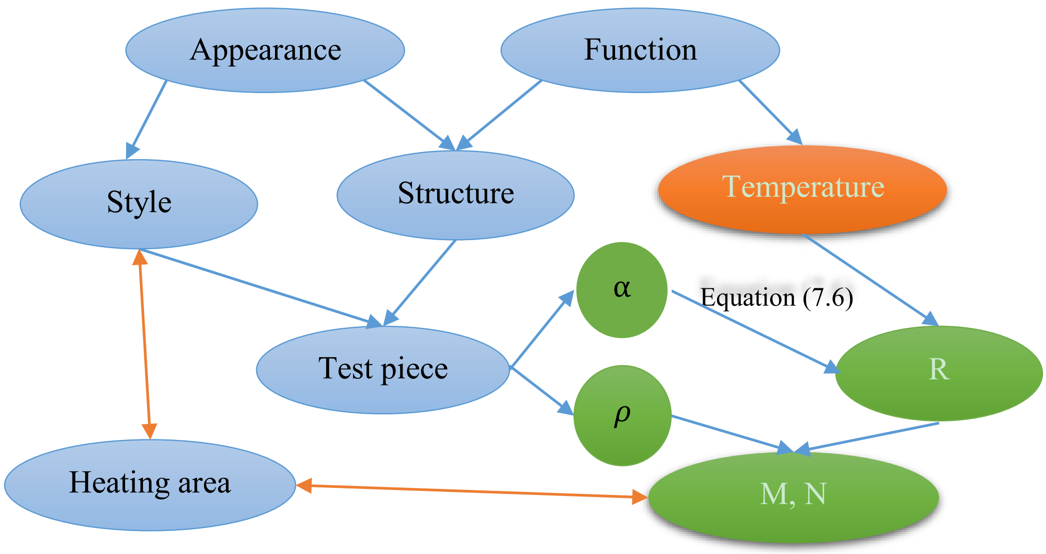

Figure 7.16 The proposed simulation models for designing the knitting structures of thermal knitwear to meet the desired heating temperature.

7.6 Conclusion

In this chapter, three thermal knitted garments that were developed with different conductive knitted structures are discussed. To compare the influence of structure differences on thermal properties, different knitted structures are used in the heating areas. In Sweater 1, the conductive yarns are embedded into the fabric by only using a knit stitch. A 1x1 float structure is used in Sweater 2 and Single Pique structure in Sweater 3 in the conductive knitted area, respectively. As well, a far-infrared camera is used to record the electrical properties of the heating area in all three sweaters.

The exceptional properties and qualities of the prototype are concluded as follows.

1. Unlike PCB panels, the conductive path and thermal area can be knitted and concealed inside garments so that the original design is not affected; however, products on the market, such as the WarmX heatable garments suffer from such a problem.
2. The prototypes in this study combine patterned design with thermal function together by using a feasible physical theory since resistance variation can be achieved by the pattern design which will thus influence the thermal function based on the proposed resistive network model and corresponding theoretical analysis.
3. Since knitted structures are an influential factor on thermal effects, it becomes possible to provide a multitude of different temperatures and heated areas with different knitted structures with the same material as shown in Figure 7.16.
4. Fully fashion technology can be adopted for flat knitting, which allows the fabric to be fabricated without extra steps, for example, cutting and sewing.
5. Lastly, the prototypes can reduce energy costs and save on energy which is environmentally friendly and conserves power.

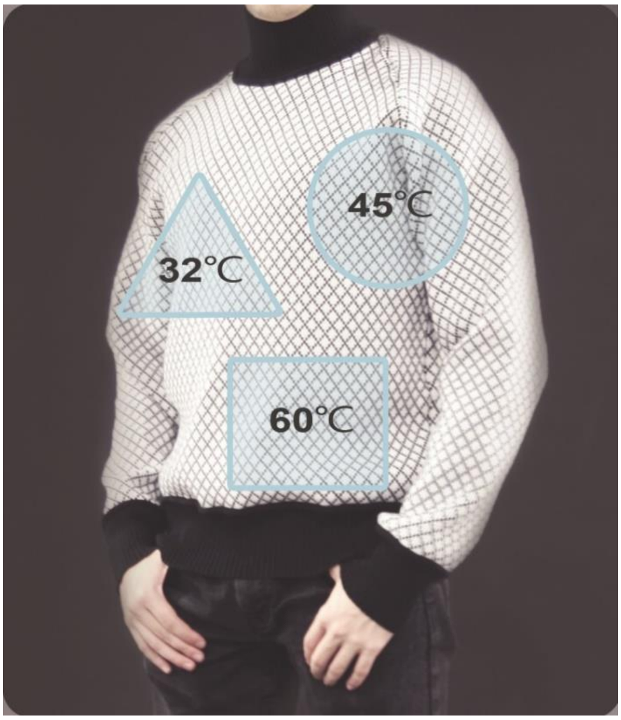

Figure 7.17 Different temperatures and heated areas in prototype.

The proposed thermal knitwear can be applied in many circumstances, such as in ordinary and outdoor clothing products, household articles, medical care products and other potential areas where soft thermal is required. As the thermal properties are not the focus of the present study, thermal performance of the sweaters will not be further discussed in this thesis.

CHAPTER 8 CONCLUSION AND FUTURE WORK

8.1 Conclusion

In this thesis, the main goal is to study the influence of different structures on resistivity of conductive knitted fabrics. To do so, the fundamental elements of knitting technology have been examined and corresponding resistive network models established based on different geometrical models. To verify the resistive network models, corresponding experiments have been carried out and a series of prototypes of thermal garments with different structures in the heating areas are developed.

First, a comprehensive related literature review has been conducted to include all aspects of current electrical textiles, the conductive paths in conductive knitted fabrics and fabrics for thermal knitwear. The information is used to determine an effective way to develop conductive knitted fabrics with different knitwear structure designs. The purpose of the review is to carry out a thorough investigation of the previous research and products of conductive knitted fabrics. This research then examined an effective means to predict the resistance value of conductive knitted fabrics with different structures. This work can therefore serve as a theoretical guide when developing conductive knitted products.

Based on a classical model developed by Munden (1959), planar geometrical models for knit, float and tuck have been established, respectively. To study the resistive properties, basic float structures and a typical tuck structure-Single Pique are selected. The resistive network models are proposed for predicting the resistance values. To simplify the models and allow the values to be calculated, contact resistance caused by the overlapping of two conductive yarns is distributed to their neighbouring branches as linear resistance. In this way, the proposed resistive models are computable and the resistance values for different knitted structures can be calculated.

Different conductive knitted fabrics with said structures have been fabricated and their resistance values measured. The resistive network models prove to be a valid means of determining the resistive properties through the conducted experiments. Therefore, the proposed models can be used to guide the development of related conductive knitwear products. Based on the models, three thermal knitted garments with different knitted structures in the heating area are designed and fabricated. The thermal performance demonstrates the predicted effects through a general observation.

The present research is a systematical study on the resistive properties of conductive knitted fabrics from the viewpoint of a single knit cell. The findings are concluded as follows.

1. Both float and tuck stitches can be used to reduce the total resistance of knitted fabrics. The resistive properties of conductive knitted products can be adjusted by changing the design of the knitwear structure.
2. For knitted structures with float stitches, the proposed model is suitable for 1x1, 1x2, 1x3 and 1x4 float structures. The model does not work for a 1x5 float structure or beyond. The reason is that the float yarn is too long so that the connectivity is weakened. Therefore, when designing a knitted structure with float stitches, it is recommended that long float structures are avoided.
3. For knitted structures that use tuck stitches (Single Pique here), it is found that these

can be the optimal structure for reducing the total resistance of knitted fabrics as opposed to float structures. As well, Single Pique fabric has a smoother and tight appearance in comparison to knitted fabric with a float structure. Therefore, to reduce the total resistance, tuck structures can be given primary consideration.

4. In thermal knitted garments, the temperature of the heating area with tuck and float structures could be over 50°C, while the garment that uses only a knit structure is about 40°C. Therefore, modifying the knit stitch to partially using tuck or float stitches could substantially improve the thermal performance.
5. The proposed models can allow the designing of thermal garments with controllable temperatures or different heating effects in different regions. Thus, smart thermal garments that are high technology and quality can be developed.

8.2 Limitations

Some limitations should be considered when applying the proposed models to produce conductive knitted products, which are discussed below.

1. The theoretical models here are based on geometrical models but not dynamic and computational intensive mechanical models. To better simulate the electromechanical properties of conductive knitted fabrics and their application in smart textiles, geometrical models are not the best for simulating electrical properties.
2. The proposed models may not really reflect the construction of 3D knitted fabric and some resistive models cannot present the real conductive conditions of the conductive fabrics, thus, the predicted resistance will be affected.

3. All of the products of the models and experiments are supposed to be used under a relaxed state. However, during wearing, the fabric may be deformed by body movement. Therefore, this is also a limitation as there are situations when body movement is frequent and irregular.

8.3 Future work

The present study focuses on the resistive properties of conductive knitted fabrics on the basis of knitted element cells. It provides a systematical means for analyzing the resistance values of conductive knitted fabrics with different structures that is understood from a micro view. Further related research can be conducted by considering the following points.

1. The research methods could be further improved by developing models that are understood from a macro view to analyze the impacts of the structure on resistance. In Chapter 6, the experiments are conducted to observe the impact of different proportions of knitting elements on the resistance of conductive fabrics. A further theoretical analysis should be carried out. This is also helpful for the prediction of complicated structures.

2. The knitted structures could be further enriched so that the system is more useful. The present study only focuses on the most basic single knit fabrics-single jersey, and basic float and Single Pique structures. In future work, different tuck structures should be considered as well as double knitted fabrics, for example, ribs, Milano, cardigan and other common structures. Therefore, a more versatile method could

be established.

3. The applications of the properties of thermal garments could be further researched. In Chapter 7, the thermal properties of conductive knitted garments are investigated by using a far-infrared camera. This just provides an approximate idea. The thermal properties could be studied in more detail and more scientifically, and as well, support with theories is necessary.

4. More intelligent thermal garments could be developed by applying different knitwear structures in different regions of garments. Since heating temperature is controllable and dimensions of the heating region can be changed, these could significantly increase the commercialization and user friendliness of thermal knitted products.

5. Some factors which can represent the dynamic tension, load force and structure deformation should be included into the models. As the garments will be stretched and deformed during wearing. A model considering external force would be better for the simulation of actual service condition. Thus, a dynamic model is preferred instead of geometrical model in the future.

This thesis uses an integrated research method to study the resistive properties of conductive knitted fabrics with different knitted structures. The related models are established on the basis of geometrical models and the resistive network models are simplified by applying the electrical theory. However, textile materials are flexible, with physical, mechanical, elastic and dynamic properties. Therefore, if future researchers with related backgrounds are interested, the work could very well be furthered, with integration of physical or mechanical models, which will greatly add to the current work.

Appendix

Clear [h,w,r,d, θ, α,AB,BC,CF,FG,GH,ID,DE,EJ,x]

h=2.04;

r=0.5;

w=1.3;

θ=Pi/6;

α=Pi/9;

d=0.33;

$$AB = Table[\{x, -\sqrt{}((0.5\sqrt{}((r*Cos[\alpha]-\frac{d}{2})^2+(\sqrt{r^2-(\frac{d}{2})^2}-r*Sin[\alpha])^2)\Big/Cos[\alpha])^2 - (x+0.5\sqrt{}((r*Cos[\alpha]-\frac{d}{2})^2+(\sqrt{r^2-(\frac{d}{2})^2}-r*Sin[\alpha])^2)\Big/Cos[\alpha] + \frac{d}{2})^2),0\},\{x,-r*Cos[\theta],-\frac{d}{2},0.005\}];$$

$$BC = Table[\{x, \frac{h-\sqrt{r^2-(\frac{d}{2})^2}}{\frac{d}{2}-r}(x+\frac{d}{2}),0\},\{x,-\frac{d}{2},-r,-0.005\}];$$

$$CF = Table[\{x, \sqrt{r^2-x^2}+h-\sqrt{r^2-(\frac{d}{2})^2}, -0.1(\sqrt{r^2-x^2}+h-\sqrt{r^2-(\frac{d}{2})^2})\text{^}2 + 0.25\},\{x,-r,r,0.005\}];$$

$$FG = Table[\{x, -\frac{h-\sqrt{r^2-(\frac{d}{2})^2}}{\frac{d}{2}-r}(x-\frac{d}{2}),0\},\{x,\frac{d}{2},r,0.005\}];$$

$$GH = Table[\{x, -\sqrt{}((0.5\sqrt{}((r*Cos[\alpha]-\frac{d}{2})^2+(\sqrt{r^2-(\frac{d}{2})^2}-r*Sin[\alpha])^2)\Big/Cos[\alpha])^2 - (x-0.5\sqrt{}((r*Cos[\alpha]-\frac{d}{2})^2+(\sqrt{r^2-(\frac{d}{2})^2}-r*Sin[\alpha])^2)\Big/Cos[\alpha] - \frac{d}{2})^2), -x\hat{}2+0.1\}, \{x, \frac{d}{2}, r*Cos[\theta], 0.005\}];$$

$$ID = Table[\{x, 2(\frac{h/2}{2rCos[\theta]-w}*(-w+r*Cos[\theta])-\sqrt{r^2-(\frac{d}{2})^2} + \frac{h/2*r*Cos[\theta]}{2r*Cos[\theta]-w}+r*Sin[\theta])-(\frac{h/2}{2rCos[\theta]-w}*x - \sqrt{r^2-(\frac{d}{2})^2}+\frac{h/2*r*Cos[\theta]}{2r*Cos[\theta]-w}+r*Sin[\theta]), -0.33\}, \{x, -w+r*Cos[\theta], -r*Cos[\theta], 0.005\}];$$

$$DE = Table[\{x, \sqrt{r^2-x^2}+h-\sqrt{r^2-(\frac{d}{2})^2}, -0.33\}, \{x, -r*Cos[\theta], r*Cos[\theta], 0.005\}];$$

$$EJ = Table[\{x, 2(-\frac{h/2}{2rCos[\theta]-w}*(w-r*Cos[\theta])-\sqrt{r^2-(\frac{d}{2})^2} + \frac{h/2*r*Cos[\theta]}{2r*Cos[\theta]-w}+r*Sin[\theta])-(-\frac{h/2}{2rCos[\theta]-w}*x - \sqrt{r^2-(\frac{d}{2})^2}+\frac{h/2*r*Cos[\theta]}{2r*Cos[\theta]-w}+r*Sin[\theta]), -0.33\}, \{x, r*Cos[\theta], w-r*Cos[\theta], 0.005\}];$$

$$ABCFGH1 = Join[AB, BC, CF, FG, GH];$$

$$ID1 = ID + Table[\{w, -h/2, i-i\}, \{i, 1, 87\}];$$

$$DE1 = DE + Table[\{w, -h/2, i-i\}, \{i, 1, 174\}];$$

$$EJ1 = EJ + Table[\{w, -h/2, i-i\}, \{i, 1, 87\}];$$

$$IDEJ1 = Join[ID1, DE1, EJ1];$$

$$unit1 = Join[AB, BC, CF, FG, GH, ID1, DE1, EJ1];$$

$$firstrow = Join[unit1, unit1 + Table[\{2w, 0, i - i\}, \{i, 1{,}793\}], unit1 + 2Table[\{2w, 0, i - i\}, \{i, 1{,}793\}], ABCFGH1 + 3Table[\{2w, 0, i - i\}, \{i, 1{,}445\}]];$$

$$ID2 = ID + Table[\{0, -h, i - i\}, \{i, 1{,}87\}];$$

$$DE2 = DE + Table[\{0, -h, i - i\}, \{i, 1{,}174\}];$$

$$EJ2 = EJ + Table[\{0, -h, i - i\}, \{i, 1{,}87\}];$$

$$IDEJ2 = Join[ID2, DE2, EJ2];$$

$$ABCFGH2 = ABCFGH1 + Table[\{w, -h/2\,, i - i\}, \{i, 1{,}445\}];$$

$$unit2 = Join[IDEJ2, ABCFGH2];$$

$$secondrow = Join[unit2, unit2 + Table[\{2w, 0, i - i\}, \{i, 1{,}793\}], unit2 + 2Table[\{2w, 0, i - i\}, \{i, 1{,}793\}], IDEJ2 + 3Table[\{2w, 0, i - i\}, \{i, 1{,}348\}]];$$

$$thirdrow = firstrow + Table[\{0, -h, i - i\}, \{i, 1{,}2824\}];$$

$$fourrow = secondrow + Table[\{0, -h, i - i\}, \{i, 1{,}2727\}];$$

$$fiverow = thirdrow + Table[\{0, -h, i - i\}, \{i, 1{,}2824\}];$$

$$sixrow = fourrow + Table[\{0, -h, i - i\}, \{i, 1{,}2727\}];$$

$$sevenrow = fiverow + Table[\{0, -h, i - i\}, \{i, 1{,}2824\}];$$

```
Graphics3D[ {Hue[0.116, 0.413, 0.63], CapForm["Butt"], Tube[BezierCurve[firstrow], 0.165], Tube[BSplineCurve[secondrow], 0.165], Tube[BSplineCurve[thirdrow], 0.165], Tube[BSplineCurve[fourrow], 0.165], Tube[BSplineCurve[fiverow], 0.165], Tube[BSplineCurve[sixrow], 0.165], Tube[BSplineCurve[sevenrow], 0.165]}, ViewPoint -> Top, Boxed -> False]
```

Reference

Abel, J., Luntz, J., Brei, D. 2012. A two-dimensional analytical model and experimental validation of garter stitch knitted shape memory alloy actuator architecture. *Smart Materials and Structures*, **21**(8), 085011.

Atalay, O., Kennon, W.R., Demirok, E. 2015. Weft-Knitted Strain Sensor for Monitoring Respiratory Rate and Its Electro-Mechanical Modeling. *Sensors Journal, IEEE*, **15**(1), 110-122.

BASHIR, T. 2013. Conjugated Polymer-based Conductive Fibers for Smart Textile Applications. *Thesis for the Degree of Doctor of Philosophy*.

Biró, L.P., Bernardo, C., Tibbetts, G., Lambin, P. 2012. *Carbon Filaments and Nanotubes: Common Origins, Differing Applications?* Springer Science & Business Media.

Bonderover, E., Wagner, S. 2004. A woven inverter circuit for e-textile applications. *Electron Device Letters, IEEE*, **25**(5), 295-297.

Bonfiglio, A., Curone, D., Secco, E.L., Magenes, G., Tognetti, A. 2011. Emergency and work. in: *Wearable Monitoring Systems*, Springer, pp. 205-219.

Bryant, K.G. 1989. Knitted fabric having improved electrical charge dissipation properties, US Patents 4815299 A.

Calvert, P., Duggal, D., Patra, P., Agrawal, A., Sawhney, A. 2008. Conducting polymer and conducting composite strain sensors on textiles. *Molecular Crystals and*

Liquid Crystals, **484**(1), 291/[657]-302/[668].

Castano, L.M., Flatau, A.B. 2014. Smart fabric sensors and e-textile technologies: a review. *Smart Materials and Structures*, **23**(5), 053001.

Çeken, F., Kayacan, Ö., Özkurt, A., Uğurlu, Ş.S. 2012a. The electromagnetic shielding properties of some conductive knitted fabrics produced on single or double needle bed of a flat knitting machine. *Journal of The Textile Institute*, **103**(9), 968-979.

Çeken, F., Pamuk, G., Kayacan, O., Ozkurt, A., Ugurlu, Ş.S. 2012b. Electromagnetic Shielding Properties of Plain Knitted Fabrics Containing Conductive Yarns. *Journal of Engineered Fabrics & Fibers (JEFF)*, **7**(4).

Chen, X. 2010. *Modelling and predicting textile behaviours*. Woodhead Publishing.

Cherenack, K., van Pieterson, L. 2012. Smart textiles: Challenges and opportunities. *Journal of Applied Physics*, **112**(9), 091301.

Chui, Y.T., Yang, C.X., Tong, J.H., Zhao, Y.F., Ho, C.P., Li, L.L. 2015. A systematic method for stability assessment of Ag-coated nylon yarn. *Textile Research Journal,* **86**(8), 787-802.

Clevertex. 2015. Report on Intelligent Textiles.

Cluster Technical Textiles Neckar-Alb. 2013. Know-How and Tradition: Technical Textiles from the Neckar-Alb Region. 978-3-9815361-1-9.

Cottet, D., Grzyb, J., Kirstein, T., Tröster, G. 2003. Electrical characterization of textile transmission lines. *Advanced Packaging, IEEE Transactions on*, **26**(2), 182-190.

Coyle, S., Lau, K.-T., Moyna, N., Gorman, D.O., Diamond, D., Di Francesco, F., Costanzo, D., Salvo, P., Trivella, M.G., De Rossi, D.E. 2010. BIOTEX—Biosensing textiles for personalised healthcare management. *Information Technology in Biomedicine, IEEE Transactions on*, **14**(2), 364-370.

De Mey, G., Ozcelik, M., Schwarz, A., Kazani, I., Hertleer, C., Van Langenhove, L., Gursoy, N.C. 2014. Designing of conductive yarn knitted thermal comfortable shirt using battery operated heating system. *TEKSTIL VE KONFEKSIYON*, **1**, 64-67.

Ding, J.T.F., Tao, X., Au, W.M., Li, L. 2014. Temperature effect on the conductivity of knitted fabrics embedded with conducting yarns. *Textile Research Journal*, **84**(17), 1849-1857.

Duran, D., Kadoğlu, H. 2015. Electromagnetic shielding characterization of conductive woven fabrics produced with silver-containing yarns. *Textile Research Journal*, **85**(10), 1009-1021.

Fayala, F., Alibi, H., Benltoufa, S., Jemni, A. 2008. Neural network for predicting thermal conductivity of knit materials. *Journal of Engineered Fibers and Fabrics*, **3**(4), 53-60.

Gonzalez, M., Axisa, F., Bulcke, M.V., Brosteaux, D., Vandevelde, B., Vanfleteren, J. 2008. Design of metal interconnects for stretchable electronic circuits.

Microelectronics Reliability, **48**(6), 825-832.

Guo, L., Berglin, L., Mattila, H. 2012. Improvement of electro-mechanical properties of strain sensors made of elastic-conductive hybrid yarns. *Textile Research Journal*, **82**(19), 1937-1947.

Hamdani, S.T.A., Potluri, P., Fernando, A. 2013. Thermo-mechanical behavior of textile heating fabric based on silver coated polymeric yarn. *Materials*, **6**(3), 1072-1089.

Holland, S.A. 2013. Conductive Textiles and their use in Combat Wound Detection, Sensing, and Localization Applications.

Hsu, F.-B., Kuo, C.-J. 2010. Conductive yarn capable of withstanding dyeing, finishing and washing, US Patents 20100300060 A1.

HTS/Amptek. 2016. DuoTape® Heating Tape, http://heatingtapes.com/collections/duo-tape-heavy, accessed in 2016 .

Hu, L., Pasta, M., Mantia, F.L., Cui, L., Jeong, S., Deshazer, H.D., Choi, J.W., Han, S.M., Cui, Y. 2010. Stretchable, porous, and conductive energy textiles. *Nano Lett*, **10**(2), 708-14.

Husain, M.D., Kennon, R., Dias, T. 2014. Design and fabrication of Temperature Sensing Fabric. *Journal of Industrial Textiles*, **44**(3), 398-417.

Inagaki, M. 2000. *New carbons-control of structure and functions*. Elsevier.

Ingle, E.M., Fisher, B.J., Finney, J.W. 2008. Silver coated nylon fibers and associated methods of manufacture and use, US Patents 20100166832 A1.

JohnA.Roberts, NorthChelmsford, JosephR.Quirk, W. 1968. Metallic yarn structure, US Patents US3378999 A.

Jon. 2005. My Mitts Are Electric..., *outdoors magic*. Accessed in 2016.

Jost, K., Stenger, D., Perez, C.R., McDonough, J.K., Lian, K., Gogotsi, Y., Dion, G. 2013. Knitted and screen printed carbon-fiber supercapacitors for applications in wearable electronics. *Energy & Environmental Science*, **6**(9), 2698-2705.

Kayacan, O., Bulgun, E., Sahin, O. 2009. Implementation of steel-based fabric panels in a heated garment design. *Textile Research Journal*, **79**(16), 1427-1437.

Kearsley, W.K. 1946. ELECTRIC BLANKET, (Ed.) US Patent 2403803 A.

Kim, H., Kim, Y., Kim, B., Yoo, H. J. 2009. A wearable fabric computer by planar-fashionable circuit board technique. *Sixth International Workshop on Wearable and Implantable Body Sensor Networks*. IEEE, 282-285.

Kinkeldei, T., Zysset, C., Cherenack, K., Troester, G. 2009. Development and evaluation of temperature sensors for textile integration. *Sensors*. IEEE, 1580-1583.

Knitting industry. 2013. Groz-Beckert interview: warmX heatable textiles, knitting industry. http://www.knittingindustry.com/grozbeckert-interview-warmx-heatable-textiles/, accessed in 2016.

Kun, Y., Guang-li, S., Liang, Z., Li-wen, L. 2009. Modelling the electrical property of

1× 1 rib knitted fabrics made from conductive yarns. *Second International Conference on Information and Computing Science*. IEEE, 382-385.

Klane F.Forsgren, Y., Sidney Melamed, E.P., Robert S. Weiner, M., Ga. 1977. PROCESS Process for producing crimped metal-coated filamentary materials, and yarns and fabrics obtained therefrom, US Patent 4042737 A.

Latifi, M., Payvandy, P. 2010. Electro-conductive textile yarns. *Technical Textile Yarns*, Woodhead Publishing Limited, 298-328.

Leaf, G., Glaskin, A. 1955. 43—The geometry of a plain knitted loop. *Journal of The Textile Institute Transactions*, **46**(9), T587-T605.

Lee, J.B., Subramanian, V. 2003. Organic transistors on fiber: a first step towards electronic textiles. *Electron Devices Meeting, 2003. IEDM'03 Technical Digest. IEEE International*. IEEE, 8-3.

Li, L. 2010. Innovative functional knitwear design with conductive yarns, Doctoral dissertation, The Hong Kong Polytechnic University.

Li, L., AU, M.W., Wan, K.M., Wan, S.H., Chung, W.Y., Wong, K.S. 2009a. A resistive network model for conductive knitting stitches. *Textile Research Journal*, **80**(10): 935-947.

Li, L., Au, W.m., Ding, F., Hua, T., Wong, K.S. 2013. Wearable electronic design: electrothermal properties of conductive knitted fabrics. *Textile Research Journal*, **84**(5), 477-487.

Li, L., Au, W.M., Hua, T., Feng, D. 2014. Smart Textiles: A Design Approach for Garments Using Conductive Fabrics. *The Design Journal*, **17**(1), 137-154.

Li, L., Au, W.M., Li, Y., Wan, K.M., Chung, W.Y., Wong, K.S. 2009b. A Novel Design Method for an Intelligent Clothing Based on Garment Design and Knitting Technology. *Textile Research Journal*, **79**(18), 1670-1679.

Li, L., Liu, S., Ding, F., Hua, T., Au, W.M., Wong, K.S. 2012. Electromechanical analysis of length-related resistance and contact resistance of conductive knitted fabrics. *Textile Research Journal*, **82**(20), 2062-2070.

Liu, L., Yu, Y., Yan, C., Li, K., Zheng, Z. 2015. Wearable energy-dense and power-dense supercapacitor yarns enabled by scalable graphene-metallic textile composite electrodes. *Nat Commun*, **6**, 7260.

Liu, R., Wang, S., Lao, T.T. 2012. A Novel Solution of Monitoring Incontinence Status by Conductive Yarn and Advanced Seamless Knitting Techniques. *Journal of Engineered Fabrics & Fibers (JEFF)*, **7**(4): 50-56.

Lymberis, A., Paradiso, R. 2008. Smart fabrics and interactive textile enabling wearable personal applications: R&D state of the art and future challenges. *30th Annual International Conference of the IEEE Engineering in Medicine and Biology Society, 2008*. IEEE, 5270-5273.

Martin, T., Jones, M., Edmison, J., Shenoy, R. 2003. Towards a design framework for wearable electronic textiles. *ISWC*, **3**: 190-200.

Mattila, H. 2006. 1 - Intelligent textiles and clothing – a part of our intelligent ambience. *Intelligent Textiles and Clothing*, Woodhead Publishing, 1-4.

McCann, J., Bryson, D. 2009. *Smart clothes and wearable technology*. Elsevier.

Meoli, D., May-Plumlee, T. 2002. Interactive electronic textile development a review of technologies. *Journal of Textile and Apparel, Technology and Management*, **2**(2) 1-12.

Meyer, J., Arnrich, B., Schumm, J., Tröster, G. 2010. Design and modeling of a textile pressure sensor for sitting posture classification. *Sensors Journal, IEEE*, **10**(8), 1391-1398.

Muller, C., Hamedi, M., Karlsson, R., Jansson, R., Marcilla, R., Hedhammar, M., Inganas, O. 2011. Woven electrochemical transistors on silk fibers. *Adv Mater*, **23**(7), 898-901.

Munden, D. 1959. 26—The geometry and dimensional properties of plain-knit fabrics. *Journal of the Textile Institute Transactions*, **50**(7), 448-471.

Nusko, R., Parzl, A., Maier, G. 2005. Electrically conductive yarn, US Patent 5927060 A.

Osman, M.A.R., Abd Rahim, M.K., Samsuri, N.A., Salim, H.A.M., Ali, M.F. 2011. Embroidered fully textile wearable antenna for medical monitoring applications. *Progress In Electromagnetics Research*, **117**, 321-337.

Özdemir, H., Kılınç, S. 2015. Smart Woven Fabrics With Portable And Wearable

Vibrating Electronics. *Autex Research Journal*, **15**(2) 99-103.

Özdil, N., Marmaralı, A., Kretzschmar, S.D. 2007. Effect of yarn properties on thermal comfort of knitted fabrics. *International journal of Thermal sciences*, **46**(12), 1318-1322.

Paradiso, R., Belloc, C., Loriga, G., Taccini, N. 2005. Wearable healthcare systems, new frontiers of e-textile. *Stud Health Technol Inform*, **117**, 9-16.

Park, S., Jayaraman, S. 2003. Smart textiles: Wearable electronic systems. *MRS bulletin*, **28**(08), 585-591.

Parkova, I., Vališevskis, A., Kašurins, A., Viļumsone, A. 2015. Integration of Flexible Keypad into Clothing. *Environment Technology Resources. Proceedings of 8th International Scientific and Practical Conference*, **2**: 173-180

Perice, F.T. 1947. Geometrical Principles Applicable to the Design of Functional Fabrics. *Textile Research Journal*, **17**(3), 123-147.

Pollini, M., Russo, M., Licciulli, A., Sannino, A., Maffezzoli, A. 2009. Characterization of antibacterial silver coated yarns. *J Mater Sci Mater Med*, **20**(11), 2361-2366.

Post, E.R., Orth, M., Russo, P., Gershenfeld, N. 2000. E-broidery: Design and fabrication of textile-based computing. *IBM Systems journal*, **39**(3.4), 840-860.

Postle, R. 1974. 17—A geometrical assessment of the thickness and bulk density of weft-knitted fabrics. *Journal of the Textile Institute*, **65**(4), 155-163.

Qureshi, W., Guo, L., Peterson, J., Berglin, L., Mehrjerdi, A.K., Skrifvars, M. 2011.

Knitted wearable stretch sensor for breathing monitoring application.

Rheaume, W.A. 1982. Heat conductive fabric, US Patent 4312913 A.

Rock, M., Sharma, V. 2005. EMI shielding fabric, US Patent 6843078 B2.

Roell, F. 1996. Electric heating element in knitted fabric, US Patent 5484983 A.

Russell, S. 2006. *Handbook of nonwovens*. Woodhead Publishing.

Šahta, I., Baltina, I., Truskovska, N., Blums, J., Deksnis, E. 2014. Selection of conductive yarns for knitting an electrical heating element. *High Performance and Optimum Design of Structures and Materials*, **137**, 91-102.

Saini, P., Arora, M. 2012. Microwave Absorption and EMI Shielding Behavior of Nanocomposites Based on Intrinsically Conducting Polymers, Graphene and Carbon Nanotubes. Polymerization Book 2, 1-42.

Sanders, J. 1981. Electrically-conductive textile fiber, US Patent 4255487 A.

School of Art & Design. 2014. Advanced Textile and Research. http://www4.ntu.ac.uk/apps/research/groups/22/home.aspx/group/143751/overview/advanced_textiles, accessed in 2016.

Schwarz, A., Van Langenhove, L. 2013. *Types and processing of electro-conductive and semiconducting materials for smart textiles*. Woodhead Publishing Limited, 26-69.

Schwarz, A., Van Langenhove, L., Guermonprez, P., Deguillemont, D. 2010. A roadmap on smart textiles. *Textile Progress*, **42**(2), 99-180.

Semnani, D., Latifi, M., Hamzeh, S., Jeddi, A. 2003. A new aspect of geometrical and physical principles applicable to the estimation of textile structures: An ideal model for the plain-knitted loop. *Journal of the Textile Institute*, **94**(3-4), 202-211.

Seymour, S. 2008. *Fashionable technology: The intersection of design, fashion, science, and technology*. Springer Publishing Company, Incorporated.

Shyr, T.-W., Shie, J.-W., Jhuang, Y.-E. 2011. The effect of tensile hysteresis and contact resistance on the performance of strain-resistant elastic-conductive webbing. *Sensors*, **11**(2), 1693-1705.

SILVERELL. 2016. MEDICAL KNITS, V Technical Textiles Inc. . http://www.shopvtechtextiles.com/Medical-Knits_c_18.html, accessed in 2016.

Soyaslan, D., Çömlekçi, S., Göktepe, Ö. 2010. Determination of electromagnetic shielding performance of plain knitting and 1X1 rib structures with coaxial test fixture relating to ASTM D4935. *The Journal of the Textile Institute*, **101**(10), 890-897.

Sparkfun. 2016. Conductive Fabric - Heavy Knit, SparkFun Electronics. https://www.sparkfun.com/products/retired/9770, accessed in 2016.

Spencer, D.J. 2001. *Knitting technology: a comprehensive handbook and practical guide*. CRC Press.

Stoppa, M., Chiolerio, A. 2014. Wearable electronics and smart textiles: a critical review. *Sensors (Basel)*, **14**(7), 11957-11992.

Swapnil, d. 2015. Wearable Technology Market Will Worth $70 billion By 2024: Technologies, Markets, Forecasts- MarketResearchReports.Biz. Daily Press. http://www.dailypress.com/news/community/spotlight/dp-ugc-article-wearable-technology-market-will-worth-70-bil-2015-10-16-story.html, accessed in 2016.

Swift Textile Metalizing. 2015. Conductive Non-Woven Fabric for Breathable Shielding Applications. http://www.swift-textile.com/conductive-nonwoven-fabric-products.html, accessed in 2016.

Textronics Inc. . 2006. Monitor the Body. http://www.textronicsinc.com/products, accessed in 2016.

Tong, J., Ding, F., Tao, X., Au, W.M., Li, L. 2014. Temperature effect on the conductivity of knitted fabrics embedded with conducting yarns. *Textile Research Journal*, **84**(17): 1849–1857.

Tong, J., Li, L. 2015. Thermal Regulation of Electrically Conducting Fabrics. *Handbook of Smart Textiles*, Springer Science+Business Media Singapore.

Van Langenhove, L., Hertleer, C. 2004. Smart clothing: a new life. *International Journal of Clothing Science and Technology*, **16**(1/2), 63-72.

Wang, J., Long, H., Soltanian, S., Servati, P., Ko, F. 2014a. Electro-mechanical properties of knitted wearable sensors: Part 2–Parametric study and experimental verification. *Textile Research Journal*, **84**(2), 200-213.

Wang, J., Long, H., Soltanian, S., Servati, P., Ko, F. 2014b. Electromechanical properties of knitted wearable sensors: part 1–theory. *Textile Research Journal*, **84**(1), 3-15.

X-STATIC. 2016. X-STATIC® - Pure Silver. Pure Protection. http://noblebiomaterials.com/xstatic-textiles/, accessed in 2016.

Xie, J., Long, H. 2014. Equivalent resistance calculation of knitting sensor under strip biaxial elongation. *Sensors and Actuators A: Physical*, **220**, 118-125.

Xie, J., Tamaki, J. 2008. An experimental study on discharge mediums used for electro-contact discharge dressing of metal-bonded diamond grinding wheel. *journal of materials processing technology*, **208**(1), 239-244.

Xue, C.-H., Chen, J., Yin, W., Jia, S.-T., Ma, J.-Z. 2012. Superhydrophobic conductive textiles with antibacterial property by coating fibers with silver nanoparticles. *Applied Surface Science*, **258**(7), 2468-2472.

Yu, Z. C., Zhang, J. F., Lou, C. W., Lin, J. H. 2015. Wicking behavior and antibacterial properties of multifunctional knitted fabrics made from metal commingled yarns. *The Journal of The Textile Institute*(ahead-of-print), **106**(8): 862-871.

Zeng, W., Shu, L., Li, Q., Chen, S., Wang, F., Tao, X.M. 2014. Fiber-based wearable electronics: a review of materials, fabrication, devices, and applications. *Adv Mater*, **26**(31), 5310-5336.

Zhang, H., Tao, X., Yu, T., Wang, S. 2006. Conductive knitted fabric as large-strain gauge under high temperature. *Sensors and Actuators A: Physical*, **126**(1), 129-140.

Zou, H. 2013. Silver-fiber medicine efficacy physiotherapy neckerchief. CN Patent 203090243 U.

ŽUravliova, S.V., StygienĖ, L., StygienĖ, L., ČEpliauskienĖ, R., ČEpliauskienĖ, R., Krauledas, S., Krauledas, S., SankauskaitĖ, A., SankauskaitĖ, A. 2013. The Influence of Three-Layer Knitted Fabrics' Structure on Electrostatic and Comfort Properties. *Materials Science*, **19**(4): 415-419.

Zysset, C., Cherenack, K., Kinkeldei, T., Tröster, G. 2010. Weaving integrated circuits into textiles. *International Symposium on Wearable Computers (ISWC)*. IEEE, 1-8.